HISTORICAL BIOLOGY
https://doi.org/10.1080/08912963.2026.2634175

Taylor & Francis
Taylor & Francis Group

RESEARCH ARTICLE

OPEN ACCESS Check for updates

A seven-million-year record from the Daroca-Calamocha area (Miocene, Spain) brings new clues to Erinaceidae phylogeny and paleobiogeography

Florentin Cailleux [1,2], Pablo Peláez-Campomanes [3], Jérôme Prieto [4] and Lars W. van den Hoek Ostende [2]

[1]Department of Geology and Palaeontology, Comenius University, Bratislava, Slovakia; [2]Vertebrate Evolution, Development and Ecology Department, Naturalis Biodiversity Center, Leiden, The Netherlands; [3]Paleobiology Department, Museo Nacional de Ciencias Naturales, Madrid, Spain; [4]Department of Earth and Environmental Science, Palaeontology & Geobiology Ludwig-Maximilians-Universität, Munich, Germany

ABSTRACT

Ninety-two localities from the Daroca-Calamocha area (central Spain), spanning seven million years, have yielded a high diversity of Miocene erinaceids, comprising six species of Galericinae (*Galerix remmerti, Galerix symeonidisi, Galerix exilis, Parasorex* sp. *Parasorex voesendorfensis, Lantanotherium* sp.) and four species of Erinaceinae (*'Amphechinus' baudeloti*, *Atelerix* cf. *depereti*, *'Mioechinus'* sp. Erinaceinae gen. et sp. indet). We identify the transition from *Galerix remmerti* to *G. exilis* during Local Zone C (MN4) and discuss the differences between *G. exilis* and *G. symeonidisi* in Spain. Detailed comparisons of the intraspecific variability of *Galerix* species lead to a new phylogeny of the genus that supports a strong basal dichotomy and two distinct dispersal events into Europe during the Early Miocene. The record of *Parasorex* sp. and *Lantanotherium* sp. in the Iberian Peninsula is constrained to the middle-late Aragonian transition and is correlated with unstable climatic conditions. The latest Aragonian and Vallesian material from Nombrevilla 2, Carrilanga 1, and Pedregueras 2A, previously identified as *Parasorex socialis*, is reattributed to *Parasorex voesendorfensis*.

ARTICLE HISTORY
Received 17 October 2025
Accepted 13 February 2026

KEYWORDS
Erinaceinae; Galericinae; Aragonian; *Galerix*; dental variability

HANDLING EDITOR
Mark T. Young, University of Edinburgh, UK

Introduction

The Erinaceidae have a rich and diverse Neogene fossil record. In western Eurasia, this high diversity is mainly explained by the success of the Galericinae, which often dominate Miocene insectivore assemblages, and for which several migration events have been identified (Van den Hoek Ostende et al., 2015). In the Neogene of Europe, Spain stands out for its rich fossil micromammal record and large number of well-dated localities, especially in the Calatayud-Montalbán, Teruel, and Vallès-Penedès Basins (e.g. Casanovas-Vilar et al., 2016; García-Paredes et al., 2016; Van der Meulen et al., 2012). This allowed the identification of peaks in eulipotyphlan diversity and their correlation with environmental and faunal phenomena during the European Miocene, such as the Miocene Climatic Optimum and the Aragonian-Vallesian transition (Furió et al., 2018). The long-term record of micromammals in Spain, combined with magnetostratigraphy, is of crucial importance for highlighting the relationship between faunal and climatic changes (e.g. Van Dam et al., 2006).

To date, insectivore studies from Spain have mainly been focused on the Ramblian (e.g. Crespo et al., 2019, 2020; Jovells-Vaqué et al., 2018; Van den Hoek Ostende, 2003) or the Vallesian (e.g. De Jong, 1988; Van Dam, 2010; Van Dam et al., 2020; Van den Hoek Ostende et al., 2012). In comparison, studies on the Aragonian Eulipotyphla are rather limited or confined to taxonomic lists (Gibert, 1975; De Jong, 1988; Van den Hoek Ostende & Furió, 2005; Álvarez Sierra et al., 2006; Furió, Casanovas-Vilar, et al., 2011a; Van Dam et al., 2011; Van der Meulen et al., 2012), partly because the overall diversity of insectivores was lower during this stage. The poorly published Aragonian record leads to an incomplete picture of the small mammal faunas and their evolution during the Miocene, despite the exceptional number of Aragonian localities. In this paper, the diversity of the Erinaceidae from the Daroca-Calamocha area, which represents the densest long-term record of insectivores in Spain and spans seven million years, is examined. Subsequently, existing phylogenetic and paleobiogeographic hypotheses will be tested on the basis of this record.

Palaeontological setting

The present work focuses on assemblages from the Daroca-Calamocha area within the Calatayud-

CONTACT Florentin Cailleux florentin.cailleux@naturalis.nl; cailleux1@uniba.sk Comenius University in Bratislava, Faculty of Natural Sciences, Department of Geology and Paleontology, Ilkovičova 6, Mlynská dolina G, Bratislava SK–842 15, Slovakia

Supplemental data for this article can be accessed online at https://doi.org/10.1080/08912963.2026.2634175

Published online 25 Mar 2026

Montalbán Basin (central Spain), a map of which is shown in Figure 1. This basin contains one of the densest long-term fossil records for micromammals (Daams, Van der Meulen, Álvarez-Sierra, et al., 1999; Daams, Van der Meulen, Peláez-Campomanes, et al., 1999; García-Paredes et al., 2016; López-Guerrero et al., 2009; López-Guerrero et al., 2018; Van Dam et al., 2020; Van der Meulen et al., 2003, 2012). Decades of fieldwork (Daams & Freudenthal, 1988) resulted in a robust stratigraphy (Álvarez Sierra et al., 2003; Daams, Freudenthal, & Van der Meulen, 1988, 1999; García-Paredes et al., 2016; Van der Meulen et al., 2011, 2012), supported by magnetostratigraphic analyses (Daams, Van der Meulen, Sierra, et al., 1999; Garcés et al., 2003; Krijgsman et al., 1994, 1996; Van Dam et al., 2014). The material attributed to Galericini consists mostly of isolated teeth and is almost continuously present in Miocene localities from Spain, ranging

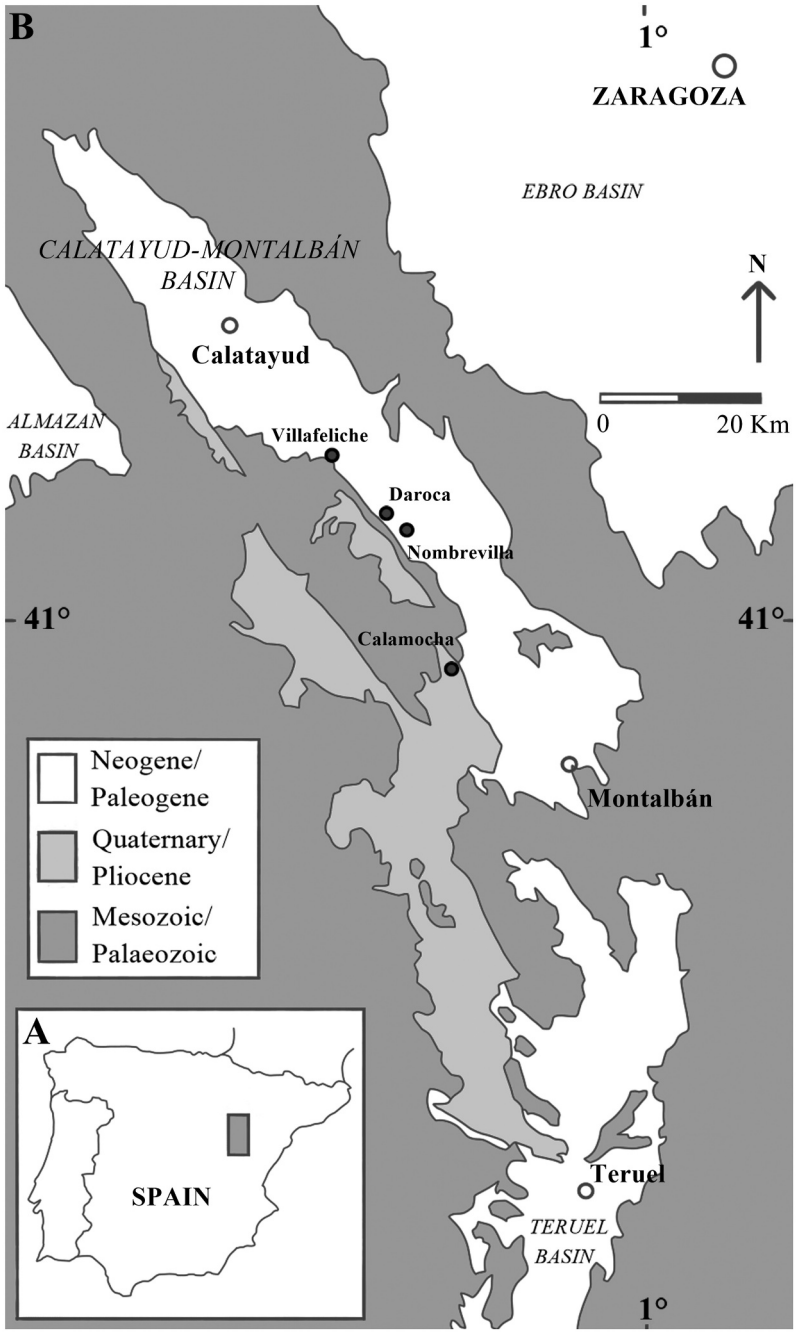

Figure 1. Simplified geological map of the Calatayud-Montalbán Basin, showing the geographic location of several localities (modified after García-Paredes et al., 2010).

from MN3 to MN15 (from ~19 Ma to ~3 Ma) (Furió et al., 2018).

The oldest species of Galericini in the Daroca-Calamocha area is found in Ramblian deposits of Navarrete del Rio (latest MN2) and identified as *Galerix remmerti* Van den Hoek Ostende, 2003. It is replaced by *Galerix symeonidisi* Doukas, 1986, and *Galerix exilis* de Blainville, 1839 during MN3 and MN4 (Van den Hoek Ostende & Doukas, 2003). The last occurrence of the genus *Galerix* Pomel, 1848 in the Daroca-Calamocha area is in the locality Carrilanga 1 (Zone G3; 11.33 Ma), where *G. exilis* is found in association with another Galericini, previously identified as *Parasorex socialis* Rabeder, 1973 (De Jong, 1988; Van den Hoek Ostende, 2001, 2003). In addition to the rich record of Galericinae, the Calatayud-Montalban and Teruel Basins are also characterised by the sporadic presence of Erinaceinae, which were temporarily attributed to ?*Amphechinus* by Van den Hoek Ostende and Furió (2005). Recently, Van Dam et al. (2020) carried out a detailed description of the Erinaceinae from the Vallesian and Turolian deposits of the Teruel Basin, describing four taxa: *Postpalerinaceus* cf. *vireti* Crusafont et Villalta, 1947, *Atelerix* aff. *depereti* Mein and Gisnburg, 2002, *Atelerix steensmai* van Dam et al., 2020, and Erinaceinae gen. sp. indet.

Materials and methods

The material studied comprises 2621 dental elements of Erinaceidae from ninety-one Aragonian localities and one Vallesian locality from the Daroca-Calamocha area (Table 1, Figure 2). We follow the dental terminology of Cailleux et al. (2023). All tooth sizes are given in millimetres (mm), and the specimens are presented in left orientation. Therefore, right specimens are reversed and indicated in figures by an underlined letter. Drawings were made using a graphics tablet (Wacom Intuos Pro) and the Autodesk SketchBook (v. 8.7.1) software. We follow Prieto and Rummel (2009) for the measurement method of length (L), labial length (L1), shortest anteroposterior length (L2), width (W), anterior width (W1), and posterior width (W2). All measurements were taken twice and averaged. They were obtained using a LEICA MZ16 A binocular, a LEICA DFC420 digital camera, two LEICA CLS 150X optical light sources, and the Leica Application Suite (v. 4.5.0; Leica Microsystems Ltd., Heerbrugg, Switzerland) software. Ages of the Daroca-Calamocha localities are taken from Daams, Van der Meulen, Álvarez-Sierra, et al. (1999), Van Dam et al. (2006), Van Dam et al. (2014), and recalibrated to the most recent time scale of Raffi et al. (2020), based on the most recent ages for chron boundaries. The specimens studied from the Daroca-Calamocha area are housed in several institutions: Museo Nacional de Ciencias Naturales (MNCN), Madrid, Spain; Rijksmuseum van Geologie en Mineralogie (RGM), now the Naturalis Biodiversity Center, Leiden, The Netherlands; University of Lyon (UCBL), Lyon, France; University of Utrecht (UU), Utrecht, The Netherlands. The repository for each locality is indicated in Table 1, alongside the collection code and age estimation used in Figure 2 and in the text. The taxonomic verdicts, identification numbers, and measurements of all the studied material are available in supplementary material (S1).

Plots were generated using the R software environment (v. 3.5.3) (R Core Team, 2019). The use of Kernel Density Estimation (KDE) was considered particularly efficient for representing one-dimensional variability, and rug plots are always presented with the default bandwidth. We also considered the use of area measurements to reveal/contrast dissimilarities. These measurements focus on the upper dental rows, which are rather variable among Eulipotyphla. The area of the trigonid of the m1 (atm1) was also considered as a possible evolutionary marker. Dental areas are considered in mm^2. They are estimated by tracing the outline with a variable number of points (about 140 for P3, 160 for P4, 200 for M1 and M2, 120 for p4, 100 for m1) and using the area line tool of Leica Application Suite (v.4.5.0). The robustness of such a method was tested by calculating the area of a M1 (LUM21-1C) and a P4 (RGM335206) once a day for 50 days. For an average area of 7.062 mm^2, we obtain values for the M1 that are contained between 7.049 mm^2 and 7.072 mm^2. For an average area of 2.533 mm^2, we obtain values for the P4 that are contained between 2.529 mm^2 and 2.537 mm^2. Considering the usually high variability of size in Erinaceidae, the error rate is considered insignificant here. We consider morphometric methods as an imperfect way to distinguish the Erinaceidae from the Daroca-Calamocha area, especially for populations with low abundance or with undiagnostic, ancestral features. The identification based on morphology and the possible identification based on area measurements have been applied independently for each specimen, as the latter can only provide a probability of identification in most cases. As a result, the open nomenclature term 'confere' is exceptionally used at the specimen level in Supplementary material 1. Only the highest degree of taxonomic certainty is used in the manuscript and the figures. To facilitate further comparison, descriptions of material include frequency as much as possible; broader terms (e.g. 'usual', 'often', 'sometimes') are used when wear stages or very thin details

subject to observation biases do not allow for an exact frequency.

Systematic Palaeontology

Order **Eulipotyphla** Waddell, Okada and Hasegawa, 1999
Family **Erinaceidae** Fischer, 1814
Subfamily **Galericinae** Pomel, 1848
Tribe **Galericini** Pomel, 1848

Remarks

We adopt the concept of Galericini from Van den Hoek Ostende (2001), except for the synonymy of *Tetracus* Aymard, 1850, and *Galerix* made in this paper and refuted by Hugueney and Adrover (2003). We follow Hugueney and Adrover (2003), Van den Hoek Ostende and Fejfar (2006), and Masini and Fanfani (2013) by including the genera *Apulogalerix* Masini & Fanfani, 2013, *Deinogalerix* Freudenthal, 1972, *Riddleria* van den Hoek Ostende, 2006, and *Tetracus* in this tribe. Our use of the term Galericini differs from that of Lopatin (2006) in that we exclude most of the morphologically conservative Palaeogene taxa (e.g. *Protogalericius* Lopatin, 2006 and *Oligochenus* Lopatin, 2005), as well as recent gymnures (e.g. *Hylomys* Müller, 1840) and their close fossil relatives (e.g. *Thaiagymnura* Mein and Ginsburg, 1997, and *Lantanotherium* Filhol, 1888).

Table 1. Abbreviations of the locality names from the Daroca-Calamocha area yielding erinaceids material.

Locality	Code	Age (Ma)	Collection	Locality	Code	Age (Ma)	Collection
Pedregueras 2A	PE2A	10.62	RGM	Valdemoros 6A	VA6A	14.53	MNCN
Carrilanga 1	CAR1	11.33	RGM	Valdemoros 7C	VA7C	14.55	MNCN
Nombrevilla 2	NO2	11.87	MNCN	Valdemoros 7B	VA7B	14.59	MNCN
Solera	SOL	12.01	RGM	Valdemoros 7A	VA7A	14.62	MNCN
Paje 2	PJE2	12.26	MNCN	Vargas 8C	VR8C	14.71	MNCN
Paje 1	PJE1	12.39	MNCN	Vargas 8B	VR8B	14.73	MNCN
Las Planas 5 H	LP5H	12.60	RGM	Caseton 2B	CS1B	14.75	RGM
Toril 2	TOR2	12.61	RGM	Caseton 1A	CS1A	14.78	RGM
Toril 1	TOR1	12.62	RGM	Moratilla 4	MOR4	–	RGM
Toril 3B	TOR3B	12.65	MNCN	Vargas 7	VR7	14.81	MNCN
Alcocer 2	AC2	12.70	RGM	Valdemoros 3D	VA3D	14.82	RGM
Villafeliche 9	VL9	12.85	RGM	Valdemoros 3B	VA3B	14.84	UU
Las Planas 5K	LP5K	13.08	RGM	Vargas 6	VR6	15.25	MNCN
Borjas	BOR	13.20	RGM	Vargas 5	VR5	15.32	MNCN
Valalto 1B	VT1B	13.30	RGM, MNCN	Villafeliche 4A	VL4A	15.50	RGM
Valalto 1A	VT1A	13.35	MNCN	Valdemoros 8A	VA8A	15.68	MNCN
Las Planas 5C	LP5C	13.55	RGM, MNCN	Moratilla 3	MOR3	15.73	MNCN
Las Umbrias 21	LUM21	13.75	MNCN	Moratilla 2	MOR2	15.78	MNCN
Las Umbrias 22	LUM22	13.76	MNCN	Fuente Sierra 4	FT4	15.82	MNCN
Las Umbrias 20	LUM20	13.80	MNCN	Fuente Sierra 3	FT3	15.82	MNCN
Las Umbrias 19	LUM19	13.95	MNCN	La Col D	COLD	15.84	MNCN
Las Planas 4B	LP4B	13.96	MNCN, UU	La Col C	COLC	15.86	MNCN
Las Umbrias 14	LUM14	13.99	MNCN	Fuente Sierra 2	FT2	15.89	MNCN
Las Umbrias 18	LUM18	14.00	MNCN	Olmo Redondo 8	OR8	15.91	RGM
Las Umbrias 17	LUM17	14.01	MNCN	Vargas 2B	VR2B	15.92	MNCN
Las Umbrias 12	LUM12	14.03	MNCN	La Col A	COLA	15.93	MNCN
Las Umbrias 16	LUM16	14.04	MNCN	Vargas 2A	VR2A	15.94	MNCN
Las Umbrias 11	LUM11	14.06	MNCN	Olmo Redondo 9	OR9	15.95	RGM
Las Umbrias 10	LUM10	14.09	MNCN	La Col B	COLB	15.98	MNCN
Regajo 2	RG2	14.16	RGM	Olmo Redondo 5	OR5	16.02	RGM
Las Umbrias 9	LUM9	14.18	MNCN	Vargas 1A	VR1A	16.11	RGM
Las Umbrias 8	LUM8	14.20	MNCN	Vargas 4BB	VR4BB	16.12	MNCN
Las Umbrias 7	LUM8	14.20	MNCN	Vargas 3	VR3	16.13	MNCN
Valdemoros 7 G	VA7G	14.24	MNCN	Vargas 4B	VR4B	16.13	MNCN
Valdemoros 7F	VA7F	14.27	MNCN	Vargas 4A	VR4A	16.15	MNCN
Valdemoros 7E	VA7E	14.29	MNCN	Olmo Redondo 4A	OR4A	16.30	MNCN, UU
Las Umbrias 5	LUM5	14.30	MNCN	San Roque 3	SR3	16.33	MNCN, UU
Las Umbrias 4	LUM4	14.32	MNCN	Artesilla	ART	16.49	MNCN
Valdemoros 7D	VA7D	14.33	MNCN	Villafeliche 2A	VL2A	16.63	UU
Las Umbrias 3	LUM3	14.37	MNCN, UCBL	Olmo Redondo 3	OR3	16.64	RGM
Vargas 11	VR11	14.38	MNCN	San Roque 5	SR5	16.65	MNCN
Valdemoros 6B	VA6B	14.39	MNCN	San Roque 2	SR2	16.66	RGM
Las Umbrias 2	LUM2	14.40	MNCN	San Marco 1	SAM	16.69	MNCN
Las Umbrias 1	LUM1	14.42	MNCN	Olmo Redondo 2	OR2	16.72	RGM
Valdemoros 3F	VA3F	14.50	MNCN	Olmo Redondo 1	OR1	16.75	RGM
Valdemoros 3E	VA3E	14.53	RGM	San Roque 1	SR1	16.77	RGM

The corresponding ages are after Daams, Van der Meulen, Álvarez-Sierra, et al. (1999) and Van Dam et al. (2014). MNCN = Museo de Ciencias Naturales, Madrid, Spain; RGM = Rijksmuseum van Geologie en Mineralogie, Leiden, The Netherlands; UCBL = University of Lyon, Lyon, France; UU = University of Utrecht, Utrecht, The Netherlands.

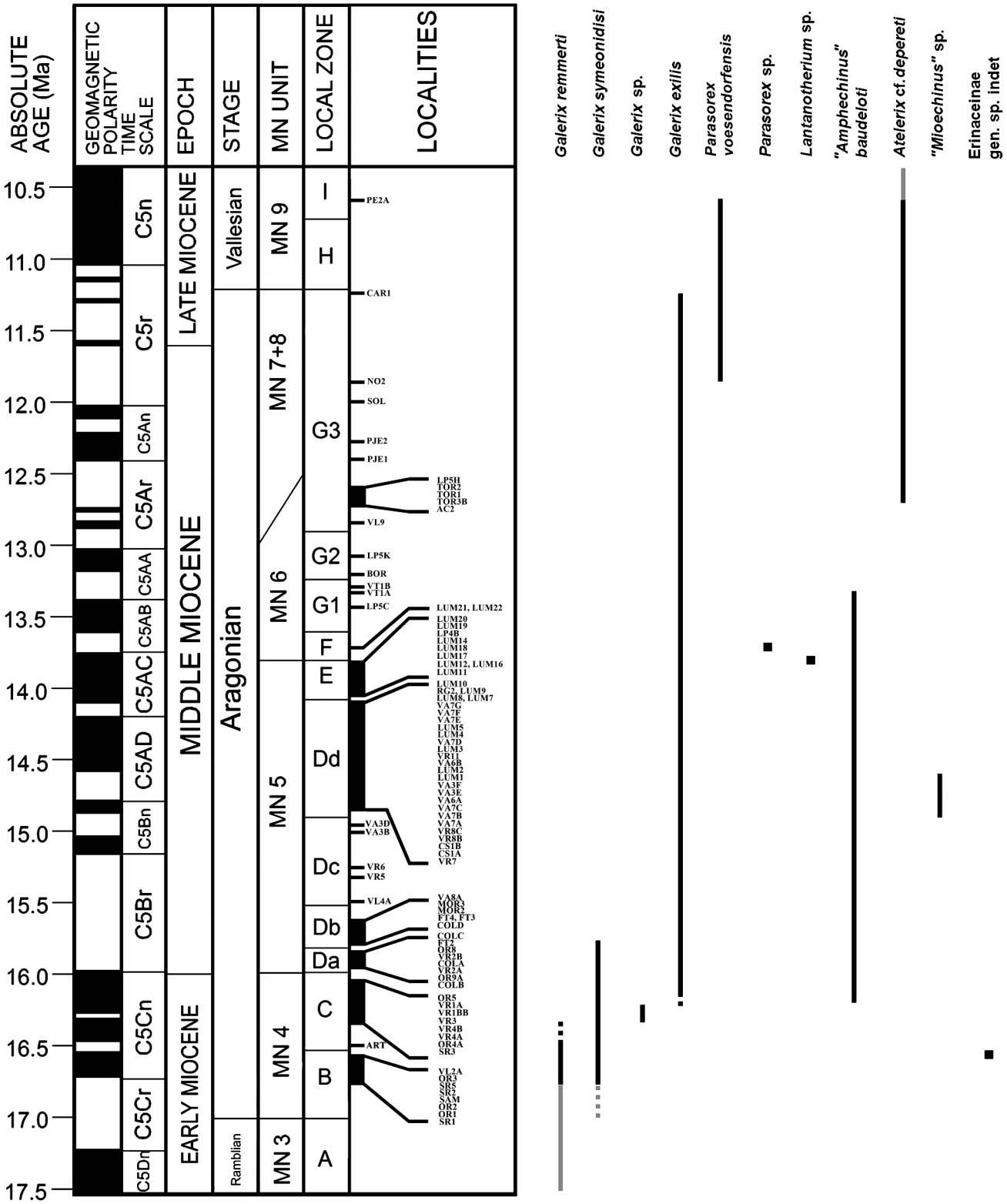

Figure 2. Temporal correlation of studied localities from the Daroca-Calamocha area, showing the distribution of identified erinaceids (Modified after Van den Hoek Ostende et al., 2016). Corresponding ages are after Daams, Van der Meulen, Álvarez-Sierra, et al. (1999) and Van Dam et al. (2014) and follow the recent time scale of Raffi et al. (2020). *Galerix* cf. *exilis*, *G.* cf. *remmerti*, and *G.* cf. *symeonidisi* are represented by dashed lines. Grey lines represent the upper Ramblian and Vallesian record of the studied species (based on Van Dam et al., 2020; Van den Hoek Ostende, 2003). Taxonomic verdicts for each assemblage is provided in Supplementary file S1.

Genus *Galerix* Pomel, 1848

Type species

Viverra exilis de Blainville, 1839

Other referred species

G. stehlini (Gaillard, 1929); *G. africana* Butler, 1956; *G. rutlandae* Munthe & West 1980; *G. symeonidisi* Doukas, 1986; *G. aurelianensis* Ziegler, 1990; *G. saratji* Van den Hoek Ostende, 1992; *G. uenayae* Van den Hoek Ostende, 1992; *G. iliensis* (Kordikova, 2000); *G. remmerti* Van den Hoek Ostende, 2003. The species names '*G.*' *ehiki* Kretzoi, 1954, '*G.*' *hipparionum* Kretzoi, 1954, '*G.*' *paraexilis* Gureev, 1979, and '*G.*' *tadzhikistanicus* Gureev, 1979 are all considered to be *nomina dubia* because of their unclear and extremely poorly described characteristics. According to Zijlstra and Flynn (2015), '*G.*' *ehiki* may correspond to a species of *Schizogalerix* Engesser, 1980, and '*G.*' *hipparionum* may correspond to a *Lantanotherium* species. The material mentioned by Gureev (1979) needs a complete description.

Remarks

Galerix species display a wide morphological and morphometric variability, because it is difficult or impossible to assign all dental elements to a particular species when more than one taxon occurs in the same locality. In the early Aragonian deposits of the Daroca-Calamocha area, the three identified species of *Galerix* have overlapping morphological and morphometric distributions. The indistinguishable elements, notably several morphologically conservative lower molars, are excluded from descriptions. The names G*alerix* cf. *remmerti*, *Galerix* cf. *symeonidisi*, and *Galerix* cf. *exilis* are used here to differentiate specimens that are closer to the variability of *G. remmerti*, *G. symeonidisi*, and *G. exilis*, respectively, but not sufficiently for a clear assignment.

Galerix remmerti Van den Hoek Ostende, 2003 and *Galerix* cf. *remmerti* Van den Hoek Ostende, 2003

Figures 3(A–H), 4, Table 2

Stratigraphic range. The type locality is Ramblar 1, Spain (Local Zone Z, MN2). *Galerix remmerti* is found from Local Zone Z to Local Zone C (latest MN 2 to early MN 4) in the Daroca-Calamocha area of Spain (Van den Hoek Ostende, 2003), and has been identified in the Vallès-Penedès Basin by Van den Hoek Ostende et al. (2020) in the MN 3 localities of Turó de les Forques, and Sant Andreu de la Barca 1 and 3 (Ramblian, Zone A). *Galerix remmerti* has also been documented in the MN3 French localities of Estrepouy (Hugueney & Bulot, 2011) and Beaulieu (see Klietmann et al., 2014).

Referred specimens

42 isolated teeth (11 P3, one P4, five M1, 11 M2, one M3, one p4, five m1, four m2 and three m3). Measurements are provided in Table 2. Additional data is provided in supplementary material (S1).

Localities

Zone B: San Roque 1, Olmo Redondo 1, San Marco 1, Villafeliche 2A.

Zone C: Artesilla.

Galerix cf. *remmerti* is identified in San Roque 3 (Zone C).

Description

The P3 is elongated and characterised by a reduced development of the lingual extension (Figures 3(A), 4(A)). The paracone has a circular base. The parastyle is distinct and isolated or consists of a thin anteroposterior ridge. The postparacrista is low and straight. It bends labially at the very end of the posterior ridge of the tooth. The lingual extension is narrow and bears a low, conical protocone. There is a thin ridge between the protocone and the parastyle. The P4 has a robust shape, with a quadrangular outline and a large lingual extension. The high paracone is connected to a rather short and transversely oriented postparacrista. From the base of the rounded paracone starts a low ridge connecting to the parastyle. The strong protocone is labially elongated; from it descends a thin ridge not reaching the parastyle. The low hypocone is connected to the base of the protocone by a straight crest.

The M1 (Figures 3(B), 4(C)) has a subrectangular outline. The metacone is connected to the paracone by a thin and direct ectoloph. The postmetacrista is curved and reaches a low metastyle. The high protocone is always connected to a robust and circular metaconule by a high crest. There is no postmetaconule crest. The premetaconule crest is weak. The postprotocrista connecting the protocone to the hypocone is blunt. The anterior cingulum is rather thick, while the posterior cingulum is narrower. As shown in Figure 3(B,C-D) and Figure 4(C,D-F), the M2 differs from the M1 by its smaller dimensions, the shorter postmetacrista, and the less posterolingual position of the hypocone. The ectoloph is always straight. The parastyle is usually connected to the paracone. The protoconule is not distinguishable, and the preprotoconule crest is separated from the paracone by a weak notch in one out of the three unworn specimens in which this character can be evaluated. The high protocone is always connected to the

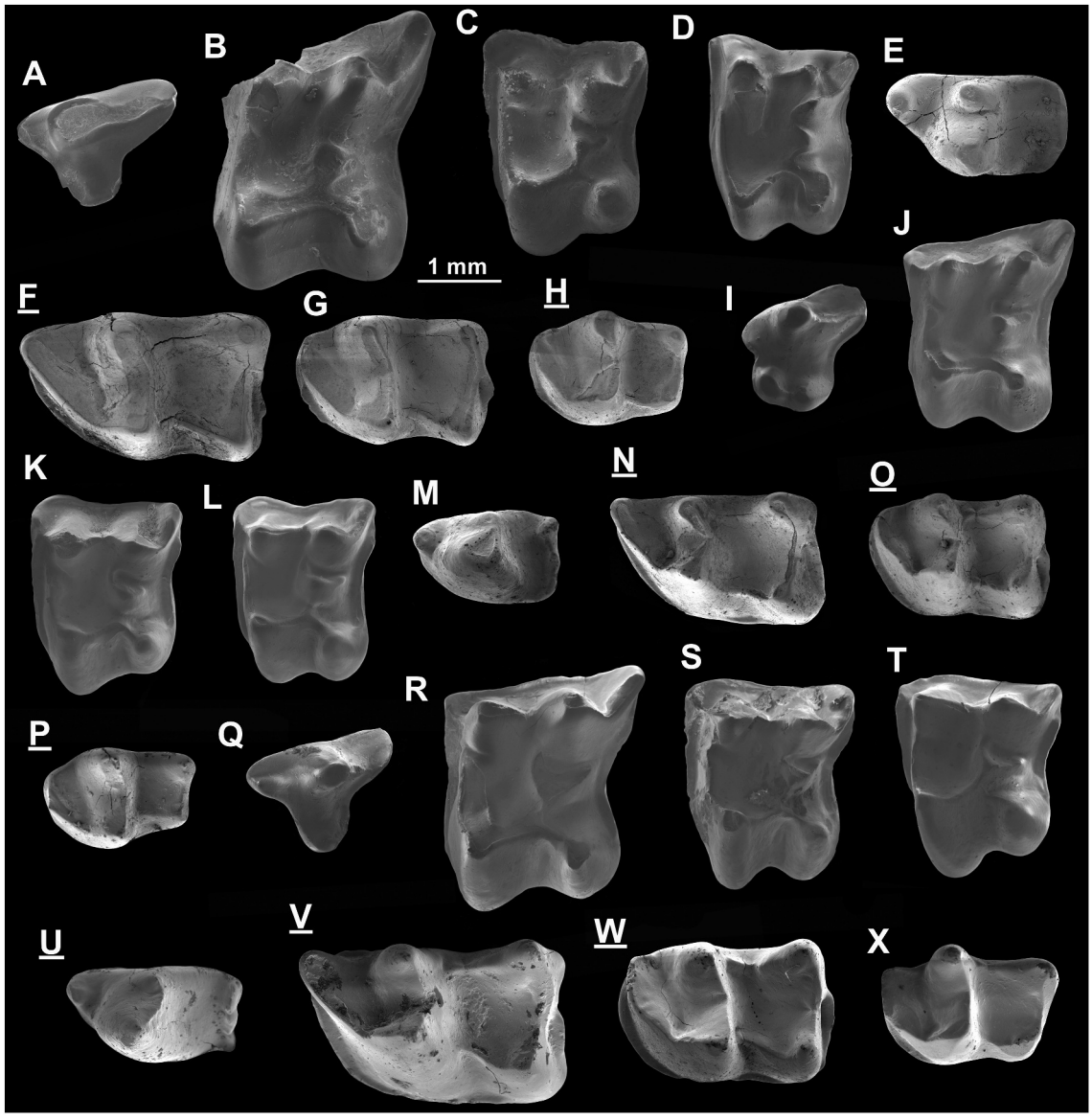

Figure 3. SEM pictures of *Galerix remmerti* (**A-H**), *Galerix symeonidisi* (**I-P**), and *Galerix exilis* (**Q-X**) from the Daroca-Calamocha area. (**A**) P3, ART, ART-111. (**B**) M1, ART, ART-121. (**C**) M2, VL2A, VL2A-1011. (**D**) M2, OR1, RGM410909. (**E**) p4, ART, ART-11. (**F**) m1, ART, ART-22. (**G**) m2, ART, ART-34. (**H**) m3, ART, ART-45. (**I**) P3, SR1, RGM410183. (**J**) M1, OR1, RGM410906. (**K**) M2, SR1, RGM410192. (**L**) M2, SAM, SAM-41. (**M**) p4, SAM, SAM-10. (**N**) m1, ART, ART-23. (**O**) m2, ART, ART-44. (**P**) m3, ART, ART-50. (**Q**) P3, VLF9, RGM334855. (**R**) M1, VLF9, RGM334847. (**S**) M2, LP5C, LP5C-B6. (**T**) M2, BOR, RGM334917. (**U**) p4, TOR1, RGM335054. (**V**) m1, SOL, RGM334663. (**W**) m2, TOR1, RGM335051. (**X**) m3, TOR1, RGM335062.

metaconule (high connection in four specimens, low in one). The postmetaconule crest is absent in four specimens and present in three. One M3 from San Roque 1 stands out by its large size and its broad and triangular shape (Figure 4(G)).

The p4 (Figures 3(E), 4(H)) has a narrow anterior part. The paraconid is conical and isolated from the high and bulbous protoconid; there is no paralophid. The metaconid is well developed and not connected to the protoconid by a crest. The talonid has a postcingulid and a thin central ridge. The lower molars are (Figure 3 (F–H)) very conservative in shape and do not differ fundamentally from those of *Galerix exilis* (below).

Remarks

Distinguishing *G. remmerti* from *G. exilis* is an arduous task. First, both species are almost identical in size. This is especially true since we noticed a slightly smaller size in our material of *G. remmerti* compared to the ones from the Ramblian assemblages (Van den Hoek Ostende, 2003). Morphologically, the two species differ mostly by the protocone-metaconule connection on the upper molars, which

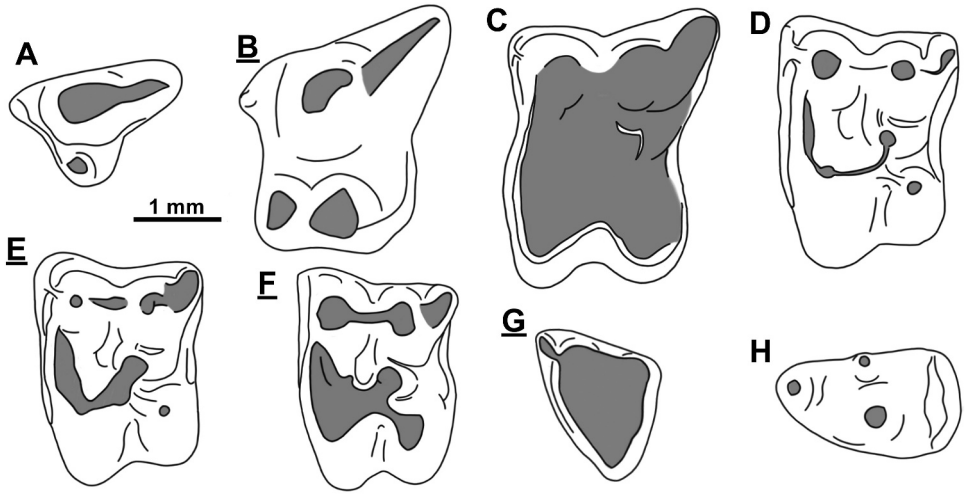

Figure 4. Drawings of *Galerix remmerti* from the Daroca-Calamocha area. (**A**) P3, ART, ART111. (**B**) P4, ART, ART-88. (**C**) M1, SR1, RGM213002. (**D**) M2, VL2A, VL2A-1011. (**E**) M2, SR1, SR1-001. (**F**) M2, OR1, OR1-909. (**G**) M3, SR1, RGM410195. (**H**) p4, ART, ART-I11.

Table 2. Measurements (in mm) of *Galerix remmerti* from Daroca-Calamocha, Spain.

	P3		P4			M1			M2		
	L	W	L	W1	W2	L	W1	W2	L	W1	W2
N	7	7	1	1	1	1	1	4	8	10	9
Min	1.63	1.16						2.79	1.86	2.42	2.00
Max	1.97	1.55						3.18	2.19	2.84	2.41
Mean	1.82	1.35	2.51	2.15	2.64	2.41	2.97	3.02	1.99	2.62	2.26
	M3			p4		m1			m2		
	L1	L2	W	L	W	L	W1	W2	L	W1	W2
N	1	1	1	1	1	4	4	4	4	4	4
Min						2.65	1.48	1.63	2.23	1.43	1.40
Max						2.92	1.72	1.82	2.30	1.57	1.47
Mean	1.50	1.37	1.85	2.02	1.25	2.78	1.67	1.74	2.26	1.49	1.43
	m3										
	L	W1	W2								
N	3	3	3								
Min	1.73	1.03	0.77								
Max	1.74	1.14	0.96								
Mean	1.73	1.10	0.86								

is always present in *G. remmerti*, whereas it is variably present in *G. exilis*. This crest is absent in *G. symeonidisi*, co-occurring in the Local Zones B and C, further hampering the identification of *G. exilis*.

Additional differences have been found between the two species. Based on the Ramblian material and the rather large specimens from Local Zone B, *Galerix remmerti* shows a reduction of the posterior width of M2 compared to *G. exilis*: In Local Zone B, the W1/W2 ratio is found to range between 1.13 and 1.21 ($n = 5$) in *G. remmerti*, whereas in Local Zones Da-Dc this ratio is found to range between 0.99 and 1.12 ($n = 18$) in *G. exilis*. Moreover, several assemblages from Local Zones B and Ca (San Roque 1, Olmo Redondo 1, San Marcos, Artesilla, San Roque 3) yielded large specimens with no postmetaconule crest. This curious feature was previously only attested in *Galerix africana* (Butler, 1956, 1984, originally described as *G. africanus*, although the term *Galerix* is feminine) and in *G. aurelianensis*, the latter being a larger geographical variant of *G. remmerti* (Klietmann et al., 2014). It is now clear that this feature was also present at the end of the biostratigraphic range of *G. remmerti*. It is worth noting that the lack of postmetaconule also sometimes occurs in *G. exilis*, although the oldest specimen displaying such a feature is found in Valdemoros 3F (14.52 Ma), almost 2 my after the extinction of *G. remmerti*.

In the relatively large sample from Artesilla (16.51 Ma), the upper molars always have a protocone-metaconule connection, and several specimens show no postmetaconule crest. The W1/W2 ratio of M2 (1.12–1.15; $n = 3$) also fits that of *G. remmerti*. The large *Galerix* from Artesilla is therefore attributed to *G. remmerti* without doubt. The last upper molar with no postmetaconule crest is attested in the small sample from San Roque 3 (16.35 Ma), which is consequently identified as *Galerix* cf. *remmerti* and represents

the youngest occurrence of the species. Therefore, *Galerix remmerti* only reaches the subzone Ca.

Klietmann et al. (2014) suggested that the lack of a postmetaconule crest has an ecological signal and may indicate a tendency towards carnivory. In our opinion, this indicates a tendency towards durophagy, that is to say, in the case of *G. remmerti*, a slightly more omnivorous or hard-bodied invertivorous diet. The wide dental variability of *G. remmerti* in Artesilla is considered to represent morphological experimentation, which later led to the emergence of *G. exilis* during the interval 16.35–16.15 Ma. This change may relate to the arrival of *G. symeonidisi* in the basin (see below). The development of a more robust morphotype in *Galerix remmerti* was apparently unsuccessful.

Galerix symeonidisi Doukas, 1986, and ***Galerix* cf. *symeonidisi*** Doukas, 1986

Figures 3(I–P), 5, Table 3

Stratigraphic range

The type locality is Aliveri, Greece (MN4). *Galerix symeonidisi* is recorded in MN4 and MN5 of western (Van den Hoek Ostende, 2003; Van den Hoek Ostende & Doukas, 2003; Van den Hoek Ostende et al., 2020), central (Bonilla-Salomón et al., 2024; Daxner-Höck, 1998; Prieto & Rummel, 2009; Ziegler, 2005; Ziegler & Fahlbusch, 1986) and southeastern Europe (Doukas, 1986; Marković & Milivojević, 2010), and perhaps in North Caucasus (Pickford et al., 2000). The identification of *Galerix symeonidisi* in Anatolia as proposed by Sen et al. (1998) has been ruled out by Van den Hoek Ostende and Doukas (2003). Ziegler (1994) suggested the presence of *Galerix symeonidisi* in MN3 based on two M3 from Wintershof-West (Germany).

Referred specimens

One fragment of a mandible with p3-m1, and 168 isolated teeth (43 P3, four P4, 34 M1, 53 M2, seven M3, four p4, seven m1, nine m2 and seven m3). Measurements are provided in Table 3. Raw data are provided as Supplementary material (S1).

Localities

Zone B: San Roque 1, Olmo Redondo 1, Olmo Redondo 2, San Marco 1, San Roque 2, San Roque 5, Olmo Redondo 3.

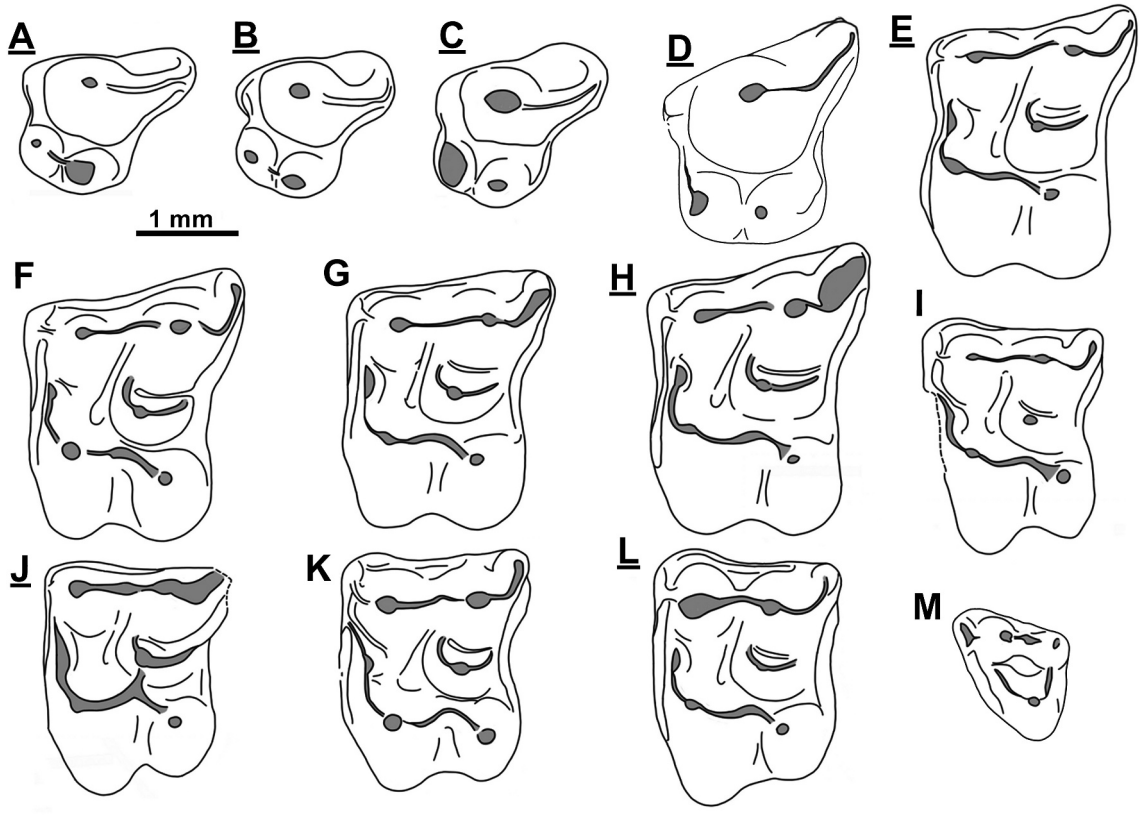

Figure 5. Drawings of *Galerix symeonidisi* (**A-C**, **E-M**) and *Galerix* cf. *symeonidisi* (**D**) from the Daroca-Calamocha area. (**A**) P3, OR3, RGM410165. (**B**) P3, SR1, RGM410183. (**C**) P3, OR2, RGM410975. (**D**) P4, ART, ART-83. (**E**) M1, ART, ART-129. (**F**) M1, OR1, RGM410906 (**G**) M1, ART, ART-125. (**H**) M1, SR1, RGM410187. (**I**) M2, SR1, RGM410191. (**J**) M2, OR2, RGM410979. (**K**) M2, SAM, SAM-42. (**L**) M2, SR1, RGM410192. (**M**) M3, SR3, SR3-16.

Zone C: Villafeliche 2A, Artesilla, San Roque 3, Olmo Redondo 4A, Vargas 4A, Vargas 4BB, Vargas 1A, Vargas 3, Olmo Redondo 5, Olmo Redondo 8.

Zone Da: Vargas 2A, Vargas 2B, Fuente Sierra 2, La Col C.

Zone Db: La Col D.

The material from Vargas 4B (Zone C) and Fuente Sierra 3 (Zone Da) is classified as *Galerix* cf. *symeonidisi*.

Description

The P3 has a compact shape (Figures 3(I), 5(A–C)). The parastyle is detached from the paracone. The postparacrista is robust and short; it turns labially at the end of the tooth and joins the labial cingulum. The lingual part has two well-developed cusps. The protocone is sometimes connected to the parastyle by a thin ridge. The hypocone is a simple, anteriorly elongated cusp lower than the protocone. A thin crest is sometimes present between the two lingual cusps (2 specimens out of 17). The P4 has a high conical paracone and a reduced parastyle area. The postparacrista has a tiny carnassial notch. The protocone is higher than the hypocone and is sometimes connected to the parastyle when present. A thin crest is found between the two lingual cusps. The posterior cingulum is well developed.

The M1 is subrectangular (Figures 3(J)). The paracone and metacone are usually connected by a curved ectoloph (concave, $n = 10$; straight, $n = 1$). The postmetacrista creates a variably strong posterolabial emargination in occlusal view. The parastyle is isolated in two specimens and connected to the paracone in eleven specimens. Usually, the preprotoconule crest bends anteriorly before reaching the base of the paracone (in 13 out of 14 specimens). The protoconule is absent ($n = 2$), distinguishable ($n = 4$), or strong ($n = 7$). The strong protocone is always connected to the hypocone. There is no protocone-metaconule connection ($n = 15$) or a low connection ($n = 2$). The metaconule is connected to the posterior cingulum in one out of 14 specimens. Anterior, posterior, and labial cingula are always present. As shown in Figure 3(J,K–L) and Figure 5(E–F, H–L), the M2 has a more anteroposteriorly compressed outline than the M1. The M2 also differs by the less curved ectoloph (concave, $n = 4$; straight, $n = 15$); the more variable preprotoconule crest which sometimes reaches the anterior cingulum (Figure 5(H,J)); the less developed protoconule (absent, $n = 7$; distinguishable, $n = 6$; strong, $n = 4$); the more frequent protocone-metaconule connection (absent, $n = 16$; low, $n = 3$; high, $n = 6$) and postmetaconule-postcingulum connection (absent, $n = 1$; short, $n = 15$; connected to the cingulum, $n = 4$). The parastyle is similar to that in M1, being connected to the paracone in 14 out of 15 specimens. The ectoloph is strong ($n = 9$) or weak ($n = 10$). The preprotoconule crest is incomplete ($n = 1$) but is generally complete and short ($n = 17$). In four out of 28 specimens, this crest joins the anterior cingulum. As usual for M2, the hypocone is reduced. The cingula are well developed. The M3 is subtriangular (Figure 5(M)). The metacone and paracone are connected by a low crest. The paracone is high and connected to a rather robust parastyle. The protocone is curved and close to the two other cusps. The preprotocrista is separated from the paracone by a notch, while the postprotocrista is fully connected to the metacone. The anterior cingulum is strong.

The mandible from Villafeliche 2A (1003) displays a slightly curved body, a broken and narrow trigonid of m1, an elongated two-rooted p4, and a small two-rooted p3. The anterior alveoli are interpreted as belonging to

Table 3. Measurements (in mm) of *Galerix symeonidisi* from Daroca-Calamocha, Spain.

	P3			P4			M1			M2		
	L	W1	W2	L	W1	W2	L	W1	W2	L	W1	W2
N	34	35	32	3	3	3	15	22	16	28	34	30
Min	1.37	1.10	1.25	2.11	1.79	2.12	2.03	2.24	2.40	1.64	2.13	1.90
Max	1.96	1.61	1.88	2.28	2.07	2.31	2.38	2.66	2.87	2.05	2.60	2.45
Mean	1.68	1.32	1.54	2.19	1.93	2.21	2.20	2.42	2.97	1.83	2.36	2.16
	M3			p3		p4		m1				
	L1	L2	W	L	W	L	W	L	W1	W2		
N	7	7	7	1	1	5	5	7	7	7		
Min	1.16	1.03	1.32			1.64	0.98	2.17	1.26	1.32		
Max	1.37	1.25	1.67			1.71	1.12	2.46	1.43	1.56		
Mean	1.29	1.15	1.45	1.10	0.67	1.66	1.06	2.34	1.34	1.45		
	m2			m3								
	L	W1	W2	L	W1	W2						
N	8	8	9	7	7	6						
Min	1.91	1.27	1.24	1.46	0.98	0.77						
Max	2.18	1.51	1.50	1.74	1.10	0.91						
Mean	2.03	1.34	1.36	1.64	1.04	0.84						

a two-rooted p2, significantly longer than the p3, and a one-rooted p1. The mandibular foramen is located below the anterior alveole of the p3.

The p3 is a narrow and simple element. The main cuspid is in a central position, and a thin ridge is visible on its anterior flank. The talon is represented by a short posterolingual cingulum. The p4 has an isolated paraconid with a rounded tip. The protoconid is relatively stout, with a distinct metaconid attached to it. The talon is broad. The posterior cingulum is higher in its lingual region. The trigonid of the m1 is narrower and usually slightly shorter than the talonid. The paraconid is distinguishable from the paralophid, and its height reached that of the entoconid. The metaconid is conical and is positioned in a more anterior position than the protoconid. The talonid bears a strong, labiolingually compressed entoconid. The hypoconid is low. The postcristid is strongly curved. Anterior and posterior cingula are present. The m2 is roughly similar to m1, but the trigonid is more compressed antero-posteriorly; the paraconid is indistinct; the postcristid is straight, and the postcingulid is present but rather weak. The anterior cingulid is broad. The m3 has a rounded trigonid and a rectangular, slightly longer talonid. The paralophid is low and curved. The trigonid basin is relatively open compared to m1 and m2. The conical metaconid is the highest cuspid of the molar. The talonid bears a slightly compressed and high entoconid and a much weaker hypoconid. The entoconid is sometimes in a more posterior position than the hypoconid.

Galerix exilis (de Blainville, 1839) and ***Galerix* cf. *exilis*** (de Blainville, 1839)

Figures 3(Q–X), 6, Table 4

Stratigraphic range

The type locality is Sansan, France (MN6). *Galerix exilis* is an extremely common member of Middle Miocene European assemblages (e.g. Ziegler, 1983), the origin of which can be tracked to early MN4 (see Van den Hoek Ostende & Doukas, 2003; this paper). Its last occurrences are from the German locality of Hammerschmiede (11.62 Ma; Lechner & Böhme, 2025; as *Galerix* cf. *exilis*, see Prieto et al., 2011) and the Local Zone G3 in the Daroca-Calamocha area (11.33 Ma; De Jong, 1988; this work).

Referred specimens

One mandible with p2-m2, one mandible with p2-p4, one mandible with p2-p3, and 1194 isolated teeth (one C, ten P1, 19 P2, 121 P3, ten dP3, 60 P4, three dP4, 121 M1, 271 M2, 135 M3, one i1, two i3, five c, three p1, 19 p2, 36 p3, 12 dp3, 74 p4, 17 dp4, 75 m1, 117 m2, 82 m3). Measurements are provided in Table 4. Raw data are provided as Supplementary material (S1).

Localities

Zone C: Vargas 1A, Olmo Redondo 5, Olmo Redondo 8, Vargas 2A.

Zone Da: Vargas 2B, Olmo Redondo 9, Fuente Sierra 2, La Col B, La Col C.

Zone Db: La Col D, Fuente Sierra 4, Moratilla 2.

Zone Dc: Villafeliche 4A, Vargas 5, Valdemoros 3B, Valdemoros 3D.

Zone Dd: Vargas 7, Moratilla 4, Caseton 1A, Caseton 2B, Vargas 8B, Vargas 8C, Valdemoros 7A, Valdemoros 7B, Valdemoros 7C, Valdemoros 6A, Valdemoros 3E, Las Umbrias 1, Las Umbrias 2, Valdemoros 6B, Las Umbrias 3, Valdemoros 7D, Las Umbrias 4, Las Umbrias 5, Valdemoros 7E, Valdemoros 7F, Valdemoros 7 G, Las Umbrias 7, Las Umbrias 8, Las Umbrias 9, Regajo 2, Las Umbrias 10.

Zone E: Las Umbrias 11, Las Umbrias 16, Las Umbrias 12, Las Umbrias 17, Las Umbrias 18, Las Umbrias 14, Las Planas 4B, Las Umbrias 19, Las Umbrias 20.

Zone F: Las Umbrias 21, Las Umbrias 22.

Zone G1: Las Planas 5C, Valalto 1A, Valalto 1B.

Zone G2: Borjas, Las Planas 5K.

Zone G3: Villafeliche 9, Alcocer 2, Toril 3B, Toril 1, Toril 2, Solera, Nombrevilla 2, Carrilanga 1.

Galerix cf. *exilis* is identified in Vargas 4BB (Zone C), La Col A (Zone Da) and Fuente Sierra 3 (Zone Da).

Description

The elongated two-rooted upper canine bears one cusp that is stretched posteriorly. There are neither crests nor cingula. The P1 is a small, elliptical, and two-rooted tooth with a main cusp in central position (Figure 6(A)). The roots are straight or slightly convergent. There is sometimes a posterior cingulum. The P2 is larger than the P1 and has a more robust central cusp. The posterior cingulum is always present and sometimes bears a very low cuspule, as shown in Figure 6(B). The anterior cingulum is inconspicuous. The roots are often bent slightly backwards. The P3 is slightly molarized and bears a strong, conical paracone. There is a straight anterior extension that does not bear a clear parastyle. The lingual part is narrow, with the protocone only represented by a ridge-like elevation. The lingual extension is variable in length (Figure 6(E) vs Figure 6(F)). In eight out of 89 specimens, the P3 bears a minute hypocone (Figure 6(E)). The protocone of the dP3 is a robust and conical cusp. The postprotocrista turns labially at the end of the tooth and joins a posterior cingular crest. The metacone is often distinguishable as an elevation in

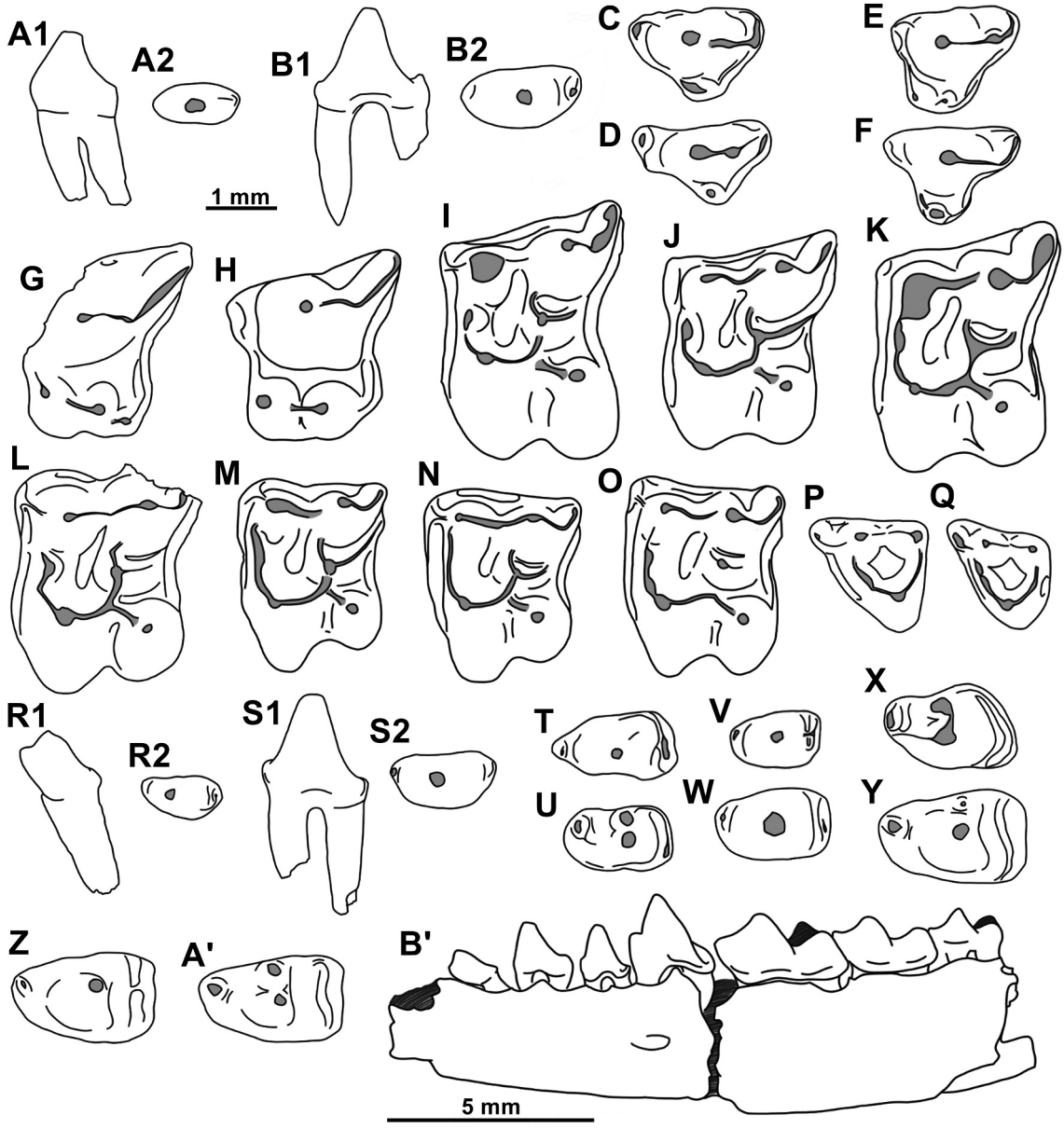

Figure 6. Drawings of *Galerix exilis* from the Daroca-Calamocha area. (**A**) P1, PJE2, PJE2A1, in labial (**A1**) and occlusal (**A2**) views. (**B**) P2, VR7, VR7-B2, in labial (**B1**) and occlusal (**B2**) views. (**C**) dP3, CS1A, RGM410334. (**D**) dP3, VA7B, VA7B-B4. (**E**) P3, CS1A, RGM410336. (**F**) P3, VL9, RGM334855. (**G**) dP4, TOR3B, TOR3B-B4. (**H**) P4, LUM8, LUM8-B3. (**I**) M1, SOL, RGM334641. (**J**) M1, NO2, NO2-A47. (**K**) M1, BOR, RGM334911. (**L**) M1, LP4B, LP4B-C1. (**M**) M2, SOL, RGM334643. (**N**) M2, BOR, RGM334917. (**O**) M2, NO2, NO2-B53. (**P**) M3, SOL, RGM334616. (**Q**) M3, CS1A, RGM410340. (**R**) p1, TOR1, RGM433629, in labial (**R1**) and occlusal (**R2**) views. (**S**) p2, SOL, RGM334583, in labial (**S1**) and occlusal (**S2**) views. (**T**) dp3, VR7, VR7-A3. (**U**) dp3, VR7, VR7-B3. (**V**) p3, VR8B, VR8B-B1. (**W**) p3, LUM22, LUM22-A1. (**X**) dp4, CS2B, RGM410380. (**Y**) p4, NO2, NO2-C7. (**Z**) p4, NO2, NO2-C8. (**A'**) p4, NO2, NO2-B10. (**B'**) Mandible with p1-m3, NO2, NO2-E1. Scales: 1 mm (**A-A'**), 5 mm (**B'**).

the middle of the crest (Figure 6(C)). The P4 bears a high paracone. The parastyle is usually distinct from the anterolabial corner. There is no connection between the parastyle and the paracone. The postparacrista is thick and shows a carnassial notch. A thin ridge sometimes connects the protocone to the anterolabial margin. The hypocone is lower than, but as strong as the protocone. The two cusps are sometimes connected by a low loph. The posthypocrista is variably developed. The DP4 has an enlarged lingual part, which often allows the development of a third lingual cusp posterior to the hypocone (Figure 6(G)). The parastyle region is also enlarged in one out of three specimens.

The shape of the subrectangular M1 is variable (Figure 6(I-L)). The paracone is sometimes connected to the parastyle by a low crest. The parastyle is usually connected to the paracone ($n = 52$) but is sometimes isolated ($n = 4$) or absent ($n = 3$). The paracone is

Table 4. Measurements (in mm) of *Galerix exilis* from Daroca-Calamocha, Spain.

	C		P1		P2		DP3		P3			DP4		
	L	W	L	W	L	W	L	W1	L	W1	W2	W1	W2	
N	1	1	8	8	11	12	6	2	89	87	4	1	2	
Min			1.17	0.53	1.38	0.71	1.77	1.29	1.50	1.06	1.51		2.57	
Max			1.39	0.79	1.72	0.90	2.06	1.49	2.25	1.84	1.57		2.70	
Mean	1.55	1.00	1.21	0.61	1.59	0.82	1.93	1.39	1.84	1.45	1.55	2.32	2.64	
	P4			M1			M2			M3			i1	
	L	W1	W2	L	W1	W2	L	W1	W2	L1	L2	W	L	W
N	26	30	31	52	77	58	143	165	146	102	110	101	1	1
Min	2.21	1.99	2.15	2.14	2.35	2.62	1.82	2.26	2.12	1.24	1.03	1.39		
Max	2.78	2.52	3.06	2.75	3.25	3.56	2.31	3.02	2.79	1.74	1.47	2.06		
Mean	2.57	2.32	2.65	2.49	2.80	3.10	2.04	2.68	2.45	1.51	1.30	1.75	0.80	1.15
	i3		c	p1		p2		Dp3		p3		Dp4		
	L	W	L	L	W	L	W	L	W	L	W	L	W	
N	1	1	5	3	2	22	19	12	12	37	36	10	13	
Min			0.85	1.03	0.59	1.27	0.67	1.51	0.75	1.10	0.67	1.70	1.02	
Max			1.06	1.31	0.67	1.72	0.98	1.90	0.95	1.71	0.98	2.18	1.36	
Mean	0.78	0.94	0.97	1.16	0.63	1.46	0.81	1.65	0.86	1.43	0.86	1.94	1.19	
	p4		m1			m2			m3					
	L	W	L	W1	W2	L	W1	W2	L	W1	W2			
N	57	57	34	43	45	83	88	87	65	73	66			
Min	1.75	1.13	2.65	1.42	1.52	2.15	1.29	1.23	1.56	1.00	0.83			
Max	2.26	1.45	3.28	1.88	1.96	2.68	1.76	1.90	2.11	1.35	1.22			
Mean	2.03	1.25	2.90	1.66	1.77	2.41	1.56	1.57	1.92	1.18	1.01			

connected to the protocone by a robust loph. The protoconule is often present (40 out of 54 specimens). Only a partial notch is usually visible between the preprotoconule and the paracone. The protocone is connected to the metaconule ($n = 68$) or not ($n = 22$). The hypocone is always connected to the protocone. The metaconule is crescent-shaped. The premetaconule crest is always connected to the base of the metacone. The postmetaconule crest is usually short ($n = 75$), sometimes connected to the postcingulum ($n = 7$), and sometimes lacking ($n = 7$). A two-segmented, robust postmetacrista descends from the steady metacone. The ectoloph is usually straight ($n = 54$) and sometimes concave ($n = 7$). Anterior and posterior cingula are well-developed, whereas the lingual cingulum is often discontinuous. The postmetaconule in the M2 is short ($n = 188$), connected to the postcingulum ($n = 18$) or absent ($n = 6$); the ectoloph is straight ($n = 145$) or concave ($n = 12$); the protocone-metaconule connection is usually present ($n = 158$) but can be absent ($n = 47$). The M2 differs also by its smaller size, the fully convex anterior border, the reduced hypocone, and the shorter and more curved metastyle (Figures 3(S-T), 6(M-O)). The M3 is a small three-cuspid tooth with a subtriangular outline. The paracone is the largest cusp and is often connected to the variably strong parastyle. The protocone is higher and more bent labially than the metacone. The trigon basin is completely closed. The ectoloph is a relatively straight and short crest, whereas the rather high preprotocrista and low postprotocrista are longer and curved. A thickening of the preprotocrista represents the paraconule. The anterior cingulum is usually broad while the posterior cingulum is narrow or absent.

In labial view, the lower outline of horizontal ramus of the mandible is slightly curved from the labial view (Figure 6(B')). The ramus is thickest under the m1. The decrease in height is more marked anterior of p2. The mandibular symphysis starts under the anterior root of p2. The mandibular foramen is situated under the anterior root of p4.

The symmetric i1 has a straight and anteroposteriorly compressed root. The main crest consists of a slightly convex wall, which has a rectangular occlusal outline. A thin posterior cingulid is present. The i3 differs from the i1 in its smaller size and asymmetrical shape, with the wall of the main cusp slightly transversely bent. The lower canine has a bent cusp and a relatively strong base. A shoulder is often visible at the posterior base of the tooth. The p1 is a one-rooted tooth and less elongated than the p2 (Figure 6(R) vs Figure 6(S)). The protoconid is rather bulbous, curved and in a rather anterior position. There is often a distinguishable anterior bulge in front of the protoconid, and a posterior slope which usually bears a low bulge or a cingulid. Some specimens have an enlarged root (Figure 6(R1)). The p2 has an oval protoconid in a central position. As in the p1, there is a small anterior bulge. The posterior slope is longer than the anterior one and ends as a cingulid. There are two straight roots. The p3 is usually smaller than the p2 (Figure 6(S) vs Figure 6(V-W)) but is more complex: the outline is more subtriangular; the protoconid is bulbous; the anterior cuspule is more distinct; the

talon usually has a thin cingular crest. In some rare specimens, a swelling (metaconid) on the lingual side of the protoconid is visible. The dp3 is a more triangular and elongated two-rooted tooth. The protoconid is gracile and pointed. The paraconid is well developed and almost always isolated. The metaconid is lacking in most specimens (Figure 6(T)) but can be prominent (Figure 6(U)). The talonid is short, more developed than p3, but not oblique as in dp4. The posterior cingulum sometimes bears a pointed cuspule. The p4 is much larger than the p3 and has a large protoconid. The paraconid is isolated and conical. The metaconid usually consists of a small cusp attached to the protoconid (Figure 6(Y)). It is sometimes stronger (Figure 6(A')) or absent (Figure 6(Z)). The talonid has a thin postcingulid, sometimes connected to the lingual border of the metaconid. The morphological variability of dp4 is high. The conical or blade-like protoconid is connected to the paraconid by a crest. The metaconid is usually strong but is sometimes absent. The talon is narrow and always shows an oblique posterior crest.

On m1, the trigonid is as long as the talonid. The protoconid and metaconid are similar in height. The conical metaconid is in a slightly more anterior position than the protoconid. The paralophid is low and angular. The paraconid can be steady or slightly procumbent. The talonid has a rectangular outline. The entoconid is higher than the hypoconid. The two cusps are connected by a low postcristid. The oblique cristid is short, straight, and lingually oriented. The broad anterior cingulid is usually not connected to the labial cingulid. The posterior cingulid is usually short but is sometimes connected to the postcristid or the entoconid. The m2 differs from the m1 by the more anteroposteriorly compressed trigonid, the more curved paralophid, a better closed trigonid basin, and the more often reduced postcingulid. On the small m3, the trigonid and talonid are of similar length, but the talonid is narrower. The conical metaconid is the highest cusp of the tooth. The paralophid descends from the protoconid as a curved crest and reaches the anterolingual border perpendicular to the length direction of the tooth. The hypoconid is weaker than in m2, and the entoconid is in a more posterior position. The anterior cingulid is always present, but the labial one can be absent. A short postcingulid can be present in some cases.

Remarks

The material from Vargas 4BB (16.15 Ma) is attributed to *G.* cf. *exilis* based on the short postmetaconule crest and the rather reduced anterior width of the incomplete M2. *Galerix exilis* is first clearly identified from Vargas 1A (Local Zone C, 16.14 Ma) based on the low W1/W2 ratio on M2 (1.09–1.15; $n = 3$). From then onwards, *G. exilis* became frequent and abundant within the Aragonian insectivore community, with a last occurrence in Carrilanga 1 (Zone G3, 11.33 Ma). The species shows a huge morphological and morphometric variability. The anagenetic evolution of this taxon in the Daroca-Calamocha area requires further analysis and will be discussed elsewhere.

Galerix sp.

Referred specimens

Four isolated teeth: one P3 (Vargas 4B, D: W = 1.49), one M1 (Olmo Redondo 4A, I5: L = 2.34, W1 = 2.71, W2 = 2.97), one broken M2 (Vargas 4B, B3), one broken M3 (Vargas 4A, B4). Additional data are provided as Supplementary material (S1).

Localities

Zone C: Olmo Redondo 4, Vargas 4A, Vargas 4B

Description

The few specimens here display the conservative morphology of *Galerix exilis* and *Galerix remmerti*. As there are no morphological characteristics that allow one of the two species to be identified, a description of this material is considered unnecessary.

Remarks

Following the disappearance of *G. remmerti*, the emergence of *Galerix exilis* is attested in the Vargas section, from Vargas 4BB (16.15 Ma). A few, rather large specimens are still found in Olmo Redondo 4 (16.32 Ma), Vargas 4A (16.18 Ma), and Vargas 4B (16.16 Ma). This material cannot be distinguished from *G. remmerti* and *G. exilis* and may represent transitional forms. These four elements are therefore attributed to *Galerix* sp.

Genus ***Parasorex*** von Meyer, 1865

Type species.
Parasorex socialis von Meyer, 1865

Other referred species

P. voesendorfensis (Rabeder, 1973); *P. depereti* (Crochet, 1986); *P. ibericus* (Mein & Martin-Suárez, 1993); *P. pristinus* (Ziegler, 2003); *P. kostakii* (Doukas & Van den Hoek Ostende, 2006).

Parasorex sp.

Figures 7(A), 8(A)

Referred specimens.

One M1 (LUM21C-A1: L = 2.70, W1 = 3.20, W2 = 3.49).

Localities

Zone F: Las Umbrias 21.

Description.

The M1 has a subrectangular outline, with a slight transversal elongation. The parastyle is connected to the base of the paracone. The protoconule is clearly distinct from the preprotocrista. A notch is present between the protoconule and the paracone. The protocone is connected to the hypocone by a high and strongly curved loph; a thinner crest connects the metaconule to this loph. The premetaconule crest is short and high. The postmetaconule crest joins the posterior cingulum. The junction between these two structures is rather low. The metacone is stronger than the paracone. The postmetacrista is two-segmented and elongated. The ectoloph is thin and curved. Anterior, posterior, and labial cingula are well developed.

Remarks.

The M1 from Las Umbrias 21 corresponds to a rather advanced MN6 galericine and shows notable similarities with the younger *Parasorex socialis*. It is also found in the upper variability of *P. socialis* from Petersbuch fissures (Ziegler, 2005). The protocone-metaconule connection on M1, usually associated with *Galerix* species,

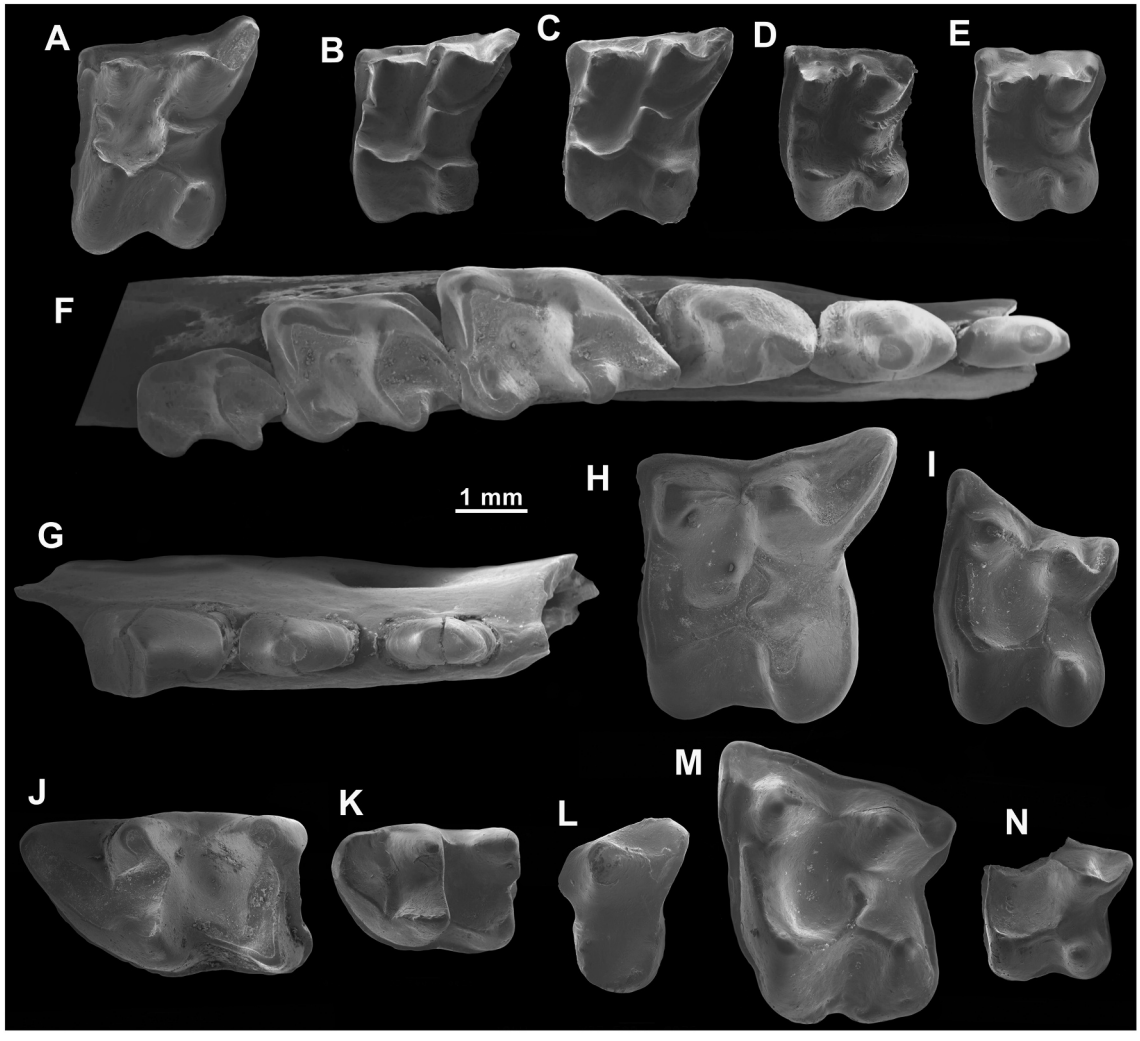

Figure 7. SEM pictures of *Parasorex* sp. (**A**), *Parasorex voesendorfensis* (**B-F**), *Lantanotherium* sp. (**G**), '*Amphechinus*' *baudeloti* (**H-K**), *Atelerix* cf. *depereti* (**L-M**), and '*Mioechinus*' sp. (**N**) from the Daroca-Calamocha area. (**A**) M1, LUM21, LUM21-C1. (**B**) M1, CAR1, RGM335277. (**C**) M1, CAR1, RGM335279. (**D**) M2, CAR1, RGM335218. (**E**) M2, CAR1, RGM335237. (**F**) p3-m3, CAR1, RGM 335,482. (**G**) p2-p4, LUM20, LUM20-A1. (**H**) M1, MOR2, MOR2-C4. (**I**) M2, MOR2, MOR2-C5. (**J**) m1, MOR2, MOR2-D2. (**K**) m2, MOR3, MOR3-B1. (**L**) P3, PE2A, RGM334439. (**M**) M2, TOR2, TOR2-A4. (**N**) M2, CA1A, RGM 213,184.

is rare in *Parasorex*: it is attested in *Parasorex* sp. from Sámsanoháza (Prieto et al., 2012), some rare *Parasorex socialis* from the Vallès-Penedès Basin (M. Furió, pers. obs.), and a vestigial crest is sometimes distinguishable in *P. ibericus* (Mein & Martin-Suárez, 1993). Considering the sample size, the absence of *P. socialis* in other assemblages from the Daroca-Calamocha area, and the chronological gap between Las Umbrias 21 (13.75 Ma) and the first late Aragonian occurrences of *P. socialis* in the Vallès-Penedès Basin (Van den Hoek Ostende et al., 2016), our material is classified as *Parasorex* sp.

Parasorex voesendorfensis (Rabeder, 1973)

Figures 7(B-F), 8(B-T), 9(A), Table 5

1988 - *Parasorex socialis*– De Jong, p. 257–269, plates 1–3.

Stratigraphic range. The type locality is Vösendorf, Austria (MN9). *Parasorex voesendorfensis* is known from the late Middle Miocene and Late Miocene (MN7/8, MN9) of western, central, and eastern Europe (Cailleux et al., 2023; Harzhauser et al., 2011; Hír et al., 2016, 2017; Kälin & Kempf, 2009; Prieto et al., 2010, 2014; Rabeder, 1973; Ziegler, 2000). Unpublished material indicates the presence of the species in Germany (J. P., pers. data), France (F.C., pers. data), and Turkey (LvdHO, pers. data).

Referred specimens. One mandible with p2-m3, one mandible with m1-m2, and 462 isolated teeth (three P1, 45 P3, 60 P4, 47 M1, 78 M2, 22 M3, six p1, ten p2, 34 p3, 37 p4, 37 m1, 50 m2, 41 m3). Measurements are provided in Table 5. Raw data are provided as Supplementary material (S1).

Localities. Zone G3: Nombrevilla 2, Carrilanga 1.

Zone I: Pedregueras 2A.

Description. The P3 has a robust and conical paracone. The parastyle is usually lacking but sometimes constitutes a low bulge at the anterolabial margin of the tooth, as in Figure 8(B). Sometimes (four out of 22 specimens), a thin crest connects the parastyle to the base of the paracone. The postparacrista is robust and slightly curved (nine out of 16 specimens); it ends by turning labially at the margin of the tooth. The conical protocone is often isolated but sometimes connected to the middle of the anterior border by a thin and low preprotocrista. The hypocone is robust and has a more elongated shape than the protocone. The posthypocrista reaches the posterior cingulum. The P4 shows only a slight oblique elongation (Figure 8(C-D)). The paracone is robust, and the postparacrista is rather sharp. The parastyle is often present and always low. The lingual extension is more developed than in P3. The conical protocone is often connected to the parastyle by a thin crest. The hypocone is conical (in one 'aberrant' specimen, it is blade-like) and connected to the wide posterior cingulum by the posthypocrista.

The M1 is rectangular to diagonally elongated. The paracone has a triangular outline and is connected to the parastyle by a thin crest (in 23 out of 25 specimens). The protoconule is always present and usually strong (23 out of 32 specimens). It is sometimes isolated from the protocone. As shown in Figure 7(B-C), a complete notch is usually present ($n = 32$); the preprotoconule crest is connected to the anterior cingulum in one specimen. The protocone is connected to the hypocone by a slightly curved loph. The posthypocrista is distinguishable in 20 specimens (out of 36). A protocone-metaconule connection is present in two molars out of 42 (Figure 7(C)). The postmetaconule crest is always connected to the postcingulum. The metacone is high and connected to a rather short postmetacrista. The ectoloph is usually sinusoidal ($n = 28$), but a few M1

Table 5. Measurements (in mm) of *Parasorex voesendorfensis* from Daroca-Calamocha, Spain.

	P1		P3			P4			M1			M2		
	L	W	L	W1	W2	L	W1	W2	L	W1	W2	L	W1	W2
N	3	3	30	34	30	42	47	41	25	28	23	39	40	39
Min	0.77	0.61	1.78	1.34	1.56	2.20	1.99	2.14	2.23	2.55	2.68	1.81	2.44	2.28
Max	0.85	0.64	2.20	1.97	2.30	2.58	2.48	2.99	2.56	3.08	3.17	2.24	3.09	2.79
Mean	0.80	0.62	1.98	1.62	1.92	2.36	2.24	2.59	2.37	2.77	2.97	1.96	2.67	2.49
	M3			p1		p2		p3		p4				
	L1	L2	W	L	W	L	W	L	W	L	W			
N	19	20	19	6	6	10	10	31	33	6	7			
Min	1.19	1.08	1.52	0.70	0.56	1.02	0.61	1.47	0.86	1.77	1.23			
Max	1.39	1.20	1.91	0.82	0.59	1.35	0.71	1.96	1.18	2.15	1.46			
Mean	1.32	1.15	1.70	0.74	0.58	1.23	0.65	1.78	1.00	1.99	1.32			
	m1			m2			m3							
	L	W1	W2	L	W1	W2	L	W1	W2					
N	3	4	5	13	15	15	17	19	17					
Min	2.63	1.47	1.70	2.29	1.53	1.50	1.84	1.13	0.93					
Max	2.87	1.75	1.95	2.53	1.68	1.77	2.21	1.32	1.17					
Mean	2.72	1.62	1.87	2.41	1.60	1.62	1.95	1.21	1.05					

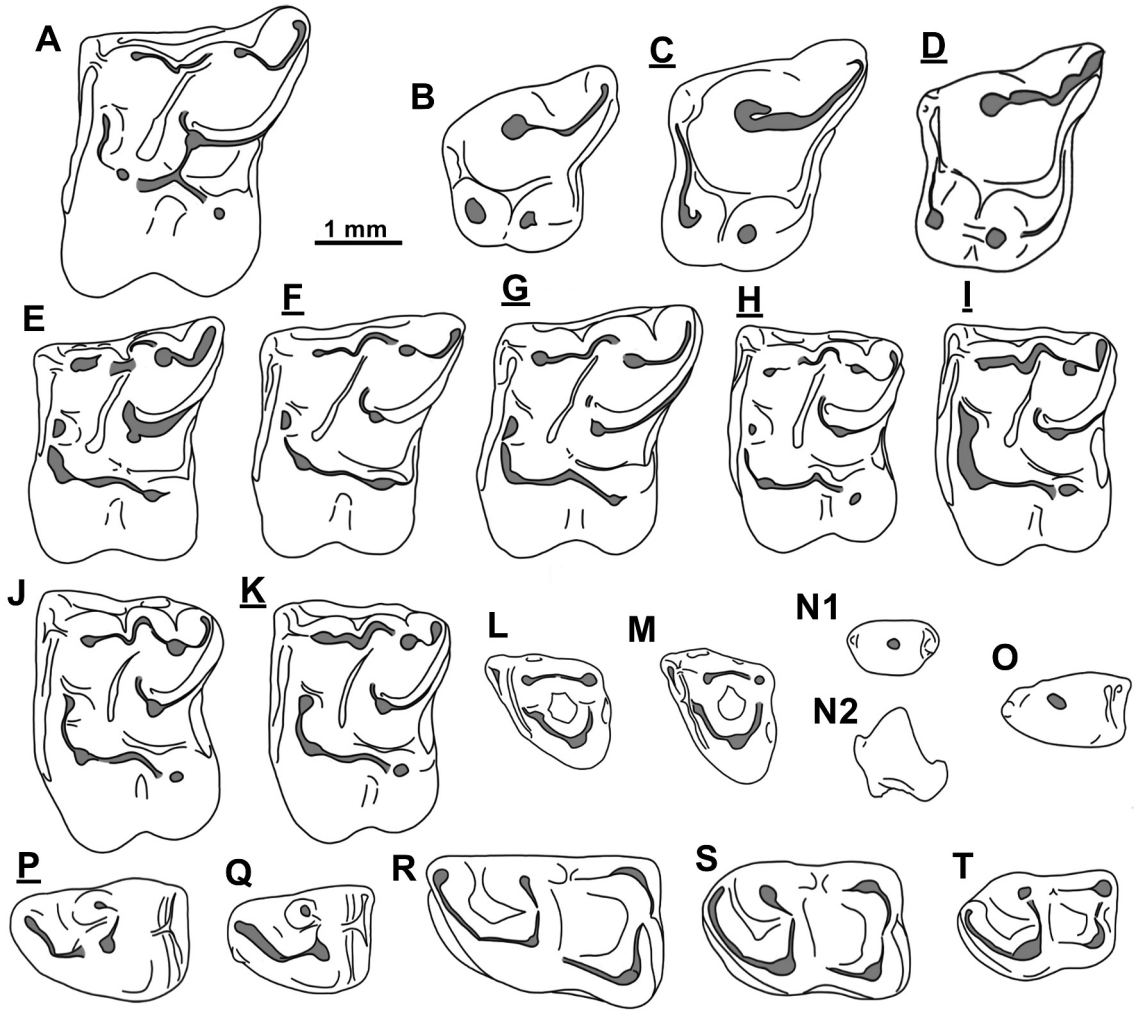

Figure 8. Drawings of *Parasorex* sp. (**A**) and *Parasorex voesendorfensis* (**B-T**) from the Daroca-Calamocha area. (**A**) M1, LUM21, LUM21-C1. (**B**) P3, NO2, NO2-C33. (**C**) P4, CAR1, RGM335230. (**D**) P4, PG2A, RGM334443. (**E**) M1, CAR1, RGM335266. (**F**) M1, CAR1, RGM335287. (**G**) M1, NO2, NO2-A44. (**H**) M2, CAR1, RGM335318. (**I**) M2, CAR1, RGM335308. (**J**) M2, NO2, NO2-D48. (**K**) M2, NO2, NO2-B49. (**L**) M3, PG2A, RGM334453. (**M**) M3, PG2A, RGM334454. (**N**) p2, PG2A, RGM334436, in labial (**N1**) and occlusal (**N2**) views. (**O**) p3, PG2A, RGM334434. (**P**) p4, NO2, NO2-B6. (**Q**) p4, PG2A, RGM334430. (**R**) m1, CAR1, RGM335421. (**S**) m2, CAR1, RGM335448. (**T**) m3, CAR1, RGM335448.

($n = 5$) have a divided crest (Figure 8(E)) or have a concave ectoloph ($n = 2$). Anterior, posterior, and labial cingula are well developed, even if the labial cingulum is often discontinuous. The parastyle in the M2 is always connected to the paracone (in 38 specimens). The notch of the preprotoconule crest is usually less pronounced. The protoconule is always present (in 35 specimens). The preprotoconule crest is incomplete ($n = 54$), connected to the base of the paracone ($n = 1$), or connected to the anterior cingulum ($n = 2$). The ectoloph curvature is sinusoidal ($n = 49$) or divided ($n = 2$); the protocone-metaconule connection is present in five out of 69 specimens; the posthypocrista is visible in seven out of 64 specimens. Finally, we also note two M2 with a discontinuous postmetaconule-postcingulum connection (out of 63 specimens). The M3 is subtriangular but variable in length: some specimens are anteroposteriorly compressed, leading to a short ectoloph. The parastyle is well developed and is usually part of the anterior cingulum. The preprotocrista and postprotocrista are similar in length. The protocone is usually distinguishable on the preprotocrista. Narrow labial and posterior cingula are present.

The mandibular body is gracile and has a constant height between p3 and m2. The ramus has a deep masseteric fossa and a marked curvature of its anterior edge of the ramus. The mental foramen is situated before the anterior root of the p4.

The p1 is a small and simple, one-rooted tooth with a bent, ovoid main cuspid. The p2 has two

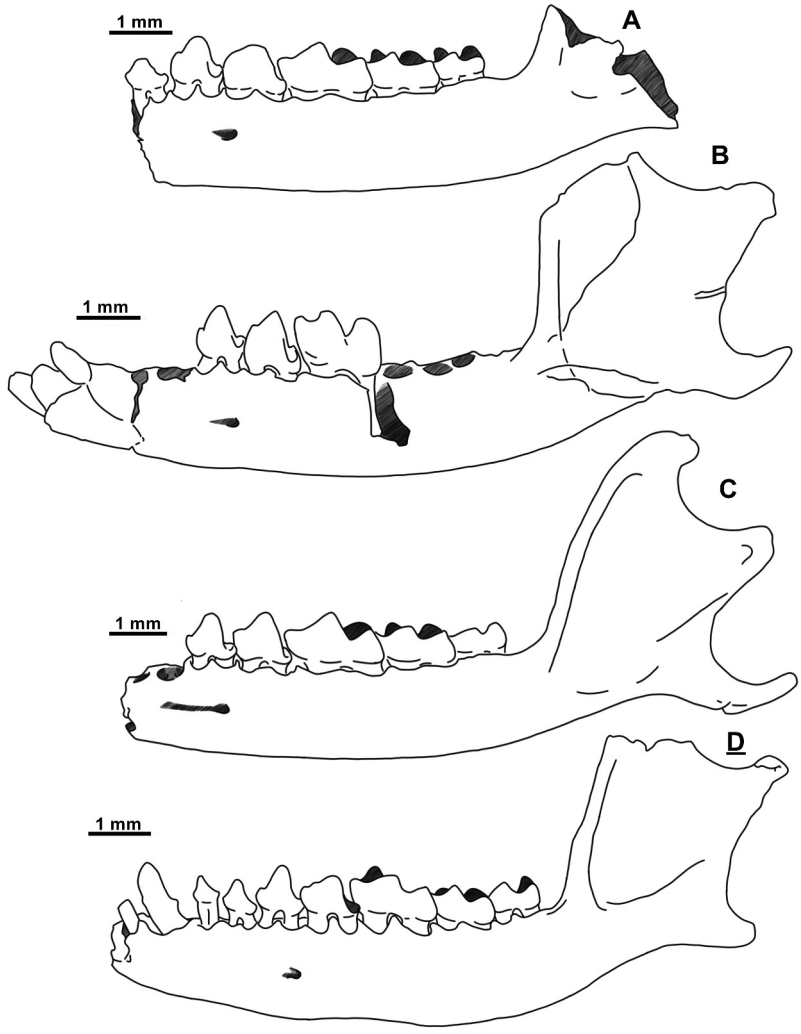

Figure 9. Drawings of *Parasorex* mandibles. (**A**) p2-m3, CAR1, RGM335482, *Parasorex voesendorfensis*. (**B**) i1-i2, p3-m1, Gratkorn, UMJGP 204,691, *Parasorex voesendorfensis*, modified after Prieto et al. (2014). (**C**) p3-m3, Petersbuch 6, NHMA P6-013B1, *Parasorex socialis*, modified after Ziegler (2005). (**D**) c-m3, Cucálon, *Parasorex ibericus*, modified after Mein and Martin-Suárez (1993).

parallel to slightly divergent roots. The main cusp is in an anterior position. An anterior cuspule is present. A small talon is distinguishable, bearing a posterior cuspule. As shown in Figure 7(F), the subtriangular p3 is longer than the p2. The protoconid is robust and placed in an anterior position. The low paraconid is conical or blade-like. In only one out of 21 specimens, the paraconid is isolated. The talonid is well developed with a posterior and a transverse crest. The subtriangular p4 is a robust tooth with a labially placed protoconid. The paraconid is always connected by a curved paralophid to the base of the protoconid. The metaconid is usually strong. The talonid is variable in length (Figure 8(P, Q)); it bears a thin central ridge (on 18 out of 23 specimens) and a strong and posterior cingular crest.

The trigonid on the m1 is subequal to the talonid (Figure 8(R)). The paralophid is elongated and consists of two segments. The paraconid is sometimes slightly procumbent. The protoconid and metaconid have the same height. The metaconid is more anteriorly placed than the protocone. The entoconid is well developed and higher than the hypoconid. The two cusps are connected by a low postcristid. The talonid basin is closed; the metacristid and entocristid are divided by a tiny notch. The oblique cristid is straight. A robust anterior cingulid is present. The labial cingulid is sometimes absent; when present, it is usually disconnected from the anterior cingulid. The connection of the postcingulid is variable: the entoconid-postcingulid connection is present in twelve specimens, the postcristid-postcingulid connection is found in eight m1, and the postcingulid is isolated in 15 m1. The m2 differs from the m1 by the anterior compression of the trigonid, the more curved paralophid, and the weaker development of the postcingulid. There is an entoconid-postcingulid

connection ($n = 8$) or a postcristid-postcingulid connection ($n = 11$). The postcingulid is isolated in 26 m2. The m3 is a small and rather elongated tooth (Figure 7(F)). The conical metaconid is the highest cusp. The paralophid descends from the protoconid as a robust and curved crest and reaches the antero-lingual border perpendicular to the length of the tooth. It is often procumbent. The talonid still presents a notch between the metacristid and the entocristid. The entoconid is in a more posterior position than the hypoconid. The postcingulid is sometimes present; it may be isolated or connected to the entoconid.

Remarks. The identification of *Parasorex socialis* in the Daroca-Calamocha by De Jong (1988) has been questioned since the discovery of new material and species of Galericini (Prieto et al., 2014). The variability of the Daroca-Calamocha specimens is considered here to be closer to *Parasorex voesendorfensis* (previously attributed to *Schizogalerix*; see below) than to *Parasorex socialis* and fits perfectly with the diagnosis of Prieto et al. (2010). It should be noted that some of the measurements published in 2010 were incorrectly reported in their Table 1 (J.P., pers. obs.). The corrected measurements are available as Supplementary Material (S2 Table). The measurements from the Daroca-Calamocha area are very similar to those from Gratkorn (S2 Table), Nebelbergweg (Kälin & Engesser, 2001), and Borský Svätý Jur (Cailleux et al., 2023). We note that the antemolar elements in Borský Svätý Jur are slightly shorter than in the oldest localities, Nombrevilla 2, Carrilanga 1, and, to a lesser extent, Gratkorn. The p4 from Pedregueras 2A is also more compact than in the two older localities (Figure 8(Q) vs. Figure 8(P)), resulting in a p4 outline similar to that of more advanced Galericini such as *P. ibericus*. This supports a progressive shortening of the mandible over time, mirroring the observations made within the assemblages of *P. ibericus* (Mein & Martin-Suárez, 1993).

The possible occurrence of *Schizogalerix* in MN7/8 Spanish deposits and the rather ancestral variability of '*S.*' *voesendorfensis* is for us the result of an incorrect generic assignment. After all, while *Schizogalerix* is mainly distinguished by the split ectoloph on M1-M2, the evolutionary stage of *P. voesendorfensis* is more similar to that of *Parasorex ibericus* (Mein & Martin-Suárez, 1993). Another variable feature on M1 and M2 is the presence or absence of a protocone-metaconule connection. This connection is considered often present in *Galerix* and always absent in *Schizogalerix*. This character was also considered absent in *Parasorex* (Van den Hoek Ostende 2001), but new evidence supports that the loss of this character appeared later in the evolutionary history of both *Parasorex* (see remarks of *Parasorex* sp.) and early *Schizogalerix* (F.C., pers. data). Moreover, *P. voesendorfensis* from Daroca-Calamocha sometimes lacks the labial cingulid on the lower molars. As far as we know, this particular character has only been described in *Parasorex ibericus* (Mein & Martin-Suárez, 1993). Finally, these authors mentioned that the most diagnostic feature of *P. ibericus*, the posthypocrista on M1, was already present in the material from Pedregueras 2C and Carrilanga based on De Jong (1988). This observation is confirmed here. This crest is not mentioned in *Parasorex socialis* from Steinheim (type-locality) and Anwil (Engesser, 1972). The slightly reduced length of the lower premolar of *P. voesendorfensis* from MN9 deposits is also consistent with an intermediate position between *P. socialis* and *P. ibericus*. Prieto et al. (2010) highlighted differences in the mandible morphology of *P. voesendorfensis* and *P. socialis*, shown in Figure 9: the former has its anterior part reduced and its incisors, canine and first premolar are more protruding. In addition, the ascending ramus is more perpendicular to the dental row in *P. voesendorfensis*. The only relatively well-preserved mandible of *P. voesendorfensis* from Carillanga 1 has a more anterior reduction of the mandible (Figure 9(A)), like the material from Gratkorn (Figure 9(B)), while the curvature of the ascending ramus appears closer to *P. socialis* (Figure 9(C)) and *P. ibericus* (Figure 9(D)). Consequently, *P. voesendorfensis* can no longer be attributed to *Schizogalerix* and should be transferred to *Parasorex*, as was previously suspected (Cailleux et al., 2023; Prieto et al., 2014).

The reattribution of our material to *Parasorex voesendorfensis* implies the possible misidentification of this species in latest Middle Miocene and early Late Miocene localities. For instance, the Galericini tentatively identified as *Parasorex socialis* from Barranc de Can Vila 1 (Furió, Casanovas-Vilar, et al., 2011a) presents a sinusoidal ectoloph on M1 and M2 that is uncommon for *P. socialis*, but not for *P. voesendorfensis*. Similarly, several specimens from La Grive-Saint-Alban identified as *P. socialis* seem out of the variability range of this species (F.C., pers. data). On the other hand, the relative abundance of *P. voesendorfensis* in Pedregueras 2A suggests that this species may have survived longer in Spain than in Central Europe. Several MN10 Spanish localities delivered early forms of *Parasorex ibericus* (Mein & Martin-Suárez, 1993), whereas some of the Vallesian material from southern France has been listed as *P.* cf. *socialis* (Jujurieux: Mein, 1999; Soblay: Ménouret & Mein, 2008) or *P.* aff. *socialis* (Montredon: Crochet & Green, 1982). It is clear that the differences between *Parasorex* species were

somewhat unclear in the early Late Miocene, and all MN9 and MN10 material should be carefully considered and properly described.

Galericinae Tribe **Incertae sedis**
Genus ***Lantanotherium*** Filhol, 1888

Type species.
Lantanotherium sansaniense (Lartet, 1851).

Other referred species. *L. robustum* (Viret, 1940); *L. sanmigueli* Villalta and Crusafont, 1944; *L. longirostre* Thenius, 1949; *L. sawini* (James, 1963); *L. dehmi* (James, 1963); *L. lactorense* (Baudelot & Crouzel, 1976); *L. sabinae* (Mein & Ginsburg, 2002); *L. observatum* (Korth and Evander, 2016); *L. anthrace* Cailleux et al., 2020.

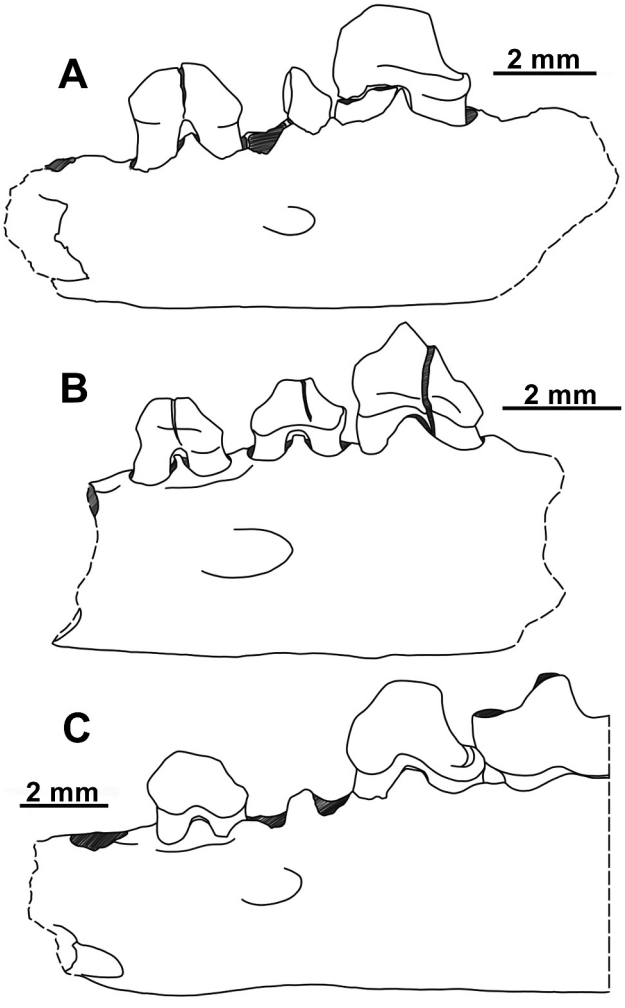

Figure 10. Drawings of *Lantanotherium* mandibles. (**A**) *Lantanotherium lactorense*, p2-p4, Navère, MHNT.PAL.2015.0.722 (holotype). (**B**) *Lantanotherium* sp., p2-p4, LUM20, LUM20-B4. (**C**) *Lantanotherium sabinae*, p2-m1 (detail), Peyre et Beau, FSL66146 (holotype). Scale: 2 mm.

Remarks. According to Baudelot and Crouzel (1976), the holotype of *Lantanotherium lactorense* was housed at the historical museum Eugène-Camoreyt of Lectoure, France. However, as it appeared, the material is unfindable (Furió, Alba, Carmona, et al., 2011). Fortunately, F. C. discovered the holotype at the Museum d'Histoire Naturelle de Toulouse (MNHT), France, under the identification number MHNT.PAL.2015.0.722. As shown in Figure 10(A), the mandible is slightly damaged, but diagnostic features are preserved.

***Lantanotherium* sp.**
Figures 7(G), 10(B)

Referred specimens. One fragment of mandible with p2 (L = 1.40, W = 0.68), p3 (L = 1.61, W = 0.87) and p4 (L = 2.06, W = 1.27) (LUM20B4); height of the mandible under p2: 3.41 mm; height of the mandible under p4: 3.97 mm.

Locality. Zone E: Las Umbrias 20.

Description. The mandible fragment is robust and rather high. In occlusal view (Figure 7(G)), the dentary slightly deviated to the labial part in the section anterior to the p2. Short diastemas are present anterior and posterior to p2. A large, partially preserved alveole is present anterior to the p2, and is interpreted as belonging to the canine. The mandibular foramen lies below the anterior root of p3 (Figure 10(B)).

The double-rooted p2 is only slightly smaller than the p3. The protoconid is elongated and placed in a slightly anterior position. The anterior margin of the tooth is short, narrow, and without cingulid. Its posterior part is also reduced. The p3 is elongated and has a narrower anterior part. The protoconid is bulbous and steady. The anterior part is just a slope without cingulid. A cingulid is visible on the posterior margin. The p4 has an ovoid outline and a rounded anterior margin. The paraconid is low and blunt. It is attached to the rather large protoconid. There is no metaconid. The talonid bears a thin postcingulid but has no basin. A narrow anterolabial cingulid is present.

Remarks. The large and simple lower premolars, each separated by a diastema, cannot be attributed to any known species of Galericini. This combination of characters is found in some members of the crown group of the gymnures. The sole representative of this group in the Miocene of Europe is *Lantanotherium*. This genus is diverse throughout the Miocene (Cailleux et al., 2020; Furió & Alba, 2011), yet it is always rare in Early and Middle Miocene European deposits. For example, although the genus originated in Asia, the first recorded

occurrence in Europe was in Lectoure, southern France (MN3/4; Baudelot & Crouzel, 1976), highlighting the very blurred biogeographic history of this group. The first occurrence of the genus in Spain is in Can Cerdà (MN4; Crusafont et al., 1955) with *L. piveteaui*, although the material consists only of a fragment of a mandible with m2 and m3, making this identification tentative and comparisons with our material impossible.

Our dental elements differ from *L. lactorense* by the reduction of the p2 (Figure 10(A) vs Figure 10(B)). The combination of a two-rooted p2 and a robust p4 without a distinct metaconid is diagnostic for the large *L. sabinae* from La Grive-Saint-Alban (MN7/8; Mein & Ginsburg, 2002) (Figure 7(G)), but this species possesses a p1, which seems to be lacking in our mandible, as in *L. sansaniense*. *Lantanotherium lactorense* already shows a progressive reduction in mandibular height after the p3 (Baudelot & Crouzel, 1976: fig. 2). This decrease in height is partly an artefact of representation (F. C., pers. obs.) but is still more pronounced than in the mandible from Las Umbrias 20 and in *L. sansaniense*. However, it is worth noting that the mandible of the latter seems to be relatively variable in this respect (Engesser, 2009). This decrease is stronger in *L. longirostre*, where it corresponds to an abrupt constriction, resulting in a very elongated mandible.

The size of the specimen from Las Umbrias 20 does not fit the increasing trend observed in the European clade of *Lantanotherium*. Therefore, the species from Daroca-Calamocha does not represent an intermediate form between *L. lactorense* and *L. sabinae*, as also suggested by the absence of p1. The small *Lantanotherium sanmigueli*, which has been found in the early Late Miocene in Eurasia (see, for example, Cailleux et al., 2023; Furió & Alba, 2011; Ziegler, 2005), represents the second migration event of the genus into Western Europe. Compared to our specimen, *L. sanmigueli* has proportionally shorter p2 and p3, a p2 with a single root, as well as a more slender p4 with a distinct paraconid and metaconid swelling (based on De Bruijn et al., 2012). Our specimen also has a much thicker mandible (based on Ziegler, 2005).

The phylogeny of Middle Miocene European *Lantanotherium* is still uncertain and is blurred by the concept of *Lantanotherium* aff. *sansaniense* (e.g. Böttcher et al., 2009; Ziegler, 2000, 2006), which is used to indicate material slightly smaller or larger than *L. sansaniense*. A revision of the European *Lantanotherium* material from MN4 to MN6 is necessary. In addition, the antemolars are subject to great morphological variation in gymnures, the absence of p1 being common in the intraspecific variability of fossil and recent Erinaceidae species (Cailleux, in press). As shown by the example of *Lantanotherium tobieni*, which was subsequently synonymised with *L. sansaniense* (see Baudelot, 1972; Engesser, 1979), the number of premolars should not be considered a reliable diagnostic feature. With this in mind, it is impossible with such a limited sample – notably without upper molars – to precisely identify the taxon from Las Umbrias 20. This MN5 specimen likely represents a local descendant of the MN3 *L. lactorense*.

Specimens from MN4 of Mas d'Antolino B3 (Local Zone C) (Crespo et al., 2019) have been attributed to cf. *Lantanotherium* sp. by Crespo et al. (2020). This material could be evidence of the first migration of the genus in Spain. However, the attribution is based on one fragment of an unmeasurable m2 and one large-sized fragment of m1 (W = 2.23 mm) with a strong but independent postcingulid. Such a large *Lantanotherium* is only known from MN6 in Europe (Prieto et al., 2015; Cailleux et al., 2020, for comparisons), and the only occurrence before MN6 is represented by our specimen from Las Umbrias 20, which is also smaller. Also, the material described does not display a high entocristid, which is a diagnostic feature of *Lantanotherium*. On the other hand, '*Amphechinus*' *baudeloti* is a relatively frequently identified hedgehog in Spanish basins during Local Zone C (see below), with well-developed postcingulid on m1 and m2. The mean width of the m1 talonid of this species (based on eight specimens from Daroca-Calamocha; see below) is 2.21 mm. Therefore, the material from Mas d'Antolino B3 should be reattributed to cf. '*Ampechinus*' *baudeloti*.

Subfamily **Erinaceinae** Fischer, 1814
Genus ***Amphechinus*** Aymard, 1850

Type species.
Amphechinus arvernensis Blainville, 1839

Other referred species. *Amphechinus* first consisted of the western European, latest Oligocene and earliest Miocene taxa *A. arvernensis* Blainville, 1839, *A. edwardsi* Filhol, 1879, and *A. pomeli* Schlosser 1926 (see Hugueney & Maridet, 2022; Viret, 1938). It was subsequently used as a wastebasket taxon for ancestral Neogene erinaceines from Eurasia, Africa, and America. It is now clear that the generic attribution of most Erinaceinae species cannot be clearly supported without sufficient evidence from antemolar dentition and cranial and mandibular elements. In Europe, *Amphechinus* is not recorded from the MN3 and from the MN4 assemblages, which exhibit notable differences compared to pre-MN3 species (see Bonilla-Salomón et al., 2024; Van Dam et al.,

2020). In Asia, the recent description of the new genera *Oligoechinus* (Li et al., 2019), *Ladakhechinus* (Wazir et al., 2022), and *Sonidolestes* (Li et al., 2024) highlights the limitations of using *Amphechinus* as the default genus for isolated specimens. Pending a detailed revision of the Neogene Erinaceinae and in addition to the aforementioned species, we provisionally consider the following species: '*A.*' *kansuensis* Bohlin, 1942; '*A.*' *rusingensis* Butler, 1956; '*A.*' *horncloudi* Macdonald, 1970; '*A.*' *ginsburgi* Baudelot, 1972; '*A.*' *baudeloti* Gibert, 1975; '*A.*' *golpeae* Gibert, 1975; '*A.*' *robinsoni* Gilbert, 1975; '*A.*' *kreuzae* Munthe and West, 1980; '*A.*' *akespensis* Lopatin, 1999; '*A.*' *microdus* Lopatin, 1999; '*A*'. *bohlini* Bi, 2000; '*A.*' *gigas* Lopatin, 2002; '*A.*' *ellicoti* Martin and Lim, 2004; '*A.*' *major* Ziegler et al., 2007; '*A.*' *minutissimus* Ziegler et al., 2007; '*A.*' *taatsiingolensis* Ziegler et al., 2007.

'Amphechinus' baudeloti Gibert, 1975

Figures 7(H-K), 11, Table 6

Stratigraphic range. The type locality is Valtorres, Spain (MN4). *Amphechinus baudeloti* is recorded from MN4 to MN6 in western and central Europe (Van den Hoek Ostende & Furió, 2005; Bonilla-Salomón et al., 2024; this paper).

Material. 74 isolated teeth (3 I3, 2 C, 1 P2, 2 P3, 1 P4, 6 M1, 13 M2, 8 M3, 3 i3, 2 c, 3 p3, five p4, 2 Dp4, 10 m1, 7

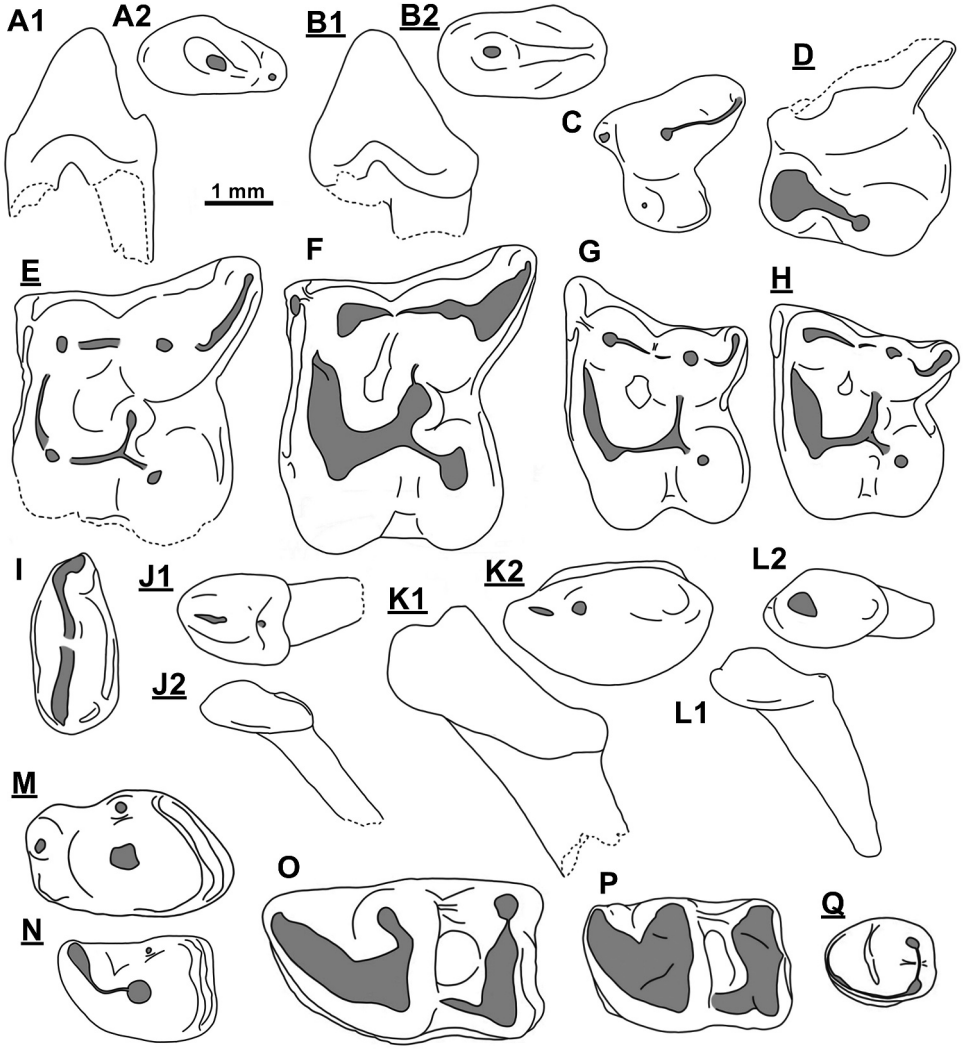

Figure 11. Drawings of *'Amphechinus' baudeloti* from the Daroca-Calamocha area. (**A**) I3, VR7B, VR7B1, in labial (**A1**) and occlusal (**A2**) views. (**B**) C, COLD, COLD-I4, in labial (**B1**) and occlusal (**B2**) views. (**C**) P3, COLC, COLC-103. (**D**) P4, VA7B, VA7B-B1. (**E**) M1, MOR2, MOR2-D4. (**F**) M1, MOR2, MOR2-C4. (**G**) M2, MOR2, MOR2-C5. (**H**) M2, VR4BB, VR4BB-A1. (**I**) M3, COLB, COLB-I20. (**J**) i3, COLD, COLD-I8, in labial (**J1**) and occlusal (**J2**) views. (**K**) c, LUM19, LUM19-A3, in labial (**K1**) and occlusal (**K2**) views. (**L**) p3, COLD, COLD-I6, in labial (**L1**) and occlusal (**L2**) views. (**M**) dp4, LUM19, LUM19-A1. (**N**) p4, LUM1, LUM1-A6. (**O**) m1, MOR2, MOR2-D2. (**P**) m2, VR4A, VR4A-C9. (**Q**) m3, VR2A, VR2A-I5.

Table 6. Measurements (in mm) of '*Amphechinus' baudeloti* from Daroca-Calamocha, Spain.

	I3		C		P2		P3		M1			M2		
	L	W1	L	W	L	W	L	W1	L	W1	W2	L	W1	W2
N	2	2	1	1	1	1	2	2	2	1	2	3	3	6
Min	1.84	1.21					2.06	1.98	3.47		4.17	2.66	2.97	2.42
Max	1.89	1.37					2.18	2.00	3.53		4.22	3.02	3.50	2.74
Mean	1.86	1.29	2.37	1.27	2.22	1.23	2.12	1.99	3.50	3.79	4.19	2.78	3.19	2.60
	M3		i3		c		p3		Dp4		p4			
	L	W	L	W1	L	W	L	W	L	W	L	W1		
N	7	8	7	7	1	1	2	2	2	2	3	4		
Min	1.06	2.23	1.51	1.09			1.51	1.12	2.56	1.56	2.20	1.41		
Max	1.40	2.76	2.15	1.41			1.77	1.14	2.84	1.74	2.58	1.63		
Mean	1.21	2.45	1.81	1.24	3.05	1.75	1.64	1.13	2.70	1.65	2.42	1.48		
	m1			m2			m3							
	L	W1	W2	L	W1	W2	L	W1						
N	1	4	8	2	4	4	4	4						
Min		1.96	2.13	2.92	1.78	1.81	1.54	1.10						
Max		2.16	2.29	2.96	1.96	1.93	1.78	1.36						
Mean	3.93	2.06	2.21	2.94	1.88	1.86	1.63	1.20						

m2, 4 m3). Measurements are provided in Table 6. Raw data are provided as Supplementary material (S1).

Localities. Zone C: Vargas 4A, Vargas 4B, Vargas 4BB, Vargas 1A, Vargas 2A.

Zone Da: Fuente Sierra 2, La Col B, La Col C.

Zone Db: La Col D, Moratilla 2, Moratilla 3, Valdemoros 8A.

Zone Dc: Vargas 6, Valdemoros 3B.

Zone Dd: Vargas 7, Valdemoros 7B, Valdemoros 7C, Valdemoros 3E, Las Umbrias 1, Vargas 11, Regajo 2.

Zone E: Las Umbrias 16, Las Planas 4B, Las Umbrias 19.

Zone G1: Valalto 1A.

Description. I3 is a sharp tooth with two elongated roots (Figure 11(A)). The crown is high and triangular from a lateral view. The anterior margin is rounded, whereas the posterior part is elongated. The main cusp continues posteriorly as a sharp and low crest and joins a minute cusp at the posterior border of the tooth. The upper canine is similar in morphology to the I3. It differs by its more robust and blunt aspect (wider tooth, stronger roots) and by the rounded posterior margin (Figure 11 (B)). The double-rooted P2 has a strong posterior root and an elevated anterior root. The main cusp is blunt and lies in an anterior position. A long central crest extends from the cusp to the very end of the posterior border. The posterior part is low and slightly wider than the anterior part. There is no cingulum. In the P3, the large paracone is connected to a weak metacone by a low postparacrista. The anterolabial corner is slightly extended and bears a minute bulge. The protocone is robust but does not reach half the height of the paracone. It is placed on a lingual extension, which is well differentiated from the labial part by a posterior constriction (Figure 11(C)). The posteriormost part of this extension bears a thin cingular ridge.

The P4 (one broken specimen, Figure 11(D)) has a well-developed lingual part. The paracone is high and labio-lingually elongated. The hypocone is low, its base is circular, and its position is lingual. A ridge connects the hypocone to the paracone. The posterior margin is rounded without a marked cingulum. The M1 has a quadrangular morphology, with the parastyle creating a right-angle corner. The postmetacrista is elongated, creating a rather strong posterolabial extension. The metacone is stronger and wider than the paracone. The protoconule is not distinct; a weak notch is visible in the preprotoconule crest in one of the two unworn specimens. The conical metaconule is robust and placed almost in the centre of the tooth. The metaconule is connected to the postprotocrista. A thin premetaconule crest is sometimes present (Figure 11(F)). Narrow cingula are present on the labial, anterior, and lingual sides. The posterior cingulum is divided, with a stronger posterolabial part. The M2 has a more compressed and irregular outline than the M1 (Figure 11(G-H)): the metastyle is short and turns labially; two specimens have a parastyle similar to the M1 (Figure 11(H)), while a third specimen has an extended parastyle (Figure 11(G)). The protoconule is absent. The metaconule is placed more posteriorly and is less pronounced than in the M1: four of the eight preserved specimens present a ridge (Figure 11 (G)) rather than a true metaconule (Figure 11(H)). The hypocone is massive and shows a slight anteroposterior compression. The anterior cingulum is continuous, whereas it is discontinuous on the other flanks. The M3 is an almond-shaped tooth with a single robust root. The protocone is strong, but the

paracone is hardly distinguishable. Both cusps are included in a robust and sinusoidal central crest. There is a strong anterior cingulum and a weak linguo-posterior cingulum.

The one-rooted i3 is subtriangular to ovoid. The main cusp is included in a low central crest. As shown in Figure 11(J), the posterior part bears a small bulge often distinguishable from the central crest. The posterior outline is variable and can be straight or concave. The lingual side is more flattened than the labial one. The one-rooted lower canine is elongated and consists of a blade-like paraconid and a robust, procumbent protoconid. The central ridge descending posterior to the protoconid turns lingually at the posterior end of the tooth. The lingual side is more flattened than the labial one. A thick lingual cingulid is present. The one-rooted p3 is similar to i3 but differs from it by the absence of a central ridge and the more rounded posterior margin (Figure 11(J) vs Figure 11(L)). There is a short extension anteriorly of protoconid, which has the form of a small bulge in unworn specimens. The p4 has a two-segmented and rather high paralophid, connecting the paraconid to the top of the protoconid. A weak metaconid is attached to the lingual flank of the protoconid. The talonid is short with a very thin posterior ridge. The two roots are wide. The deciduous p4 is a massive element with a higher dental complexity than the p4: the paraconid is low and isolated; the protoconid is conical and placed in the centre of the tooth; the metaconid is low and attached to the paraconid. A curved and low descending ridge connects the metaconid to the postcingulid. The narrow talon has an oblique posterior margin.

The m1 is robust and has a strong two-segmented paralophid. The trigonid is larger than the talonid and has a weakly developed and largely open trigon basin. On the talonid, the entoconid is strong and connected to the hypoconid. The postcingulid is connected to the entoconid in three specimens, to the postcristid in three specimens, and is weak in two specimens. The m2 differs from the m1 in size and by the compressed trigonid. The postcingulid is connected to the postcristid in one specimen and is weak in two. The ovoid m3 consists only of a trigonid. The protoconid and metaconid are low and connected to each other by a thin ridge. The paralophid is elongated and almost completely closes the basin. The paraconid is but a thickening of the paralophid.

Remarks. Gibert (1975) described '*Amphechinus*' *baudeloti* as a medium-sized species with a well-developed metastyle on M1, a distinct metaconule, and a hypocone connected to the protoloph on M1 and M2. Our material shows no significant variation from this pattern, although the presence of a distinct metaconule is not observed on all M2 specimens. The acquisition of a distinct metaconule on M2 is likely subject to variation in this species. This is further supported by the more ancestral MN4 material from Mokrá-Quarry (Czechia), attributed to '*A.*' cf. *baudeloti* by Bonilla-Salomón et al. (2024). As discussed by these authors, '*A.*' *baudeloti* differs from Oligocene and earliest Miocene forms by its more square-shaped M1 and its more compressed M2. Based on the material from the Daroca-Calamocha area, the antemolar elements are also more molarised than *Amphechinus edwardsi* from the MN1 and MN2 of France and Germany (Viret, 1938; Ziegler et al., 2005).

Genus ***Atelerix*** Pomel, 1848

Type species. *Atelerix albiventris* (Wagner, 1841)

Other referred species. *A. frontalis* (Smith, 1831); *A. algirus* (Lereboullet, 1842); *A. sclateri* Anderson, 1895; *A. depereti* Mein and Ginsburg, 2002; *A. rhodanicus* Mein and Ginsburg, 2002; *A. steensmai* Van Dam et al., 2020.

Atelerix* cf. *depereti Mein and Ginsburg, 2002

Figures 7(L-M), 12(A-D)

Stratigraphic range. The type locality is La Grive Saint-Alban, fissure L5, France (MN7/8). *Atelerix* (cf.) *depereti* is also recorded in western and central Europe from MN6 to MN9 (Mein & Ginsburg, 2002; Van Dam et al., 2020; Cailleux et al., 2023; this paper).

Referred specimens. One P3 (PE2A, RGM334439: L = 2.08, W = 1.77), one fragment of maxillar with P4 (TOR2-C2: W1 = 2.94), one M2 (TOR2-A4: L = 3.38, W1 = 3.89, W2 = 3.34), one c (TOR2-C3: L = 2.42, W = 1.24), one i3 (TOR3-B10: L = 1.55, W = 1.16), one fragment of m1 (PJI-A1). Additional data are provided in supplementary material (S1).

Locality. Zone G3: Toril 3B, Toril 2, Paje 1.
Zone I: Pedregueras 2A.

Description. The P3 is strongly anteroposteriorly compressed. The conical paracone has a large base and is connected by a low and short crest to the metacone. The lingual part is relatively wide but only bears a small protocone on its anterior border. The P4 (Figure 12(A)) has a very high paracone. A reduced anterior cingulum is present, independent from the paracone. The

labial part of the tooth is separated from the lingual part by a posterior constriction. The protocone is robust and labially elongated. Compared to the protocone, the hypocone is lower, has a wider base, and is placed in a more lingual position. A short ridge connects the top of the protocone to the posterior flank of the hypocone.

As shown in Figure 12(B), the M2 is a bunodont, trapezoidal tooth with robust cusps. The base of the high paracone is connected to a well-developed, elongated parastyle. A thin ectoloph is present between the paracone and the metacone. The metacone has a wider base than the paracone but is lower. The postmetacrista is strongly compressed, and the metastyle is reduced. The protocone is connected to the paracone by a large, almost straight preprotocrista. The protocone is strong and is as high as the metacone. It is directly connected to a conical metaconule by a blunt and low loph. The conical hypocone is connected to the loph by a lower crest. The trigon basin is deep and oval-shaped. Posterior and anterior cingulums are wide, whereas the labial cingulum is narrow. A short but robust cingulum is present between the paracone and the hypocone.

The i3 is blunt and almost entirely flat (Figure 12 (C)). This simple ovoid tooth bears a small anterior cusp from which a worn posterolabial ridge runs down to the margin. The anterior part of the crown is slightly procumbent. The lower canine is large and simple, with a large, compressed cuspid in anterior position (Figure 12(D)). This cuspid is included in a central crest reaching the anterior margin. It is also connected to a small cuspule situated at the posterior margin of the tooth by a hardly distinguishable crest. The lingual cingulum is well developed. The lower m1 has a strong entoconid, which is higher than the hypoconid. The entocristid is low and leaves the talonid basin slightly open. The postcingulid is large and connected to the entoconid.

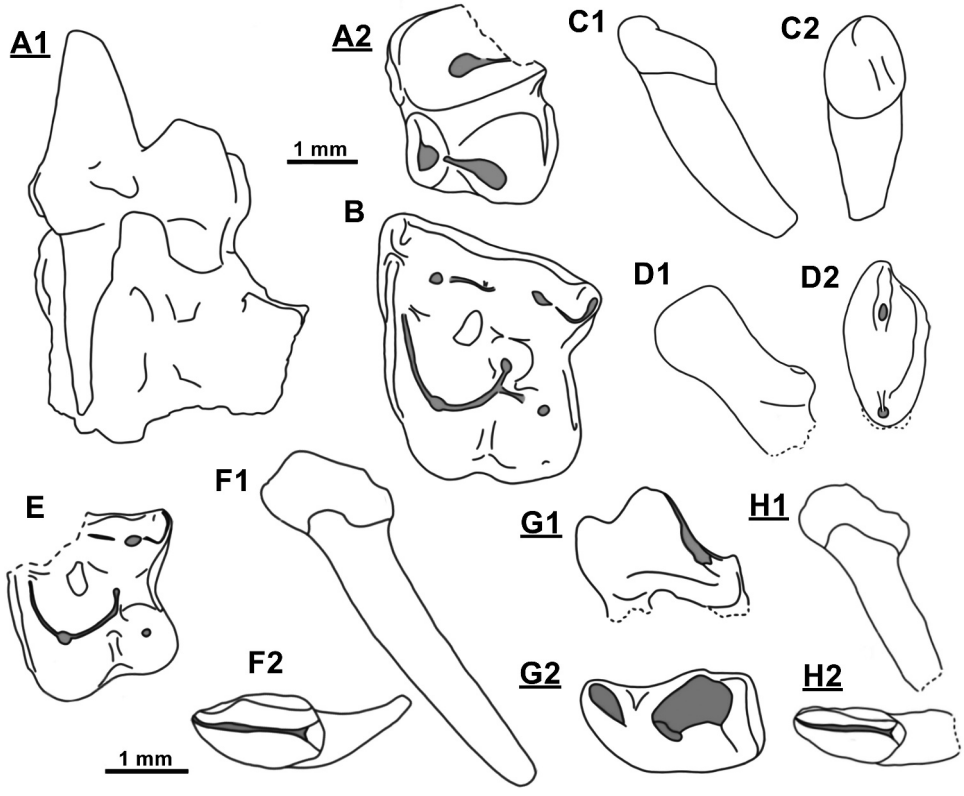

Figure 12. Drawings of *Atelerix* cf. *depereti* (**A-D**), '*Mioechinus*' sp. (**E-G**), and Erinaceinae gen. sp. indet. (**H**) from the Daroca-Calamocha area. (**A**) P4, TOR2, TOR2-C2, in anterior (**A1**) and occlusal (**A2**) views. (**B**) M2, TOR2, TOR2-A4. (**C**) i3, TOR3B, TOR3B-B10, in labial (**C1**) and occlusal (**C2**) views. (**D**) c, TOR2, TOR2-C6, in labial (**D1**) and occlusal (**D2**) views. (**E**) M2, CS1A, RGM213184. (**F**) M3, VA3B, VA3B-2152, in labial (**F1**) and occlusal (**F2**) views. (**G**) p4, VA7B, VA7B-A1, in labial (**G1**) and occlusal (**G2**) views. M3, VL2A, VL2A-1019, in labial (**H1**) and occlusal (**H2**) views. Scales (A-D) (E-K): 1 mm.

Remarks. The hypothesis of a migration of *Atelerix depereti* to Spain was formulated by Van Dam et al. (2020), who described *Atelerix* cf. *depereti* in Pedregueras 2C and *A.* aff. *depereti* in younger Spanish localities. In general, these specimens show a progressive increase in size compared to the type material from La Grive Saint-Alban (Mein & Ginsburg, 2002), although it should be noted that the specimens from the different fissures already show a large variation in size. Our sample does not differ significantly from the type material, except for our smaller i3 and lower canine. Considering the limited material, we name the material from Daroca-Calamocha *Atelerix* cf. *depereti*. *Atelerix* aff. *depereti* sensu Van Dam et al. (2020) appeared as a more advanced form occurring in western and central Europe during the Late Miocene (Cailleux et al., 2023).

Genus ***Mioechinus*** Butler, 1948

Type species. *Mioechinus oeningensis* (Lydekker, 1886)
Other referred species. We follow Ziegler (2005) and Prieto et al. (2015) by considering that only the type species can be included without doubt into the genus. Therefore, the other referred species are: '*M.*' *butleri* Crusafont et al., 1955; '*M.*' *tobieni* Engesser, 1980; '*M.*' *gobiensis* Qiu, 1996.

'*Mioechinus*' sp.

Figures 7(N), 12(E-G)

Referred specimens

Two M2 (CS1A, RGM213184: L ≈ 1.75, W2 = 1.97; VA7B, VA7B-D9: W2 = 2.28), three M3 (VA3B, VA3B-2152: L = 0.96, W = 1.42; VA3B2153: L = 0.88, W = 1.47; VA3B, VA3B-2155: L = 0.79, W = 1.57), one p4 (VA7B, VA7B-A1: L = 2.09, W = 1.15).

Localities

Zone Dc: Valdemoros 3B.
Zone Dd: Caseton 1A, Valdemoros 7B.

Description. The M2 has a large and deep trigon basin. The metacone is slightly labiolingually compressed, and the postmetacrista is extremely reduced. The ectoloph is thin and straight. The metacone is high and conical. The protocone is the largest cusp of the molar. The preprotocrista does not completely reach the paracone, and there is no protoconule. The postprotocrista ends freely, lingually to the metacone, without joining a distinct metaconule. The hypocone is small but uncompressed. Anterior, posterior, and lingual borders have rather strong cingula. The M3 has a simple shape. This one-rooted tooth has an almond-shaped outline (Figure 12(F)). The paracone is strong, and the protocone is not distinguishable from the high central crest. The lingual cingulum is wide.

The p4 is a narrow premolar (Figure 12(G)). The paraconid is elongated and robust, whereas the protocone is relatively gracile. The metaconid is not distinct. The talonid is well developed with a rectangular shape and a thin postcingulid.

Remarks. These specimens are considered to represent a single species. Our material is surprisingly small compared to other Spanish Erinaceinae and is close in size to *Mioechinus*? sp. from the Middle Miocene Tunggur Formation, China (Qiu, 1996). The specimens from Daroca-Calamocha fit perfectly with the dimensions of this indeterminate '*Mioechinus*', sharing with it a narrow p4, a metaconule crest without a distinct metaconule on M2, a protocone-hypocone connection on M2, and a continuous crest on M3. Crespo et al. (2020) attributed a small M3 from Mas d'Antolino B3 (Local Zone C) to cf. *Atelerix* sp., which could correspond to our '*Mioechinus*' sp. The presence of '*Mioechinus*'-like form in Spain was previously attested by the occurrence of '*M.*' *butleri* in the MN4 of Sant Mamet (Van den Hoek Ostende & Furió, 2005). It is worth noting that this generic attribution for small-sized erinacein is, at best, tentative. The taxonomic nature of the Miocene '*Mioechinus*' is one of the important questions that requires a detailed revision of the entire subfamily.

Erinaceinae gen. sp. indet.

Figure 12(H)

Material.

One M3 (VL2A, VL2A-1019: L = 0.65, W = 1.35).

Localities.

Zone B: Villafeliche 2A.

Description. The M3 (Figure 12(H)) is a narrow tooth with a robust single root. The compressed central crest includes the paracone and the protocone. There is an almost complete lingual cingulum, narrower on the anterolingual part.

Remark. The M3 from Villafeliche 2A is too small to belong to the species of Erinaceinae described above, including '*Mioechinus*' sp.

Discussion

General comments on Erinaceidae biostratigraphy and palaeoecology

Because of their slower evolutionary rate and lower abundance compared to rodents, Eulipotyphla are rarely used as biostratigraphic markers. However, their presence/absence can be of great help in the relative dating of localities. For example, the genus *Parasorex* is considered a good biostratigraphic marker in the North Alpine Foreland Basin (NAFB) and appears to be the result of an abrupt migration into this basin (Van den Hoek Ostende et al., 2016, and references therein). In Germany, *Parasorex socialis* has been identified in numerous localities from the NAFB, from the Swabian and Franconian Jura (Ziegler, 2005, 2006; Ziegler et al., 2005), and from the fissure of Petersbuch 68 (Prieto & Rummel, 2009). For the latter locality, correlation based on the rodent fauna gives an age of about 14.2 Ma, corresponding to the oldest occurrence in the area. A similar dating has been estimated in Switzerland based on the assemblage from Rutzentobel (Van den Hoek Ostende et al., 2016). However, in the Iberian Peninsula, *Parasorex socialis* has so far only been identified from the latest Aragonian (Furió, Casanovas-Vilar, et al., 2011b; Furió et al., 2017; Prieto et al., 2011). Therefore, the presence of *Parasorex* sp. in Las Umbrias 21 (13.75 Ma), close to the boundary between the middle and the late Aragonian (~ 13.78 Ma according to García-Paredes et al., 2016), is the first occurrence of the genus in the Iberian Peninsula. This occurrence cancels the significant diachrony of the genus observed between Spain and Central Europe (Van den Hoek Ostende et al., 2016), despite the first migration of *Parasorex* in the area being apparently unsuccessful.

According to Prieto et al. (2011, p. 185), 'the migration of *Parasorex* in the NAFB coincides with a global cooling event around 14 to 13.5 Ma (Böhme, 2003; Shevenell et al., 2004)'. Similarly, the transition between the middle and the late Aragonian is marked by a strong faunal turnover in the Calatayud-Montalbán Basin (Van der Meulen et al., 2005), coinciding with the end of the Middle Miocene Climate Transition (MMCT) and the beginning of a Coolhouse period (e.g. García-Paredes et al., 2016). This colder climate apparently favoured the spread of *Parasorex* across central and western Europe. This period is also characterised by the presence of *Lantanotherium* in the Calatayud-Montalbán Basin. Given the occurrence of *Lantanotherium* species in the MN3/4 of southern France (*L. lactorense*, Lectoure; Baudelot & Crouzel, 1976) and already in the MN4 of the Iberian Peninsula (*L. piveteaui*, Can Cerdà; Crusafont et al., 1955), the specimen from Las Umbrias 20 May represent a more permanent presence of the genus in the area during the early Middle Miocene. The occurrence of both *Parasorex* and *Lantanotherium* fits particularly well with the astronomical obliquity nodes identified in the interval 13.85–13.6 Ma and correlated to temporarily drier conditions (Van Dam et al., 2006), whereas *Lantanotherium* is a taxon usually associated with humid environments (Cailleux et al., 2020; Furió & Alba, 2011; Prieto et al., 2011).

The re-identification of late Aragonian and early Vallesian material to *Parasorex voesendorfensis* promises major advances in the biostratigraphic understanding of trans-European faunal exchange, as the species apparently spread widely throughout Europe at the very end of the Middle Miocene. However, many taxonomic problems remain to be solved. As discussed in the remark section, *Parasorex voesendorfensis* appears to be a convenient transitional species between MN7/8 *P. socialis* and MN10 *P. ibericus*. This requires further investigations, notably regarding the Spanish and French Vallesian assemblages.

Erinaceinae are identified in 31 out of the 91 localities studied from the Daroca-Calamocha area and are always present in only a few specimens. Only one of these localities yielded two erinacein species (Valdemoros 3B, 14.85 Ma). Both '*Amphechinus*' *baudeloti* (from 16.18 to 13.35 Ma) and *Atelerix* cf. *depereti* (from 12.65 to 10.25 Ma) can be confidently considered resident species. The occurrences of the invertivorous '*Amphechinus*' *baudeloti* indicate that this species preferred a rather warm climate, in line with its maximal geographic distribution in the late MN4 and with the Miocene Climatic Optimum (based on Daams, Freudenthal, & Van der Meulen, 1988; Van Dam et al., 2006). The identification of the species in the MN4 of Czech Republic (Bonilla-Salomón et al., 2024) suggests that '*Ampechinus*' *beaudeloti* does not originate from Western Europe. This provides a convenient explanation for the stratigraphic and morphological gap observed between the true, earliest Miocene *Amphechinus* and the Middle Miocene '*Ampechinus*'. The last occurrence of '*Ampechinus*' *beaudeloti* in

Local Zone G1 suggests that the species was a late victim of the trend towards colder environments (based on Van der Meulen et al., 2005). As *Amphechinus* has been used as a wastebasket taxon, its composition, decline, and replacement remain unclear. In Europe, the late Middle Miocene saw the apparent end of the advanced '*Amphechinus*', alongside the progressive success of *Atelerix* and *Postpalerinaceus*.

Atelerix cf. *depereti* shows a more omnivorous dental pattern than '*Amphechinus*' (Van Dam et al., 2020) and entered the Calatayud-Montalbán Basin in the latest Aragonian (Local Zone G3, Toril 3B, 12.65 Ma), together with the Castoridae that re-entered the area in Toril 3A (12.65 Ma; Álvarez Sierra et al., 2003; García-Paredes et al., 2016) and with the overall higher precipitation (Daams, Freudenthal, & Van der Meulen, 1988). From *Atelerix depereti* emerged the Vallesian and Turolian *Atelerix* aff. *depereti*, and later *Atelerix steensmai*, two species that were able to survive significant Vallesian drying (Cailleux et al., 2025; Van Dam et al., 2020).

Distinguishing Galerix symeonidisi *from* Galerix exilis

The existence of *Galerix symeonidisi* in the Daroca-Calamocha area is evidenced by the presence of P3s with hypocone and the high frequency of small-sized upper molars (Van den Hoek Ostende & Doukas, 2003). Although the type material from Aliveri (Doukas, 1986) displays enough characteristics to distinguish it from *G. exilis*, we concur with Van den Hoek Ostende and Doukas (2003) that the Spanish material presents fewer diagnostic characters. Consequently, 528 out of the 2621 dental elements of Erinaceidae from the Daroca-Calamocha area have been classified as *Galerix* indet. (S1).

Figure 13 shows that the measurements of *G. exilis* and *G. symeonidisi* overlap considerably and only rarely produce a bimodal distribution. This is the case for the area of P4, which shows the most pronounced bimodality, but also for the area of M2, the posterior width of M2, the antero-posterior length of M3, the length of p3, and the talonid width of m2. Thus, only six out of 29

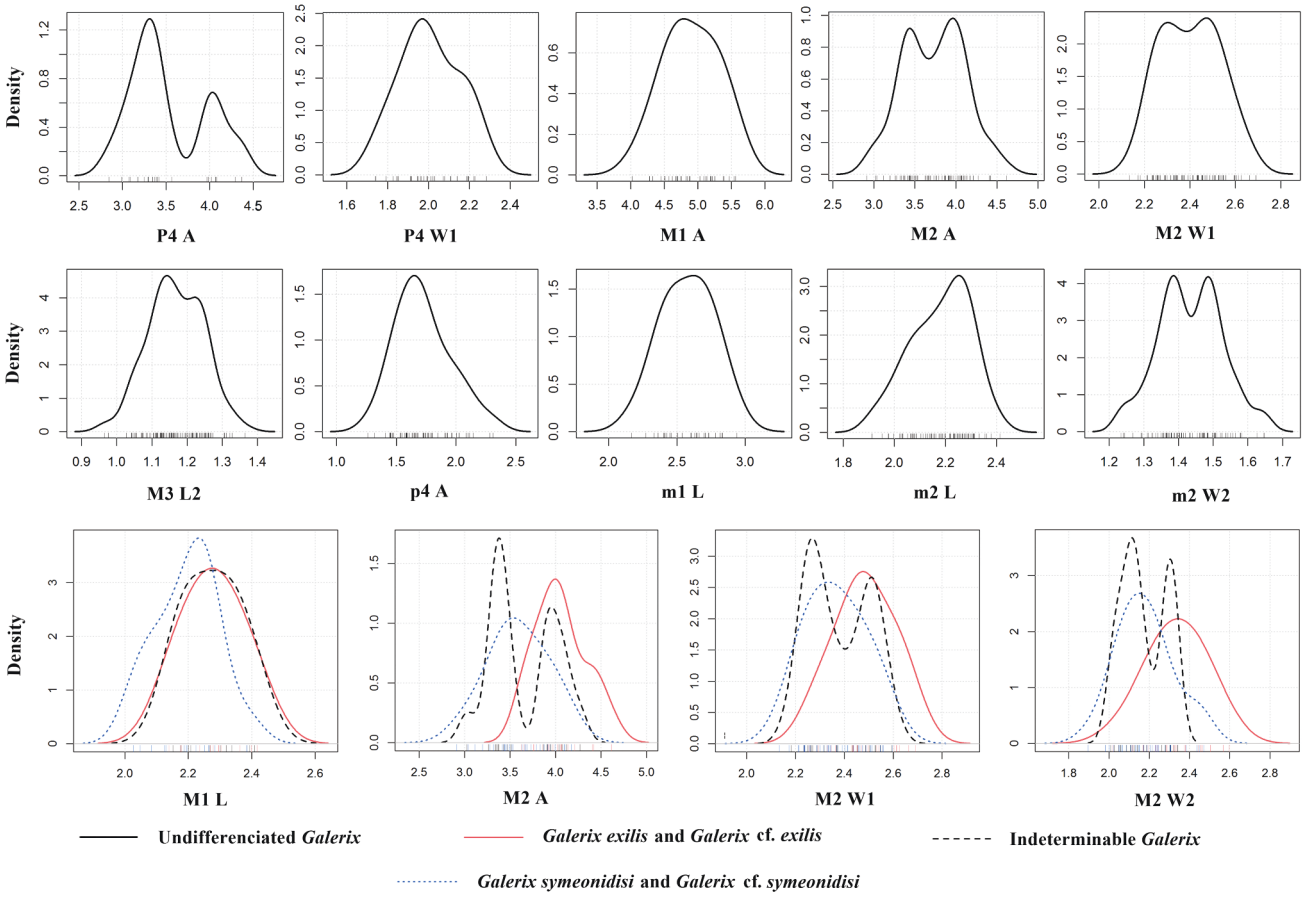

Figure 13. Rugplots of *Galerix* measurements from the Daroca-Calamocha area (from San Roque 1, 16.78 Ma, to Villafeliche 4A, 15.51 Ma). *Galerix remerti* is excluded from the dataset. Kernel density estimation is used with the default bandwidth.

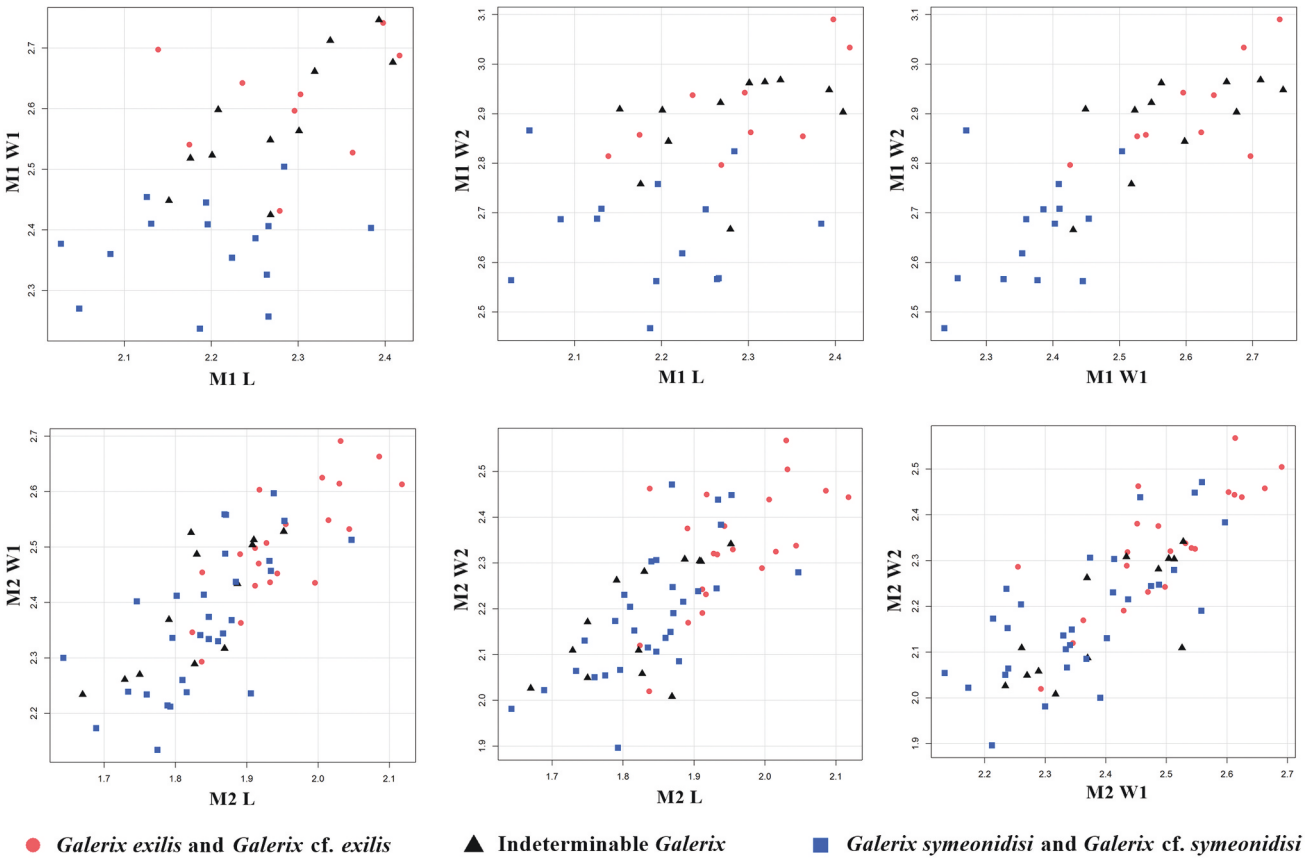

Figure 14. Size distribution of M1 and M2 of *Galerix* from San Roque 1 (16.78 Ma) to Villafeliche 4A (15.51 Ma). *Galerix remerti* is excluded from the dataset.

measurements (two out of seven area measurements, four out of 22 classic measurements) help distinguish the two species. This confirms the remark of Van den Hoek Ostende and Doukas (2003) about the smaller size of *Galerix* from Daroca-Calamocha during the time of presence of *G. symeonidisi*. The strong bimodality of P4 May imply a difference in proportion along the dental row between the two species, with *G. symeonidisi* having a proportionally smaller P4.

The identification of *Galerix symeonidisi* in this paper, based on the morphological characters described by Doukas (1986) and Van den Hoek Ostende and Doukas (2003), can be tested on the basis of size bimodality. The distribution of the groups *Galerix exilis*, *Galerix symeonidisi*, and *Galerix* indet. often produces unimodal densities when combined with Kernel density estimation (Figure 13). Therefore, the morphological elements used to differentiate the M1 and M2 of the two species are relevant, which is also justified by the scatterplots shown in Figure 14. However, *Galerix* indet. often shows a bimodal distribution. This indicates a morphological overlap between the two species, especially for M1: almost all indeterminate M1 are found in the morphometric region of *Galerix exilis*, but cannot be identified with certainty based on morphological grounds.

Between 16 Ma and 15.5 Ma, we observe a decrease in the overall morphological variability of the *Galerix* material, which is partly explained by the disappearance of *G. symeonidisi*. These elements, considered as diagnostic of the Spanish *Galerix symeonidisi* (at least, diagnostic of an 'hyper-*symeonidisi*' morphology), are: P3 always bearing a hypocone; relatively large P3 and small P4; M1 and M2 with rare postmetaconule-postcingulum connection; M1 and M2 with distinguishable to strong protoconule; M2 with a frequently pronounced preprotocrista notch (sometimes connected to the precingulum); reduced M3 with rounded corners.

Phylogenetic and paleobiogeographic consequences of Galerix symeonidisi variability

The assemblages attributed to *Galerix symeonidisi* show regional differences (Van den Hoek Ostende & Doukas, 2003). Compared to the type material from Aliveri (MN4, Greece), the specimens from Daroca-

Calamocha show a weaker hypocone on P3, mainly a low ectoloph on M1 and M2 (always high in Aliveri), mainly a concave ectoloph on M1 (mainly straight in Aliveri), mainly a strong protoconule on M1 (only distinguishable in Aliveri), and the presence of a protocone-metaconule crest connected to the upper part of the metaconule on M2 (when present, only connected to the base of the metaconule in Aliveri). The presence of a postmetaconule-postcingulum connection is variable in ancestral *Galerix*, such as in the type material of *G. wesselsae* (present in one M2 out of ten and absent in M1) and *G. saratji* (often present on M1 and sometimes on M2), but is invariably present on both M1 and M2 in *P. kostakii*, a close ally of *G. symeonidisi*. *Galerix symeonidisi* from Aliveri has this connection on two out of seven M1 and on five out of 12 M2. The material from Daroca-Calamocha does not present this connection on M1, and only on five out of 22 M2.

Some character states present in *G. symeonidisi* from Daroca-Calamocha are not observed in the material from Aliveri, and the upper molar variability of the Spanish *G. symeonidisi* actually shows similarities with those of more ancestral *Galerix* taxa, such as *G. saratji* and *G. wesselsae* (Van den Hoek Ostende, 1992; Van den Hoek Ostende et al., 2015; Zijlstra & Flynn, 2015). These similarities indicate that the Spanish *G. symeonidisi* has a more ancestral morphology than the Greek type population. This is further supported by the overall smaller p4, P3, M1, and M2 in our material, considering the progressive increase in molar size observed between the eastern *G. wesselsae*, *G. symeonidisi*, and *Parasorex kostakii*. It is, however, worth noting that the first Spanish finds are older than the estimated age of Aliveri (Van den Hoek Ostende et al., 2015).

Compared to the type material of *G. symeonidisi*, the type material of *Parasorex kostakii* from Karydia and *G. symeonidisi* from Daroca-Calamocha share the presence of a concave ectoloph in almost all M1; the presence of M1 with low ectoloph (common in Daroca-Calamocha, rare in *P. kostakii*); a higher frequency of strong protoconule on M1; and the presence of a high protocone-metaconule crest on M2. These character states are also attested in *G. saratji* (Van den Hoek Ostende, 1992). The type material of *Galerix symeonidisi*

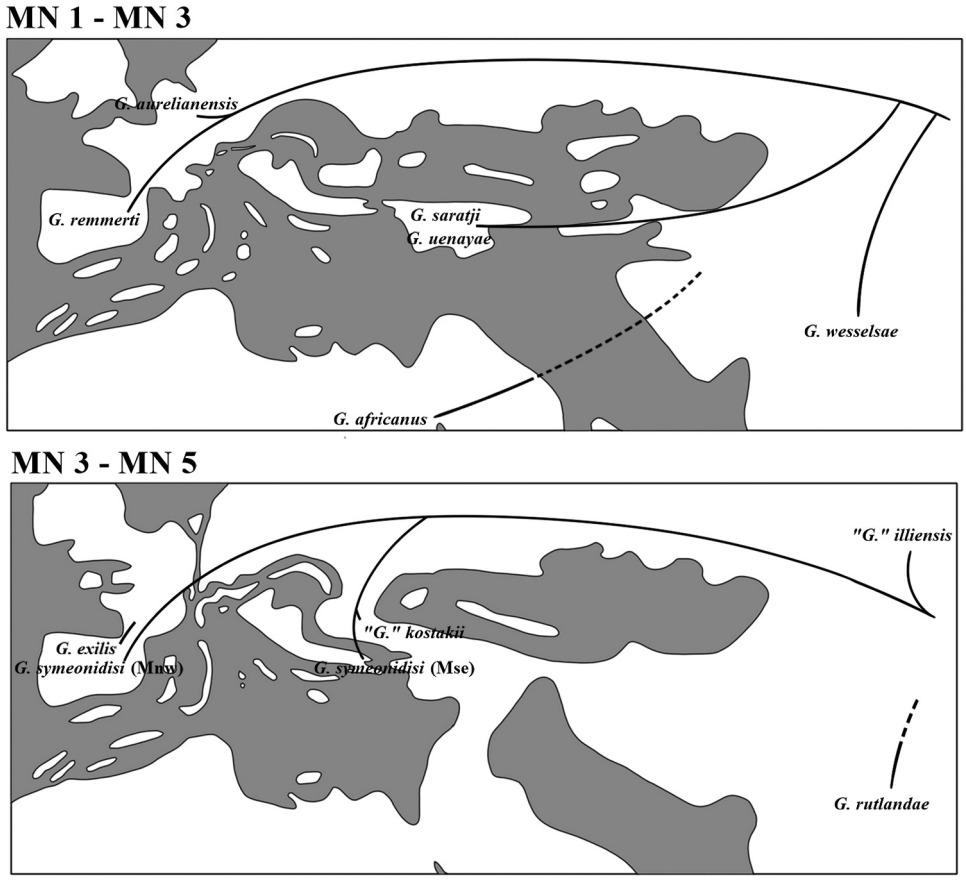

Figure 15. Model of *Galerix* dispersion, from MN 1 to MN 3 and from MN3 to MN5, showing the split between the Mnw and the Mse metapopulations of *Galerix symeonidisi*.

shows the following derived characters: the absence of a low ectoloph and strong protoconule on M1; the presence of a connection between the protoconule and the anterior cingulum (in one M1); and the absence of a high protocone-metaconule crest on M2. These observations suggest that *Parasorex kostakii* originated from a less derived population than the assemblage of Aliveri. The appearance of *P. kostakii* seems, therefore, attributable to a cladogenetic evolution.

Whereas the form from Daroca-Calamocha does not display subsequent apomorphies and therefore likely belongs to a basal form of the species *G. symeonidisi*, the Balkan representatives evolved in two separate groups: a more advanced form of *G. symeonidisi* and *Parasorex kostakii* (Figure 15). This appears evident because of the anterior structure of the p4, which consists of a crest-like paraconid in the type material of *G. symeonidisi* (Doukas, 1986), a paralophid in *P. kostakii* (Doukas & Van den Hoek Ostende, 2006), but a conical and independent paraconid in *G. saratji* (Van den Hoek Ostende, 1992), *G. wesselsae* (Zijlstra & Flynn, 2015), and in *G. symeonidisi* from Spain (this paper). The lack of this derived character in *G. symeonidisi* assemblages from central Europe (based on Bonilla-Salomón et al., 2024; Prieto & Rummel, 2009) also indicates a closer similarity with the Spanish group. Therefore, we support that the acquisition of a blade-like paraconid is specific to the Greek paleopopulation of *G. symeonidisi*. The clear, continuous paralophid is then acquired in the early *Parasorex*, *P. kostakii* (MN4/5, Doukas & Van den Hoek Ostende, 2006) and *P. pristinus* (MN5, Ziegler, 2003; 15.1 Ma according to Harzhauser et al., 2003; Ziegler, 2003).

Consequently, it is clear that *Galerix symeonidisi* is a taxon that is represented by two European metapopulations, as shown in Figure 15: the northern and western metapopulation (Mnw) and the south-eastern metapopulation (Mse). We also support two regional constraints for *G. symeonidisi*: the Mnw preserved ancestral characters and does not show any significant variation (based on its first and last occurrences at the Daroca-Calamocha area), suggesting a process of stabilising selection for tooth morphology; the Mse acquired new characters, leading to a speciation event and supporting a directional selection towards a more *Parasorex*-like morphology. Presumably, mutual gene flow was reduced, as they occupied two land masses that were only weakly connected south of the Transdanubian High, possibly with interruptions allowing intermittent exchange between the Mediterranean and western Paratethys (Kováč et al., 2017).

The apparent absence of the Mse and *Parasorex kostakii* in Anatolia supports the idea of a selective barrier, as discussed by Van den Hoek Ostende et al. (2015) and based on small mammal taxa (e.g. eomyids). *Galerix* was actually present in Anatolia during the late Early Miocene with *G. uenayae*, a species belonging to a more ancestral lineage (Van den Hoek Ostende, 1992, Van den Hoek Ostende, 2001; this paper). This species finally coexisted at the end of its biostratigraphic range with the earliest *Schizogalerix* species, *S. evae*, as in Sabuncubeli (local zone D, ~MN3; De Bruijn et al., 2006) and Hisarçik (Van den Hoek Ostende & Doukas, 2003). This first *Schizogalerix* is a migrant taxon that likely reached the Aegean-Anatolian block from the east (see reconstruction in Van den Hoek Ostende et al., 2015: fig. 3). Considering the known ecomorphological convergence between *Parasorex* and *Schizogalerix*, it is plausible that both *Schizogalerix* and pre-*Parasorex* forms were subject to similar selective pressures in the Aegean-Anatolian block, favouring the presence of the former and adaptation of the latter. In this sense, strictly speaking, *Parasorex* is already the result of a convergence phenomenon of *Galerix* with *Schizogalerix*. This hypothesis is consistent with a drying trend as observed for the late Early Miocene of Anatolia (local zone E; based on Bilgin et al., 2021), as already expressed by the insectivores assemblage from Keseköy (local zone D, ~MN3; Van den Hoek Ostende et al., 2015), and with the tentative ecological reconstruction of *Parasorex* and *Schizogalerix*, depicting these taxa as being at least more environmentally tolerant than *Galerix* (Doukas & Van den Hoek Ostende, 2006; Prieto et al., 2010, Cailleux, 2024; Van den Hoek Ostende, 2001). This gives credit to the idea of at least one distinct biome characterising the Aegean-Anatolian block. This, however, does not answer the limited eastward spread of the pre-*Parasorex* taxa and likely also the limited westward spread of *Schizogalerix*. Confirming the latter would require additional material, with a special focus on the forms identified from Komotini ('*Galerix*' sp., MN4/5, Greece; Doukas & Van den Hoek Ostende, 2006) and Antonios ('*Schizogalerix*' sp., MN5, Greece; Vasileiadou & Koufos, 2005). Despite a limited early spatial distribution, the Mse realised a relative diversification, as shown with the progressive success of true *Parasorex* at least after 15.1 Ma (see above), whereas the less adapted Mnw is last recorded in the earliest MN5 of Els Casots (16.15–15.94 Ma, Vallès-Penedès Basin; Casanovas-Vilar et al., 2022) and La Col D (15.84 Ma, Teruel Basin; this paper), which is somewhat in line with the German findings (Ziegler et al., 2005).

Biogeographic and phylogenetic history of Galerix: *a phylogenetic overview*

The increase during the last two decades in our knowledge of the Miocene eulipotyphlan faunas allowed several authors to propose a new phylogeny for Galericini. Borrani et al. (2017) selected well-known species to perform a morphology-based phylogenetic analysis of Galericini, resulting in a classification with a hard polytomy, i.e. low resolution. Several species with debated generic attributions were excluded, hindering a complete view of the evolution of Galericini (see Van den Hoek Ostende, 2018). Recently, Crespo et al. (2021) also proposed a complete revision of the Galericini, discarding the hypothesis of *Galerix-Parasorex* transitional forms. This new configuration implies a 20 my. temporal gap between *Parasorex* and *Schizogalerix* from their purported closest ancestor, the Eocene genus *Eogalericius* Lopatin, 2004. This phylogeny is provided with emended diagnoses for *Tetracus*, *Galerix*, *Parasorex*, and *Schizogalerix*, largely focused on characters found in the lower dentition. Species with intermediate variability are included in a 'doubtful species' list. Within these ten excluded species, there are notably *Parasorex kostakii* and *Parasorex pristinus*; these two taxa are at the very centre of our supported *Galerix-Parasorex* transition hypothesis. *Galerix remmerti* is also considered a 'doubtful species'. The new classification of Crespo et al. (2021) thus differs greatly from the traditional classification in both results and methods and does not resolve, from a phylogenetic point of view, the data collected in this paper on the evolution of *Galerix symeonidisi* and *Parasorex kostakii*.

The Galericinae consists of highly variable species. Similar morphological evolution can be found in species and populations from different times and spaces. Therefore, reconstructing the phylogeny of Galericini requires looking at relationships between species and between assemblages, and not between higher taxa. Obviously, this requires special attention to changes in variability, mostly found in the

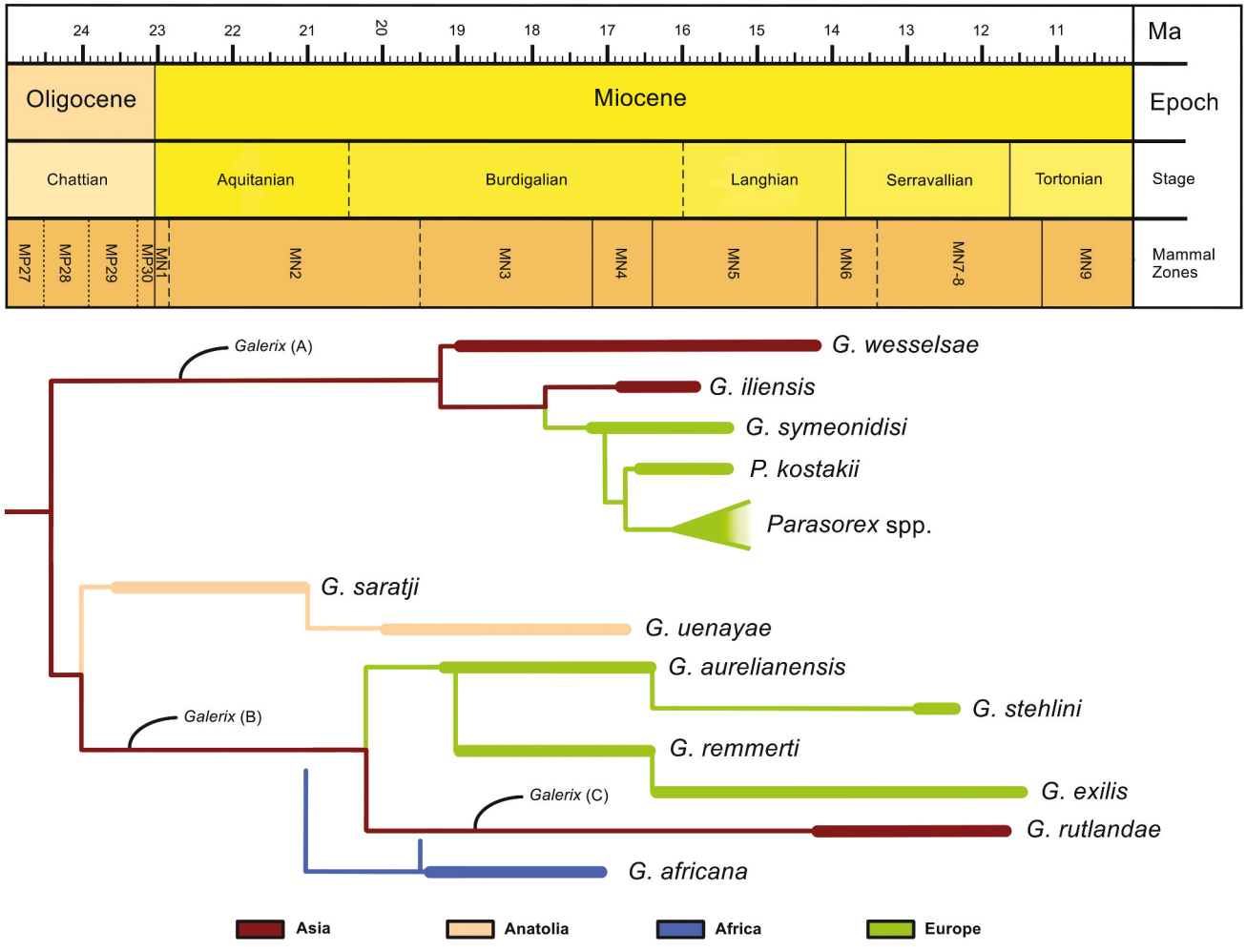

Figure 16. Tentative phylogeny of *Galerix* based on dental characters and spatial and temporal distributions (see Discussion and S3).

upper dentition and leading to polytomy if not considered. For example, the p3:p2 ratio is sometimes taken as an absolute character allowing *Galerix* to be distinguished from *Parasorex* and *Schizogalerix* (Borrani et al., 2017; Crespo et al., 2021). However, *Galerix rutlandae* has a larger p3, *Galerix africana* has a p3 equal to p2 (Butler, 1984), and some p3 are also equal to p2 in the material of *Galerix exilis* described by Ziegler (1988) and in the type locality of *Galerix stehlini* (F.C., pers. obs.). The unknown p2 and p3 of *Galerix iliensis* and *Parasorex kostakii* also hamper a clear view of their relationships with *Parasorex*.

We provide in supplementary data (S3) an in-depth comparison of *Galerix* material, based on their original diagnoses, focusing on similarities in variability between known species (Figure 16). This comparative work is not the result of a phylogenetic analysis; we opted here for a more stratophenetic approach, looking for temporal and spatial parsimony without excluding any published assemblages. We support that *Tetracus* represents an early wave of post- Grand Coupure galericine in Europe and does not represent a direct ancestor of *Galerix*, a view supported by Borrani et al. (2017) and Crespo et al. (2021). Hence, *Tetracus* is here not synonymous with *Galerix*, unlike Borrani et al. (2017) and Hugueney and Maridet (2022).

We observe a strong basal dichotomy within the genus *Galerix*, making it paraphyletic (Figure 16) and strongly supporting the hypothesis of a *Galerix-Parasorex* transitional lineage. These pre-*Parasorex* species include *G. wesselsae*, *G. iliensis*, and *G. symeonidisi*. They represent a second wave of migration into Europe at the end of MN3, preceded by the *G. aurelianensis-remmerti* species complex (Figure 15). The latter taxa, together with *G. saratji*, *G. uenayae*, *G. stehlini*, *G. exilis*, *G. rutlandae*, and G. *africana*, are considered to form a monophyletic subgroup.

As Prieto et al. (2012) discussed, distinguishing between advanced *Galerix* and early *Parasorex* requires identifying the least variable feature and therefore the most reliable one in the crown group of Galericini: either the presence of paralophid on p4, or the absence of a connection between the protocone and metaconule on M1-2. This connection is still present in the *Parasorex* specimens described from both the Sámsonháza 3 (Prieto et al., 2012) and Las Umbrias 21 site (this work). This character also rarely occurs in advanced *Parasorex* (see taxonomic remarks). By contrast, although a paralophid is present in the p4 of *Galerix rutlandae*, we concur with Zijlstra and Flynn (2015) that this angular paralophid is not equivalent to the structure observed in early *Parasorex*. Therefore, in line with Prieto et al. (2012) and other researchers (Van den Hoek Ostende, 2018; Zijlstra & Flynn, 2015), we classify *P. kostakii* as the earliest species of *Parasorex*. However, it is worth noting that the anterior structure of the p4 remains variable within this species (see Doukas & Van den Hoek Ostende, 2006, for a description). The position of *Schizogalerix* in this context remains unclear, as it may correspond to an early Asian offshoot of the pre-*Parasorex* group (*Galerix* (A) in Figure 16), or it may have an earlier origin. Considering the already particularly advanced morphology of *Schizogalerix evae* and *S. duolebulejinensis*, the latter hypothesis seems more plausible.

A complete phylogenetic reconstruction of the Galericini is beyond the scope of this paper and, as shown in the analyses of Borrani et al. (2017) and Crespo et al. (2021), would require careful consideration of the cases of morphological convergence, which are known to occur between *Galerix* and *Parasorex* (this paper), *Parasorex* and *Schizogalerix* (e.g. Cailleux et al., 2023), as well as between Early Miocene *Galerix* and *Schizogalerix* (F.C., pers. obs.). The morphological peculiarities of *Riddleria* and *Deinogalerix* are also expected to make any supra-generic reconstruction more complex. As a model, the phylogenetic reconstruction of *Galerix* supported in Figure 16 should be tested by its predictive efficiency, which is mainly as follows:

(1) The existence of a *Galerix* (A) species in western or central Asia between 24 and 20 Ma, characterised by the combination of: a small size, a hypocone on P3, a rare or absent postmetaconule-postcingulum connection on M1 and M2, a straight and low ectoloph on M1 and M2, a weak protoconule on M1, p2 longer than p3, a lack of paralophid on p4, and no postcingulid-entoconid connection on m1-2. This species could be distinguished from *G. wesselsae* by its more frequent protocone-metaconule connection on M1 and M2, its weaker protoconule on M1, and its less developed hypocone on P3. *Galerix* (A) would also differ from *G. saratji* and *G. uenayae* by the invariable presence of a hypocone on P3, and from early *Schizogalerix* species by the shorter postmetaconule crest on M1-2 and the p2:p3 ratio.
(2) The existence of a *Galerix* (B) species in western Asia between 23 Ma and 20 Ma. characterised by the combination of: a small-to-medium size, the lack or rare presence of a hypocone on P3, a concave labial outline of M1 (long metastyle), the absence of paralophid on p4, and a rather frequent postcingulid-entoconid connection on

m1-2. This species could be distinguished from *G. aurelianensis/remmerti* by its smaller size, and from *G. rutlandae* by the absence of a crest-like paraconid on p4, as well as by the p2/p3 ratio. *Galerix* (B) would also differ from *G. saratji* in having a more frequent postcingulid-entoconid connection of m1-2 and a shorter postmetaconule crest on M1-2.

(3) The existence of a *Galerix* (C) species in western or southern Asia between 19 Ma and 14 Ma characterised by the combination of: a small size, no or rare presence of a hypocone on P3, a notch of the labial outline of M1 (long metastyle), a short postmetaconule crest on M1-2, a p3 longer than p2, a crest-like paraconid on p4, and a frequent postcingulid-entoconid connection on m1 and m2. The more basal structure of the lower premolars would be the most effective means of distinguishing this species from its structural descendant *Galerix rutlandae* (14.3-11.6 Ma; Zijlstra & Flynn, 2015).

Conclusion

A total of six Galericinae and four Erinaceinae species were extracted from 92 Aragonian and early Vallesian localities in the Daroca-Calamocha area. Despite the low abundance of insectivores in these deposits, a substantial collection of specimens was obtained. The Erinaceinae subfamily is relatively frequently recorded in the area, but always in small numbers. The presence of '*Amphechinus*' *beaudeloti* confirms its preference for warm environments, whereas the late Middle Miocene and Late Miocene *Atelerix depereti* apparently had a broader climatic tolerance. The extensive material attributed to the Galericini enabled a detailed study of each identified taxon, focusing particularly on the metric and morphological variability of *Galerix exilis* and *G. symeonidisi*. Alongside the (re)identification of *Galerix remmerti*, *Parasorex* sp., and *Parasorex voesendorfensis*, this has enabled a comprehensive reconstruction of the biogeographic and phylogenetic history of the *Galerix* genus. Our reconstruction confirms the recurrent role of environmental parameters and events (e.g. MCO, MMCT, astronomical obliquity nodes, and new land bridges) in the migration, ecomorphological diversification, success, and eventual decline of the Galericini during the Neogene.

Acknowledgments

We are deeply grateful to the two anonymous reviewers for their detailed and constructive comments and suggestions, which greatly improved the manuscript. We also thank Marc Furió for his valuable remarks on the insectivore fauna from Vallès-Penedès. We also wish to thank Wilma Wessels, Emmanuel Robert, Suzanne Jiquel, Yves Laurent, and Peter Joniak for giving access to comparative material.

Author contributions

CRediT: **Florentin Cailleux:** Conceptualization, Formal analysis, Funding acquisition, Investigation, Methodology, Resources, Software, Validation, Writing – original draft, Writing – review & editing; **Pablo Peláez-Campomanes:** Conceptualization, Funding acquisition, Investigation, Resources, Writing – review & editing; **Jérôme Prieto:** Conceptualization, Resources, Validation, Writing – review & editing; **Lars W. van den Hoek Ostende:** Conceptualization, Data curation, Methodology, Project administration, Resources, Supervision, Validation, Writing – original draft, Writing – review & editing.

Disclosure statement

No potential conflict of interest was reported by the author(s).

Funding

This research was funded by the research project PID2023-151089NB-I00 funded by MCIU/AEI/10.13039/501100011033/FEDER, UE. Additionnaly, F.C. was supported throughout the research period by an Erasmus mobility grant Erasmus+ (agreement n° 99570), the Martin & Temminck Fellowship (Naturalis Biodiversity Center, Leiden, the Netherlands), the Comenius University research grants [UK/27/2022, UK/221/2023 and UK/1068/2024], the Scientific Grant Agency of the Ministry of Education, Science, Research and Sport of the Slovak Republic and Slovak Academy of Sciences (VEGA) under the contract [VEGA 1/0533/21], and the Slovak Research and Development Agency [projects APVV-20-0120 and APVV-20-0079].

ORCID

Florentin Cailleux http://orcid.org/0000-0002-1558-2088
Pablo Peláez-Campomanes http://orcid.org/0000-0002-6551-1026
Jérôme Prieto http://orcid.org/0000-0002-7485-9112
Lars W. van den Hoek Ostende http://orcid.org/0000-0003-3114-0121

Data availability statement

All data underlying the findings of this study are available within this article and in the supplementary material, which can be accessed via the Figshare repository at https://doi.org/10.6084/m9.figshare.30264655.

References

Álvarez Sierra, M. A., Calvo, J. P., Morales, J., Alonso-Zarza, A. M., Azanza, B., García Paredes, I., Hernández Fernández, M., Van der Meulen, A. J., Peláez-Compomanes, P., Quiralte, V., Salesa, M. J., Sanchez, I. M., Soria, D. (2003). El tránsito Aragoniense-Vallesiense en el área de Daroca-Nombrevilla (Zaragoza, España). López-Martinez N, Peláez-Campomanes P, Hernández Fernández M, editors. En torno a fósiles de mamíferos: datación, evolución y paleoambiente. *Coloquios de Paleontología Volumen Extraordinario*, *1*, 25–33.

Álvarez Sierra, M. A., Paredes, I. G., Van den Hoek Ostende, L. W., Van der Meulen, A. J., Peláez-Campomanes, P., & Sevilla, P. (2006). The middle Aragonian (Middle Miocene) micromammals from La Retama (intermediate depression, Tagus basin) province of Cuenca, Spain. *Estudios Geológicos*, *62*(1), 401–428. https://doi.org/10.3989/egeol.0662135

Baudelot, S. (1972). *Etude des Chiroptères, Insectivores et Rongeurs du Miocène de Sansan (Gers)* [Doctoral dissertation]. Université de Toulouse, 364.

Baudelot, S., & Crouzel, F. (1976). Insectivore et lagomorphe à Navère (Lectoure) Burdigalien inférieur du Gers. *Bulletin de La Société d'Histoire Naturelle de Toulouse*, *112*(3-4), 47–52.

Bilgin, M., Joniak, P., Mayda, S., Göktaş, F., Peláez-Campomanes, P., & Van den Hoek Ostende, L. W. (2021). Micromammals from the late Early Miocene of Çapak (western Anatolia) herald a time of change. *Journal of Paleontology*, *95*(5), 1079–1096. https://doi.org/10.1017/jpa.2021.27

Böhme, M. (2003). The Miocene climatic optimum: Evidence from ectothermic vertebrates of central Europe. *Palaeogeography, Palaeoclimatology, Palaeoecology*, *195*(3/4), 389–401. https://doi.org/10.1016/S0031-0182(03)00367-5

Bonilla-Salomón, I., Cailleux, F., Joniak, P., Ivanov, M., & Sabol, M. (2024). Herpetotheriidae, talpidae, and erinaceidae from the Early Miocene fissures of mokrá-quarry (South Moravia, the Czech Republic). *Fossil Imprint*, *80*(2), 269–284. https://doi.org/10.37520/fi.2024.021

Borrani, A., Savorelli, A., Masini, F., & Mazza, P. P. (2017). The tangled cases of *Deinogalerix* (Late Miocene endemic erinaceid of Gargano) and Galericini (Eulipotyphla, Erinaceidae): A cladistic perspective. *Cladistics*, *34*(5), 542–561. https://doi.org/10.1111/cla.12215

Böttcher, R., Heizmann, E. P., Rasser, M. W., & Ziegler, R. (2009). Biostratigraphy and palaeoecology of a Middle Miocene (Karpathian, MN 5) fauna from the northern margin of the North Alpine foreland basin (Oggenhausen 2, SW Germany). *Neues Jahrbuch fur Geologie und Palaontologie-Abhandlungen*, *254*(1), 237–260.

Butler, P. M. (1956). Erinaceidae from the Miocene of East Africa. *Fossil Mammals of Africa*, *11*, 1–75.

Butler, P. M. (1984). Macroscelidea, Insectivora and Chiroptera from the Miocene of east Africa. *Palaeovertebrata*, *14*(3), 117–198.

Cailleux, F. (2024). *Late Miocene Eulipotyphla and Chiroptera from the Pannonian Region* [Doctoral dissertation]. Comenius University In Bratislava, Faculty of Natural Sciences, 340.

Cailleux, F. (in press). Dental disorders and mandibular trauma: The last stand of the Miocene gymnure *Galerix stehlini* (Mammalia, Eulipotyphla). *Journal of Mammalian Evolution*.

Cailleux, F., Chaimanee, Y., Jaeger, J.-J., & Chavasseau, O. (2020). New Erinaceidae (Eulipotyphla, Mammalia) from the Middle Miocene of Mae Moh (Northern Thailand). *Journal of Vertebrate Paleontology*, *40*(3), e1783277. https://doi.org/10.1080/02724634.2020.1783277

Cailleux, F., Van Dam, J., Furió, M., Joniak, P., & Van den Hoek Ostende, L. W. (2025). Revised taxonomy and ecology of the Late Miocene Erinaceinae (Eulipotyphla, Mammalia) from Kohfidisch, Austria. *Historical Biology*, 1–17. Advance online publication. https://doi.org/10.1080/08912963.2025.2526058

Cailleux, F., Van den Hoek Ostende, L. W., & Joniak, P. (2023). The Late Miocene Erinaceidae (Eulipotyphla, Mammalia) from the Pannonian Region, Slovakia. *Journal of Paleontology*, *97*(4), 777–798. https://doi.org/10.1017/jpa.2023.50

Casanovas-Vilar, I., Garcés, M., Marcuello, A., Abella, J., Madurell-Malapeira, J., Jovells-Vaqué, S., Cabrera, L., Galindo, J., Beamud, E., Ledo, J. J., Queralt, P., Martí, A., Sanjuan, J., Martín-Closas, C., Jiménez-Moreno, G., Luján, À. H., Villa, A., DeMiguel, D. Sánchez, I. M., … Moyà-Solà, S. (2022). Els Casots (Subirats, Catalonia), a key site for the Miocene vertebrate record of SouthWestern Europe. *Historical Biology*, *34*(8), 1494–1508. https://doi.org/10.1080/08912963.2022.2043296

Casanovas-Vilar, I., Madern, A., Alba, D. M., Cabrera, L., García-Paredes, I., Van den Hoek Ostende, L. W., DeMiguel, D., Robles, J. M., Furió, M., Van Dam, J., Garcés, M., Angelone, C., & Moyà-Sola, S. (2016). The Miocene mammal record of the Vallès-Penedès Basin (Catalonia). *Comptes Rendu Palevol*, *15*(7), 791–812. https://doi.org/10.1016/j.crpv.2015.07.004

Crespo, V. D., Goin, F. J., Montoya, P., & Ruiz-Sánchez, F. J. (2020). Early Miocene marsupialiforms, gymnures, and hedgehogs from Ribesalbes-Alcora Basin (Spain). *Journal of Paleontology*, *94*(6), 1213–1227. https://doi.org/10.1017/jpa.2020.58

Crespo, V. D., Montoya, P., Marquina-Blasco, R., & Ruiz-Sánchez, F. J. (2021). *Parasorex ibericus* from Venta del Moro: A new light on the tribe Galericini. *Palaeontographica, Abteilung A: Palaeozoology – Stratigraphy Article*, *320*(1–3), 65–86. https://doi.org/10.1127/pala/2021/0116

Crespo, V. D., Suárez-Hernando, O., Murelaga, X., Ruiz-Sánchez, F. J., & Montoya, P. (2019). Early Miocene mammal assemblages from the Campisano ravine in the Ribesalbes-Alcora Basin (E Spain). *Journal of Iberian Geology*, *45*(1–2), 181–194. https://doi.org/10.1007/s41513-018-0093-z

Crochet, J. Y., & Green, M. (1982). Contributions à l'étude des micromammifères du gisement Miocène supérieur de Montredon (Hérault), 3-Les insectivores. *Palaeovertebrata*, *12*(3), 119–131.

Crusafont, M., Villalta, J. F., & Truyols, J. (1955). El Burdigaliense continental de la cuenca del Vallés Penedés. *Memorias y Comunicaciones del Instituto Geológico*, *12*, 1–272.

Daams, R., & Freudenthal, M. (1988). Synopsis of the Dutch-Spanish collaboration program in the Aragonian type area, 1975-1986. *Scripta Geologica*, *1*(1), 3–18.

Daams, R., Freudenthal, M., & Van der Meulen, A. J. (1988). Ecostratigraphy of micromammal faunas from the Neogene of Spain. *Scripta Geologica, Special Issue*, *1*, 287–302.

Daams, R., Van der Meulen, A. J., Álvarez-Sierra, M. A., Peláez-Campomanes, P., Calvo, J. P., Alonzo Zarza, M. A., & Krijgsman, W. (1999). Stratigraphy and sedimentology of the Aragonian (Early to Middle Miocene) in its type area (North-Central Spain). *Newsletters on Stratigraphy*, *37*(3), 103–139. https://doi.org/10.1127/nos/37/1999/103

Daams, R., Van der Meulen, A. J., Peláez-Campomanes, P., & Álvarez-Sierra, M. A. (1999). Trends in rodent assemblages from the Aragonian (Early-Middle Miocene) of the Calatayud-Daroca Basin, Aragon, Spain. In J. Agustí, L. Rook, & P. Andrews (Eds.), *Hominoid Evolution and Climatic Change in Europe*. The Terrestrial Miocene Record of Europe (Vol. 1, pp. 127–139). Cambridge University Press.

Daams, R., Van der Meulen, A. J., Sierra, M. A., Peláez-Campomanes, P., & Krijgsman, W. (1999). Aragonian stratigraphy reconsidered, and a re-evaluation of the Middle Miocene mammal biochronology in Europe. *Earth and Planetary Science Letters*, *165*(3–4), 287–294. https://doi.org/10.1016/S0012-821X(98)00273-8

Daxner-Höck, G. (1998). Palaeozoological investigations from the Early Miocene lignite opencast mine Oberdorf (N Voitsberg, Styria, Austria). *Jahrbuch der Geologischen Bundesanstalt*, *140*(4), 477–481.

De Bruijn, H., Doukas, C. S., van den Hoek Ostende, L. W., & Zachariasse, W. J. (2012). New finds of rodents and insectivores from the Upper Miocene at Plakias (Crete, Greece). *Swiss Journal of Palaeontology*, *131*(1), 61–75. https://doi.org/10.1007/s13358-011-0030-7

De Bruijn, H., Mayda, S., van den Hoek Ostende, L., Kaya, T., & Saraç, G. (2006). Small mammals from the Early Miocene of Sabuncubeli (Manisa, SW Anatolia, Turkey). *Beiträge zur paläontologie*, *30*, 57–87.

De Jong, F. (1988). Insectivora from the upper Aragonian and the lower Vallesian of the Daroca-Villafeliche area in the Calatayud-Teruel Basin (Spain). *Scripta Geologica, Special Issue*, *1*, 253–285.

Doukas, C. S. (1986). The mammals of the lower Miocene of Aliveri (Island of Evia, Greece), part 5, the insectivores. *Proceedings Koninklijke Nederlandse Akademie van Wetenschappen*, *89*(1), 15–38.

Doukas, C. S., & Van den Hoek Ostende, L. W. (2006). Insectivores (Erinaceomorpha, Soricomorpha; Mammalia) from Karydia and Komotini (Thrace, Greece; MN 4/5). *Beiträge zur paläontologie*, *30*, 109–131.

Engesser, B. (1972). *Die obermiozäne Säugetierfauna von Anwil, Baselland* [dissertation]. University of Basel, 147.

Engesser, B. (1979). Relationships of some insectivores and rodents from the Miocene of North America and Europe. *Bulletin of Carnegie Museum of Natural History*, *14*, 1–68. https://doi.org/10.5962/p.228593

Engesser, B. (1980). Insectivora und Chiroptera (Mammalia) aus dem Neogen der Türkei. *Schweizerische Paläontologische Abhandlungen*, *102*, 45–149.

Engesser, B. (2009). The insectivores (Mammalia) from Sansan (Middle Miocene, south-western France). *Schweizerische Paläontologische Abhandlungen*, *128*, 1–91.

Furió, M., & Alba, D. (2011). Aspectos problemáticos del género *Lantanotherium* (Galericinae, Erinaceidae, Mammalia). Pérez-García A., Gascó F., Gasulla J.M., Escaso F., editors. *Viajando a Mundos Pretéritos, Ayuntamiento de Morella*, *1*, 123–130.

Furió, M., Alba, D., Carmona, R., & Rifà, E. (2011). New fossil remains of Lantanotherium (Erinaceidae, Mammalia) from the Vallesian (Late Miocene) of Viladecavalls (NE Spain). *Journal of Vertebrate Paleontology, 71st Annual Meeting Society of Vertebrate Paleontology* (pp. 113), Las Vegas, Nevada, USA.

Furió, M., Casanovas-Vilar, I., Moyà-Solà, S., Köhler, M., Galindo, J., & Alba, D. M. (2011a). Insectivores (Eulipotyphla; Mammalia) from the Middle Miocene of Barranc de Can Vila 1 (Vallès-Penedès Basin, Catalonia, Spain). *Geobios*, *44*(2–3), 199–213. https://doi.org/10.1016/j.geobios.2010.10.002

Furió, M., Casanovas-Vilar, I. W., & van den Hoek Ostende, L. W. (2011b). Predictable structure of Miocene insectivore (Lipotyphla) faunas in western Europe along a latitudinal gradient. *Palaeogeography, Palaeoclimatology, Palaeoecology*, *304*(3–4), 219–229. https://doi.org/10.1016/j.palaeo.2010.01.039

Furió, M., Van den Hoek Ostende, L. W., Agustí, J., & Minwer-Barakat, R. (2017). Evolución de las asociaciones de insectívoros (Eulipotyphla, Mammalia) en España y su relación con los cambios climáticos del Neógeno y el Cuaternario. *Ecosistemas*, *27*(1), 38–51. https://doi.org/10.7818/ECOS.1454

Furió, M., van den Hoek Ostende, L. W., Agustí, J., & Minwer-Barakat, R. (2018). Evolución de las asociaciones de insectívoros (Eulipotyphla, Mammalia) en España y su relación con los cambios climáticos del Neógeno y el Cuaternario. *Ecosistemas*, *27*(1), 38–51. https://doi.org/10.7818/ECOS.1454

Garcés, M., Krijgsman, W., Peláez-Campomanes, P., Álvarez-Sierra, M. A., & Daams, R. (2003). *Hipparion* dispersal in Europe: Magnetostratigraphic constraints from the Daroca area (Spain). *Coloquios de Paleontología*, *216*(1-4), 171–178.

García-Paredes, I., Álvarez-Sierra, M. A., Van den Hoek Ostende, L. W., Hernández-Ballarín, V., Hordijk, K., López-Guerrero, P., Oliver, A., & Peláez-Campomanes, P. (2016). The Aragonian and Vallesian high-resolution micromammal succession from the Calatayud-Montalbán basin (Aragón, Spain). *Comptes Rendus Palevol*, *15*(7), 781–789. https://doi.org/10.1016/j.crpv.2015.09.014

García-Paredes, I., Peláez-Campomanes, P., & Álvarez-Sierra, M. Á. (2010). *Microdyromys remmerti*, sp. nov. a new Gliridae (Rodentia, Mammalia) from the Aragonian type area (Miocene, Calatayud-Montalbán basin, Spain). *Journal of Vertebrate Paleontology*, *30*(5), 1594–1609. https://doi.org/10.2307/40864370

Gibert, J. (1975). New insectivores from the Miocene of Spain. *Proceedings van de Koninklijke Nederlandse Akademie van Wetenschappen, Series B*, *78*(1), 108–133.

Harzhauser, M., Daxner-Höck, G., Boon-Kristkoiz, E., Ćorić, S., Mandic, O., Miklas-Tempfer, P., Roetzel, R., Rögl, F., Schultz, O., Spezzaferri, S., Ziegler, R., & Zorn, I. (2003). Paleoecology and biostratigraphy of the section Mühlbach (Gaindorf formation, lower Middle Miocene, lower Badenian, Austria). *Ann naturhist Mus Wien*, *104A*, 323–334. https://www.jstor.org/stable/41702050

Harzhauser, M., Daxner-Höck, G., Göhlich, U. B., & Nagel, D. (2011). Complex faunal mixing in the early Pannonian palaeo-Danube Delta (Late Miocene, Gaweinstal, lower Austria). *Annalen des Naturhistorischen Museums in Wien*, *113*, 167–208.

Hír, J., Venczel, M., Codrea, V., Angelone, C., Van den Hoek Ostende, L. W., Kirscher, U., & Prieto, J. (2016). Badenian and Sarmatian s. str. from the Carpathian area: Overview and ongoing research on Hungarian and Romanian small vertebrate evolution. *Comptes Rendus Palevol*, *15*(7), 863–875. https://doi.org/10.1016/j.crpv.2016.08.001

Hír, J., Venczel, M., Codrea, V., Rossner, G. E., Angelone, C., Van den Hoek Ostende, L. W., Rosina, V. V., Kirscher, U., & Prieto, J. (2017). Badenian and Sarmatian s. str. from the Carpathian area: Taxonomical notes concerning the Hungarian and Romanian small vertebrates and report on the ruminants from the Felsőtárkány Basin. *Comptes Rendus Palevol*, *16*(3), 312–332. https://doi.org/10.1016/j.crpv.2016.08.001/

Hugueney, M., & Adrover, R. (2003). *Tetracus daamsi*, une nouvelle espèce de Galericinae (Erinaceidae, Mammalia) dans l'Oligocène de Majorque (Espagne). *Coloquios de Paleontologia*, *Volumen Extra 1*, 311–324.

Hugueney, M., & Bulot, C. (2011). Les petits Mammifères du Burdigalien (MN3; Miocène) d'Estrepouy (Gers, France): liste faunique actualisée. *Estudios Geológicos*, *67*(2), 427–442. https://doi.org/10.3989/egeol.40584.200

Hugueney, M., & Maridet, O. (2022). The Erinaceidae from the Late Oligocene of Coderet-Bransat and Peublanc (Allier, France; MP 30): New data on *Amphechinus pomeli* (Schlosser, 1925-1926) and *Galerix minor* (Filhol, 1880). *Revue de Paléobiologie*, *41*, 267–279. https://doi.org/10.5281/zenodo.6858371

Jovells-Vaqué, S., García-Paredes, I., Furió, M., Angelone, C., Van den Hoek Ostende, L. W., Berrocal Barberà, M., DeMiguel, D., Madurell-Malapeira, J., & Casanovas-Vilar, I. (2018). Les Cases de la Valenciana, a new Early Miocene small-mammal locality from the Vallès-Penedès Basin (Catalonia, Spain). *Historical Biology*, *30*(3), 404–421. https://doi.org/10.1080/08912963.2017.1317768

Kälin, D., & Engesser, B. (2001). Die jungmiozäne Säugetierfauna vom Nebelbergweg bei Nünningen (Kanton Solothurn, Schweiz). *Schweizerische Paläontologische Abhandlungen*, *121*, 4–61.

Kälin, D., & Kempf, O. (2009). High-resolution stratigraphy from the continental record of the Middle Miocene northern Alpine Foreland Basin of Switzerland. *Neues Jahrbuch für Geologie und Paläontologie - Abhandlungen*, *254*(1–2), 177–235. https://doi.org/10.1127/0077-7749/2009/0010

Klietmann, J., Nagel, D., Rummel, M., & Van den Hoek Ostende, L. W. (2014). *Amphiperatherium* and Erinaceidae of Petersbuch 28. *Bulletin of Geosciences*, *89*, 1–20. https://doi.org/10.3140/bull.geosci.1454

Kordikova, E. G. (2000). Insectivora (Mammalia) from the lower Miocene of the Aktau Mountains, south-eastern Kazakhstan. *Senckenbergiana Lethaea*, *80*(1), 67–79. https://doi.org/10.1007/BF03043665

Kováč, M., Hudáčková, N., Halásová, E., Kováčová, M., Holcová, K., Oszczypko-Clowes, M., Báldi, K., Less, G., Nagymarosy, A., Ruman, A., Klučiar, T., & Jamrich, M. (2017). The central paratethys palaeoceanography: A water circulation model based on microfossil proxies, climate, and changes of depositional environment. *Acta Geologica Slovaca*, *9*(2), 75–114.

Krijgsman, W., Garcés, M., Langereis, C. G., Daams, R., Dam, J., Van der Meulen, A. J., Agustí, J., & Cabrera, L. (1996). A new chronology for the Middle to Late Miocene continental record in Spain. *Earth and Planetary Science Letters*, *142*(3–4), 367–380. https://doi.org/10.1016/0012-821X(96)00109-4

Krijgsman, W., Langereis, C. G., Daams, R., & Van der Meulen, A. J. (1994). Magnetostratigraphic dating of the Middle Miocene climate change in the continental deposits of the Aragonian type area in the Calatayud-Teruel basin (central Spain). *Earth and Planetary Science Letters*, *128* (3–4), 513–526. https://doi.org/10.1016/0012-821X(94)90167-8

Lechner, T. S., & Böhme, M. (2025). The early Late Miocene hominid locality Hammerschmiede (Bavaria, southern Germany). *Senckenberg Monographs*, *2*, 1–97.

Li, L., Cailleux, F., Mutu, E., Van den Hoek Ostende, L. W., & Qiu, Z. (2024). *Sonidolestes wendusui*, a new genus of Erinaceinae (Eulipotyphla, Mammalia) from the lower Miocene of Inner Mongolia, China. *Historical Biology*, *36* (1), 1–11. https://doi.org/10.1080/08912963.2022.2141628

Li, Z., Li, Y., Xue, X., Li, W., Zhang, Y., & Yang, F. (2019). A new fossil Erinaceidae from the Shajingyi area in the Lanzhou Basin, China. *Acta Geologica Sinica*, *93*(4), 789–798. https://doi.org/10.1111/1755-6724.13797

Lopatin, A. V. (2006). Early Paleogene insectivore mammals of Asia and establishment of the major groups of Insectivora. *Paleontological Journal*, *40*(3), 205–405.

López-Guerrero, P., Álvarez-Sierra, M. A., García-Paredes, I., Carro-Rodríguez, P. M., & Peláez-Campomanes, P. (2018). Species of *Hispanomys* from the late Aragonian and early Vallesian (Middle-Late Miocene) of the Calatayud–Daroca Basin, Zaragoza, Spain. *Journal of Iberian Geology*, *45*(1), 163–180. https://doi.org/10.1007/s41513-018-0081-3

López-Guerrero, P., Álvarez-Sierra, M. A., García-Paredes, I., López-Antoñanzas, R., & Oliver, A. (2009). Cricetodontini (Rodentia, Mammalia) from the upper Aragonian and lower Vallesian of the Toril-Nombrevilla section (Middle and Upper Miocene, Calatayud-Daroca basin, Zaragoza, Spain). *Journal of Vertebrate Paleontology*, *29*(3), 161A.

Marković, Z., & Milivojević, M. (2010). The Neogene small mammals from Serbia—collection methods and results. *Bulletin of the Natural History Museum*, *3*, 105–114.

Masini, F., & Fanfani, F. (2013). *Apulogalerix pusillus* nov. gen. nov. sp. the small-sized Galericinae (Erinaceidae, Mammalia) from the "Terre Rosse" fissure filling of the Gargano (Foggia, south-eastern Italy). *Geobios*, *46*(1–2), 89–104. https://doi.org/10.1016/j.geobios.2012.10.008

Mein, P. (1999). The Late Miocene small mammal succession from France, with emphasis on the Rhône Valley localities. In J. Agustí, L. Rook & P. Andrews (Eds.), *Hominoid evolution and climatic change in Europe, 1* (Vol. 1, pp. 140–164). Cambridge University Press.

Mein, P., & Ginsburg, L. (2002). Sur l'âge relatif des différents dépôts karstiques miocènes de La Grive-Saint-Alban (Isère). *Publications du musée des Confluences*, *5*(2), 7–47. https://doi.org/10.3406/mhnly.2002.1328

Mein, P., & Martin-Suárez, E. (1993). *Galerix iberica* sp. nov. (Erinaceidae, Insectivora, Mammalia) from the Late

Miocene and early Pliocene of the Iberian Peninsula. *Geobios*, *26*(6), 723–730. https://doi.org/10.1016/S0016-6995(93)80055-V

Ménouret, B., & Mein, P. (2008). Les vertébrés du Miocène supérieur de Soblay (Ain, France). *Travaux et Documents des Laboratoires de Géologie de Lyon*, *165*, 3–97.

Pickford, M., Gabunia, L., Mein, P., Morales, J., & Azanza, B. (2000). The Middle Miocene mammalian site of Belometchetskaya, North Caucasus: An important biostratigraphic link between Europe and China. *Geobios*, *33*(2), 257–267. https://doi.org/10.1016/S0016-6995(00)80023-6

Prieto, J., Angelone, C., Casanovas-Vilar, I., Gross, M., Hír, J., Van den Hoek Ostende, L. W., Maul, L., & Vasilyan, D. (2014). The small mammals from Gratkorn: An overview. *Palaeobiodiversity and Palaeoenvironments*, *94*(1), 135–162. https://doi.org/10.1007/s12549-013-0147-3

Prieto, J., Gross, M., Böhmer, C., & Böhme, M. (2010). Insectivores and bats (mammalia) from the late Middle Miocene of Gratkorn (Austria): Biostratigraphic and ecologic implications. *Neues Jahrbuch für Geologie und Paläontologie, Abhandlungen*, *258*(1), 107–119. https://doi.org/10.1127/0077-7749/2010/0088

Prieto, J., & Rummel, M. (2009). Erinaceidae (Mammalia, Erinaceomorpha) from the Middle Miocene fissure filling Petersbuch 68 (southern Germany). *Zitteliana*, *48*(49), 75–88.

Prieto, J., Van den Hoek Ostende, L. W., Böhme, C., & Braze, M. (2011). Reappearance of *Galerix* (Erinaceomorpha, Mammalia) at the Middle to Late Miocene transition in south Germany: Biostratigraphic and palaeoecologic implications. *Contributions to Zoology*, *80*(3), 179–189. https://doi.org/10.1163/18759866-08003002

Prieto, J., Van den Hoek Ostende, L. W., & Hír, J. (2012). The Middle Miocene insectivores from Sámsonháza 3 (Hungary, Nógrád County): Biostratigraphical and palaeoenvironmental notes near to the Middle Miocene cooling. *Bulletin of Geosciences*, *87*(2), 227–240. https://doi.org/10.3140/bull.geosci.1296

Prieto, J., Van den Hoek Ostende, L. W., Hír, J., & Kordos, L. (2015). The Middle Miocene insectivores from Hasznos (Hungary, Nógrád County). *Palaeobiodiversity and Palaeoenvironments*, *95*(3), 431–451. https://doi.org/10.1007/s12549-015-0193-0

Qiu, Z. (1996). *Middle Miocene micromammalian fauna from Tunggur, Nei Mongol*. Science Press.

Rabeder, G. (1973). *Galerix* und *Lanthanotherium* (Erinaceidae, Insectivora) aus dem Pannon des Wiener Beckens. *Neues Jahrbuch für Geologie und Paläontologie, Monatshefte*, *1973*(7), 429–446.

Raffi, I., Wade, B. S., & Pälike, H. (2020). Chapter 29 - the Neogene period. In F. M. Gradstein, J. G. Ogg, M. D. Schmitz & G. M. Ogg (Eds.), *The geologic time scale 2020* (Vol. 2, pp. 1141–1215). Elsevier.

R Core Team. R. (2019). *A language and environment for statistical computing*. R Foundation for Statistical Computing.

Sen, S., Seyitoglu, G., Karadenizli, L., Kazanci, N., Varol, B., & Araz, H. (1998). Mammalian biochronology of Neogene deposits and its correlation with the lithostratigraphy in the Çankiri-Çorum Basin, central Anatolia, Turkey. *Eclogae geologica Helvetiae*, *91*(3), 307–320.

Shevenell, A. E., Kennet, J. P., & Lea, D. W. (2004). Middle Miocene southern ocean cooling and antarctic cryosphere expansion. *Science*, *305*(5691), 1766–1770. https://doi.org/10.1126/science.1100061

Van Dam, J. A. (2010). The systematic position of Anourosoricini (Soricidae, Mammalia): Paleontological and molecular evidence. *Journal of Vertebrate Paleontology*, *30*(4), 1221–1228. https://doi.org/10.1080/02724634.2010.483553

Van Dam, J. A., Aziz, H. A., Alvarez-Sierra, M. A., Hilgen, F. J., Van den Hoek Ostende, L. W., Lourens, L. J., Mein, P., Van der Meulen, A. J., & Paláez-Campomanes, P. (2006). Long-period astronomical forcing of mammal turnover. *Nature*, *443*(7112), 687–691. https://doi.org/10.1038/nature05163

Van Dam, J. A., Krijgsman, W., Abels, H. A., Alvarez-Sierra, M. A., García-Paredes, I., López-Guerrero, P., Oliver, A., & Paláez-Campomanes, P. (2014). Updated chronology for Middle to Late Miocene mammal sites of the Daroca area (Calatayud-Montalbán basin, Spain). *Geobios*, *47*(5), 325–334. https://doi.org/10.1016/j.geobios.2014.07.002

Van Dam, J. A., Mein, P., & Alcalá, L. (2020). Late Miocene Erinaceinae from the Teruel Basin (Spain). *Geobios*, *61*, 61–81. https://doi.org/10.1016/j.geobios.2020.06.002

Van Dam, J. A., Van den Hoek Ostende, L. W., & Reumer, J. W. (2011). A new short-snouted shrew from the Miocene of Spain. *Geobios*, *44*(2), 299–307. https://doi.org/10.1016/j.geobios.2010.11.007

Van den Hoek Ostende, L. W. (1992). Insectivore faunas from the lower Miocene of Anatolia, part 1: Erinaceidae. *Proceedings Koninklijke Nederlandse Akademie van Wetenschappen*, *95*(4), 437–467.

Van den Hoek Ostende, L. W. (2001). A revised generic classification of the Galericini (Insectivora, Mammalia) with some remarks on their palaeobiogeography and phylogeny. *Geobios*, *34*(6), 681–695. https://doi.org/10.1016/S0016-6995(01)80029-2

Van den Hoek Ostende, L. W. (2003). *Riddleria atecensis* nov. gen. nov. sp. a peculiar erinaceid (Erinaceomorpha, Mammalia) from the lower Miocene of Spain. *Beiträge zur paläontologie*, *28*, 1–7.

Van den Hoek Ostende, L. W. (2018). Cladistics and insular evolution, an unfortunate marriage? Another tangle in the Deinogalerix analysis of Borrani et al. (2017). *Cladistics*, *34*(6), 708–713. https://doi.org/10.1111/cla.12238

Van den Hoek Ostende, L. W., Casanovas-Vilar, I., & Furió, M. (2020). Stuck in the middle. A geographical appraisal of the oldest insectivores–and a marsupial–from the Vallès-Penedès Basin (early Miocene, Catalonia, Spain). *Comptes Rendus Palevol*, *19*(1), 1–25. https://doi.org/10.5852/cr-palevol2020v19a1

Van den Hoek Ostende, L. W., & Doukas, C. S. (2003). Distribution and evolutionary history of the Early Miocene erinaceid *Galerix symeonidisi* Doukas, 1986. *Deinsea*, *10*, 287–304.

Van den Hoek Ostende, L. W., & Fejfar, O. (2006). Erinaceidae and talpidae (Erinaceomorpha, Soricomorpha, Mammalia) from the lower Miocene of Merkur-Nord (Czech Republic, MN 3). *Beiträge zur paläontologie*, *30*, 175–203.

Van den Hoek Ostende, L. W., & Furió, M. (2005). The fossil record of the Eurasian Neogene insectivores

(Erinaceomorpha, Soricomorpha, Mammalia): Part I. *Scripta Geologica, Special Issue*, *5*, 149–284.

Van den Hoek Ostende, L. W., Furio, M., Madern, A., & Prieto, J. (2016). Enters the shrew, some considerations on the Miocene palaeobiogeography of Iberian insectivores. *Comptes Rendus Palevol*, *15*(7), 813–823. https://doi.org/10.1016/j.crpv.2016.03.006

Van den Hoek Ostende, L. W., López-Guerrero, P., Peláez-Campomanes, P., Álvarez-Sierra, M. A., & García-Paredes, I. (2012). Early Late Miocene insectivores (Eulipotyphla, Mammalia) from the Canada section (province of Zaragoza, east central Spain). *Comptes Rendus Palevol*, *11*(7), 495–506. https://doi.org/10.1016/j.crpv.2012.06.003

Van den Hoek Ostende, L. W., Mayda, S., Oliver, A., Madern, A., Hernández-Ballarín, V., & Peláez-Campomanes, P. (2015). Aliveri revisited, a biogeographical appraisal of the Early Miocene mammals from the eastern Mediterranean. *Palaeobiodiversity and Palaeoenvironments*, *95*(3), 271–284. https://doi.org/10.1007/s12549-015-0199-7

Van der Meulen, A. J., García-Paredes, I., Álvarez-Sierra, M. A., van den Hoek Ostende, L. W., Hordijk, K., Oliver, A., López-Guerrero, P., Hernández-Ballarín, V., & Peláez-Campomanes, P. (2011). Biostratigraphy or biochronology? Lessons from the Early and Middle Miocene small mammal events in Europe. *Geobios*, *44*(2–3), 309–321. https://doi.org/10.1016/j.geobios.2010.11.004

Van der Meulen, A. J., García Paredes, I., Álvarez Sierra, M., van den Hoek Ostende, L. W., Hordijk, K., Oliver Pérez, A., & Peláez-Campomanes, P. (2012). Updated Aragonian biostratigraphy: Small mammal distribution and its implications for the Miocene European chronology. *Geologica Acta*, *10* (2), 159–179. https://doi.org/10.1344/105.000001710

Van der Meulen, A. J., Peláez-Campomanes, P., & Daams, R. (2003). Revision of medium-sized Cricetidae from the Miocene of the Daroca-Villafeliche area in the Calatayud-Teruel basin (Zaragoza, Spain). *Coloquios de Paleontología*, *Volumen Extraordinario 1*, 385–441.

Van der Meulen, A. J., Peláez-Campomanes, P., & Levin, S. A. (2005). Age structure, residents, and transients of Miocene rodent communities. *The American Naturalist*, *165*(4), 108–125. https://doi.org/10.1086/428683

Vasileiadou, K., & Koufos, G. D. (2005). The micromammals from the Early/Middle Miocene locality of Antonios, Chalkidiki, Greece. *Annales de Paléontologie*, *91*(3), 197–225. https://doi.org/10.1016/j.annpal.2005.06.002

Viret, J. (1938). Étude sur quelques Erinaceidés fossiles spécialement sur le genre *Palaerinaceus*. *Travaux et Documents des Laboratoires de Géologie de Lyon*, *34*, 1–35.

Wazir, W. A., Cailleux, F., Sehgal, R. K., Patnaik, R., Kumar, N., & van den Hoek Ostende, L. W. (2022). First record of insectivore from the late Oligocene, Kargil formation (Ladakh Molasse group), Ladakh Himalayas. *Journal of Asian Earth Sciences: X*, *8*, 100105. https://doi.org/10.1016/j.jaesx.2022.100105

Ziegler, R. (1983). *Odontologische und osteologische Untersuchungen an Galerix exilis (Blainville)(Mammalia, Erinaceidae) aus den miozänen Ablagerungen von Steinberg und Goldberg im Nördlinger Ries, Süddeutschland* [dissertation]. Ludwig Maximilian University, 277.

Ziegler, R. (1990). Didelphidae, Erinaceidae, Metacondontidae und Dimylidae (Mammalia) aus dem Oberoligozän und Untermiozän Süddeutschlands. *Stuttgarter Beiträge zur Naturkunde B*, *158*, 1–99.

Ziegler, R. (1994). Bisher übersehene Insectivora (Mammalia) aus dem Untermiozän von Winterhof-West bei Eichstätt (Bayern). *Mitteilungen der Bayerische Staatssammlung für Paläontologie und historische Geologie*, *34*, 291–306.

Ziegler, R. (2000). The Miocene Fossil-Lagerstätte Sandelzhausen, 17: Marsupialia, Lipotyphla and Chiroptera (Mammalia). *Senckenbergiana Lethaea*, *80*(1), 81–127. https://doi.org/10.1007/BF03043666

Ziegler, R. (2003). Insektenfresser (Lipotyphla) aus dem Mittel-Miozän von Mühlbach am Manhartsberg und Grund, Niederösterreich. *Annalen des Naturhistorischen Museums in Wien, Serie A*, *104*, 251–265.

Ziegler, R. (2005). Erinaceidae and Dimylidae from the late Middle Miocene of south Germany. *Senckenbergiana Lethaea*, *85*(1), 131–152. https://doi.org/10.1007/BF03043423

Ziegler, R. (2006). Miocene insectivores from Austria and Germany – an overview Beiträge zur Paläontologie. *30*, 481–494.

Ziegler, R., Dahlmann, T., Reumer, J. W. F., & Storch, G. (2005). Germany. LW Van Den Hoek Ostende, CS Doukas, JWF Reumer, editors. The fossil record of the eurasian Neogene insectivores (Erinaceomorpha, Soricomorpha, Mammalia) part I. *Leiden: Scripta Geologica, Special Issue*, *5*, 61–98.

Ziegler, R., & Fahlbusch, V. (1986). Kleinsäuger-faunen aus der basalen Oberen Süßwasser-Molasse Niederbayerns. *Zitteliana*, *14*, 3–58.

Zijlstra, J., & Flynn, L. J. (2015). Hedgehogs (Erinaceidae, Lipotyphla) from the Miocene of Pakistan, with description of a new species of *Galerix*. *Palaeobiodiversity and Palaeoenvironments*, *95*(3), 477–495. https://doi.org/10.1007/s12549-015-0190-3